NEGATIVE ION-MOLECULE REACTIONS: AN INVESTIGATION OF FLUORIDE ION TRANSFER REACTIONS IN SELECTED NONMETAL FLUORIDES

by

Thomas Crowell Rhyne

Thesis submitted to the Graduate Faculty of

Virginia Polytechnic Institute and State University

in partial fulfillment of the requirements for the degree of

DOCTOR OF PHILOSOPHY

in

Chemistry

APPROVED:

Dr. John G. Dillard

Dr. Alan F. Clifford

Dr. John C. Schug

Dr. Raymond E. Dessy

Dr. Larry T. Taylor

Date

January, 1971

Blacksburg, Virginia

ACKNOWLEDGMENTS

The completion of this period of study would not have been possible without the aid of many individuals, and it is both desirable and appropriate to express appreciation to these persons at this time.

I wish to express my sincere appreciation to Dr. John G. Dillard for his unfailing guidance and assistance. His enthusiasm for chemistry and his devotion to duty and principle provided encouragement and incentive throughout this endeavor.

The opportunity of doing nonthesis research in the laboratory of Dr. A. F. Clifford and the research assistantship provided by him during that summer are gratefully acknowledged. Appreciation is also extended to the members of the advisory committee for their assistance.

Thanks are due Mr. G. W. Dulaney for his advice and assistance in programming the laboratory computer and interfacing it with the mass spectrometer. Messrs. Frans Van Damme, Andrew Mollick, Don Bodell, Frank Shelor, S. J. Ensogna, and R. L. Miller are gratefully acknowledged for their assistance in the construction of the apparatus used in this study.

A special thanks is reserved for Billie Sue for her understanding throughout this endeavor and for her typing of the initial versions of this manuscript. The author's parents and his wife's parents also deserve special gratitude for their encouragement.

The Research Corporation, the donors to the Petroleum Research Fund administered by the American Chemical Society, the Research Division of V.P.I., and the Department of Chemistry of V.P.I. are acknowledged for financial support during this study.

TABLE OF CONTENTS

CHAPTER

CHAPTER

LIST OF TABLES

TABLE PAGE

LIST OF FIGURES

FIGURE PAGE

CHAPTER I

INTRODUCTION

Sir J. J. Thomson was first to recognize the importance of mass spectrometry as an analytical tool, and in 1913 (1) he described the use of his parabola mass spectrograph in the analysis of very small samples of gases and for the determination of atomic and molecular weights. The wealth of chemical information which could be extracted from mass spectral data prompted researchers to devise many techniques for mass spectrometric investigation of chemical systems, and by the 1950's the mass spectrometer had achieved the status of a necessary tool for chemical research.

The mass spectrometer is an instrument designed to produce ions from a gaseous sample, separate the ions according to their mass-to-charge (m/q) ratio, and measure the relative number of ions of a given m/q value. The mass spectrometer is often used for both qualitative and quantitative analysis of mixtures, and the mass spectral fragmentation pattern enables structural analysis of many complex molecules. The mass spectrum, a plot of relative ion abundance as a function of m/q value, is familiar to chemists as a tool for compound identification, but mass spectrometric data also provides valuable information about the energetics and bonding in molecules. Since the use of the mass spectrometer to obtain energetic measurements is often less familiar to the chemist than is the recording of mass spectra, a description of these measurements is presented here to facilitate later discussion of the experiments conducted in this study.

I. STUDIES OF IONS IN THE MASS SPECTROMETER

Ions are produced in a conventional mass spectrometer by bombardment of a gaseous sample with a beam of collimated electrons. The energy necessary for ionization is imparted to the molecule through a collision with an electron having sufficient energy to cause ionization. This process occurs so rapidly that, according to the Franck-Condon principle, the nuclei do not move a significant distance during the electronic transition.

Formation of Positive Ions

The minimum energy required to remove an electron from the highest occupied molecular orbital is the ionization potential of the molecule, and positive ions formed in this manner are called molecular or parent ions. If more than the minimum quantity of energy is imparted to the molecule, fragment ions are formed by decomposition of the molecular ion, and the minimum energy required to produce a given fragment is called the appearance potential of that ion. It should be noted that the ionization potential is a special case of the appearance potential.

Appearance potentials are determined by measuring the ion current as the electron energy is varied. An ionization efficiency curve is constructed by plotting ion current for a particular m/q as a function of electron energy, and the point at which the curve intercepts the electron energy axis gives the appearance potential of that ion. More sophisticated methods for determining the appearance potentials of positive ions are described by Kiser (2) and will not be discussed here since this study is primarily concerned with studies of negative ions.

Formation of Negative Ions

Negative ions are formed in the mass spectrometer by electron capture processes

$$AB + e^- \rightarrow AB^- \quad (1)$$

$$AB + e^- \rightarrow A + B^- \quad (2)$$

and by ion pair production

$$AB + e^- \rightarrow A^+ + B^- + e^- \quad (3)$$

The electron capture processes illustrated above are resonance processes which occur in the low energy region (<10 eV) and are characterized by the ionization efficiency curve shown in Figure 1. Whereas positive ion formation (and ion pair processes) are characterized by a minimum energy required for ionization with excess energy being carried away by the product electron, electron capture can occur only when electrons of specific energy collide with a molecule. The appearance potential for reaction 1 is given by the relationship

$$AP(AB^-) = -EA(AB) + U + W \quad (4)$$

where EA(AB) is the electron affinity of the molecule, U is the excitation energy associated with the product, and W is the total kinetic energy of the product. For the dissociative electron capture process (reaction 2) the appearance potential is given by

$$AP(B^-) = D(A-B) - EA(B) + U + W \quad (5)$$

where D(A-B) is the bond dissociation energy for the bond broken in the formation of the negative ion. In each of these processes the electron

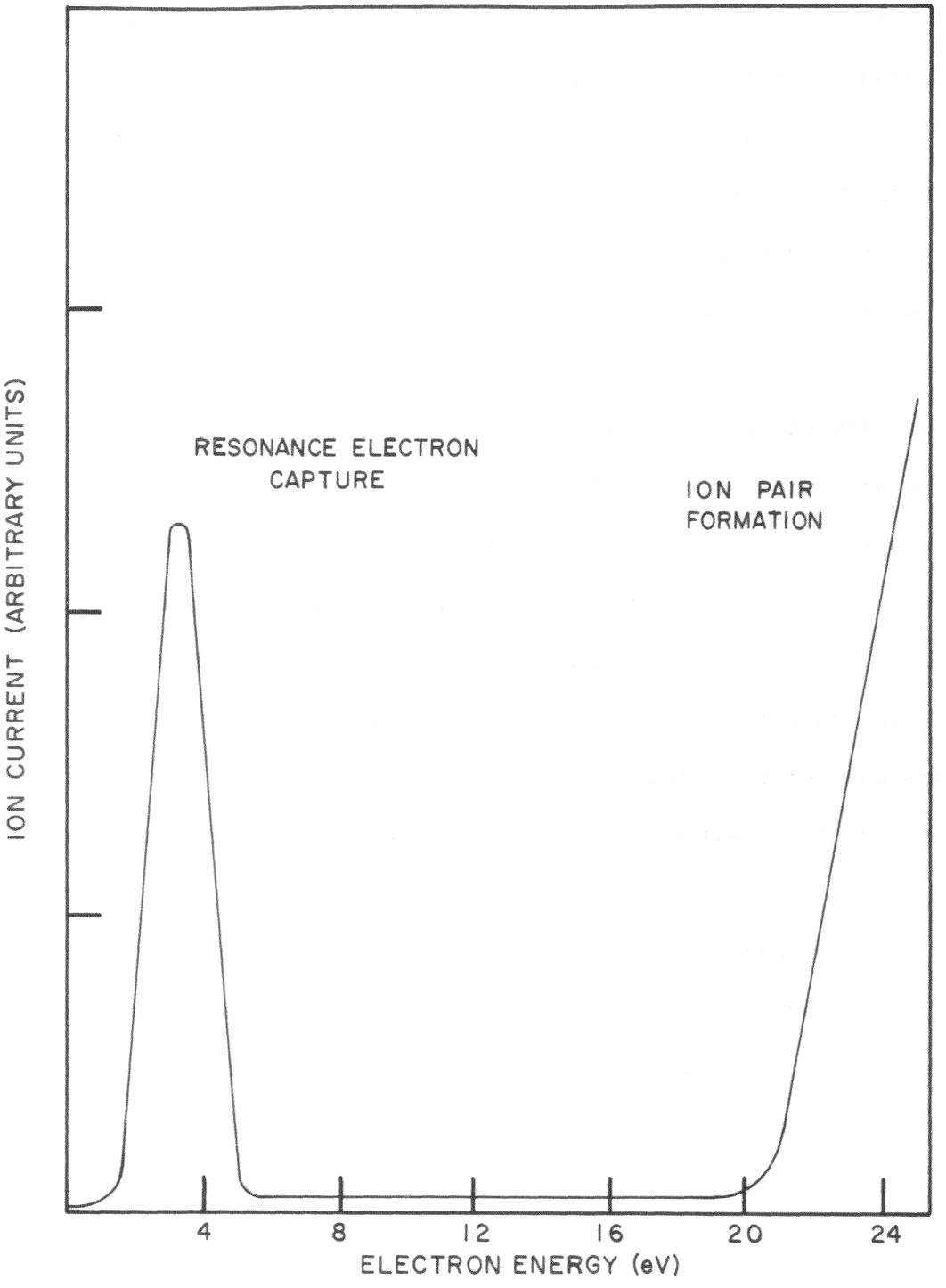

FIGURE I. REPRESENTATIVE IONIZATION EFFICIENCY CURVES FOR THE FORMATION OF NEGATIVE IONS

is captured by the molecule and must have exactly the right amount of energy to satisfy the appearance potential relationship. If the kinetic energy of the products may vary, i.e., if ions are formed having a range of kinetic energies, then electrons of a corresponding range of energies will produce negative ions. Electrons having excess energy are spontaneously ejected or cause decomposition of unstable negative ions to a more stable species, and a resonance process is not observed.

Ion pair formation (reaction 3) is observed at electron energies high enough to cause the heterolytic cleavage of the A-B bond to form both a positive and a negative ion, and stable ions may be formed by collisions with electrons having more than the minimum energy requirement since the product electron retains most of the excess energy. B^- is thus less likely to be formed in an unstable excited state by high energy electrons than are the negative ions formed via reactions 1 and 2, and negative ions are generated by reaction 3 at electron energies well above the onset energy for this process.

Conventional mass spectrometers are operated at low pressures (10^{-7} Torr) so that ions formed by the processes described above may be detected without being destroyed by collisions with other species in the instrument. Routine analytical applications of mass spectrometry are characterized by low pressure measurements which insure that only processes involving single collisions of atoms or molecules with electrons are observed.

Ion-Molecule Reactions

Ions formed by processes described above are termed primary ions

since they are formed as the result of single collisions with electrons. Another mechanism by which ions may be formed in the mass spectrometer is the bimolecular collision of a primary ion and a neutral molecule to produce a secondary ion by processes such as

$$AB^+ + CD \rightarrow ABC^+ + D \quad (6)$$

$$AB^- + CD \rightarrow A + BCD^- \quad (7)$$

$$AB^- + CD \rightarrow AB + CD^- \quad (8)$$

Reactions 6 and 7 involve atom and ion transfer, respectively, and may result in the formation of ions of higher m/q value than that of the molecular ion of the gases present. Reaction 8 involves electron transfer and is often the mechanism of formation of parent negative ions at high pressure. Processes resulting in the formation of secondary ions are enhanced by high sample pressures since ion-molecule collisions are more likely at higher concentrations of molecules. Thus investigations of secondary collision processes are characterized by mass spectrometric measurements conducted at high pressures, usually greater than 10^{-4} Torr.

II. IMPORTANCE OF ION-MOLECULE REACTIONS

Gas-phase ion-molecule reactions received little attention before the past decade, but recent studies of gaseous ion chemistry have demonstrated that ionic reactions are important in many systems in which gaseous ions are formed. The presence of ions in flames and gaseous discharges has been known for over fifty years, but two recent studies (3,4) illustrate the importance of gaseous ions in these media. Since the rates of gas-phase ion-molecule reactions are very large (several orders of

magnitude faster than free radical reactions) ionic reactions must be considered in any system in which ions are present. Radiation chemistry (5) and chemistry of the ionosphere (6), in addition to flames and gaseous discharges, are systems in which investigations have demonstrated the significant role of ion-molecule reactions in determining the chemical behavior of the system.

But the importance of gas-phase ion-molecule reactions is not restricted to gaseous systems. Ions in solution are not free ions, but rather are solvated entities surrounded by a sheath of molecules which provide stabilization energy and also participate in the chemical behavior of the ion (7). The structures of ions in solution are often dependent on the nature of the solvent medium (7), and the effect of ionic structure on reactivity is difficult to ascertain from solution studies. Thus studies of gaseous ion-molecule reactions may contribute to an understanding of the role of the solvent in condensed phase reactions of ions, as is illustrated by the following example. Hughes and Tiernan (8) have determined the gas-phase acidities of a series of alcohols by investigating the negative ion-molecule reactions

$$ROH + R'O^- \rightarrow R'OH + RO^- \quad (9)$$

$$R'OH + RO^- \rightarrow ROH + R'O^- \quad (10)$$

From the principle of microscopic reversibility the ratio of forward and reverse reactions is the equilibrium constant, and hence the relative Bronsted acidity of the alcohols may be determined. A scale of acidities determined in this way serves to remove entirely any effect of solvent, and in fact the order of acidity was found to be reverse of that determined from solution studies. This result suggests that the order determined

in solution is actually the result of solvent effects such as hydrogen bonding or dipole interactions between the solvent and alkoxide ions.

With only two exceptions (9,10), all evidence suggests that free negative ions can accomodate only a single net charge for times long enough to permit observation in a mass spectrometer (11), whereas multiply-charged negative ions are stabilized in crystals and in solutions by interaction with neighboring ions or the solvent. Thus the relatively simple structure of negative ions lends itself to an evaluation of the contribution of molecular parameters such as structure to reactivity of the ion.

Ionic reactions account for many of the phenomena observed in studies of inorganic chemical systems, and a large number of inorganic molecules undergo reactions involving negative ions. Since inorganic molecules composed of different elements and elements in different oxidation states may have different molecular geometries, examination of negative ion-molecule reactions in inorganic systems is particularly suitable for alucidating the importance of factors such as molecular structure, formal oxidation state, bond order, and electronegativity in determining reactivity of free negative ions.

The system of inorganic nonmetal fluorides provides a particularly attractive group of molecules for such investigations since these compounds exhibit a variety of structures, oxidation states, and other molecular parameters which might be related to chemical behavior. Among the nonmetal fluorides, sulfur hexafluoride (SF_6) is somewhat unique in that it is in general chemically inert. Case and Nyman (12) reported the reaction of SF_6 with several "fluorophilic" Lewis acids which resulted in

transfer of fluorine from SF_6 to the Lewis acid. Demitras and MacDiarmid (13) have reported condensed-phase reactions of SF_6 with sodium in diphenylethylene glycol dimethyl ether solution and with sodium in liquid NH_3 solution. Brewer, Chang, and King (14) reacted SF_6 with potassium and cesium in liquid NH_3, and Asmus and Fendler (15) studied the reaction of SF_6 with hydrated electrons produced in water by a ^{60}Co gamma source and by a 1.5 MeV Van de Graaf electron accelerator. In each of these reactions the initial formation of the SF_6^- ion is postulated as an important initial step with subsequent transfer of a fluoride ion yielding the fluorinated product and the SF_5 radical.

The SF_6^- radical anion is readily obtained in the gas phase since SF_6 is known to have a high electron capture cross section for thermal electrons at 0.08 eV (16). Based on solution studies described above, it seemed reasonable that SF_6^- might react with simple inorganic molecules in the gas phase where single collision events occur.

The simple phosphorus fluorides (PF_5 and PF_3) were chosen as the neutral reactants in initial experiments, since transfer of a fluoride ion to PF_5 and PF_3 would yield the anions PF_6^- and PF_4^-, respectively. Reports of the isolation of compounds containing the PF_6^- anion are numerous (17,18,19) but PF_4^- apparently is unstable in solution (17). Studies of these ions in the gas phase might suggest a basis for the difference in reactivity of these molecules and reveal the influence of molecular parameters on reactivity. Since transfer of a fluoride ion to these molecules corresponds to transfer of a pair of electrons, the measured rate constants and reaction cross sections give a relative measure of the Lewis acidity of the molecule. Thus studies of negative

ion reactions of SF_6 may provide a quantitative basis for a scale of Lewis acidities of inorganic molecules which is independent of solvent effects. In addition, studies of negative ion-molecule reactions could yield useful information on reactions and mechanisms of gaseous discharges and photolysis, and conceivably the investigations described here could lead to analytical techniques for detecting trace quantities of gaseous materials.

In summary, the purpose of this research is threefold: (1) to investigate the chemistry of free inorganic negative ions and determine the effect of molecular parameters on reactivity; (2) to add to the knowledge of negative ion-molecule reactions and enable the eventual correlation between gas-phase kinetic studies and condensed-phase chemical behavior; and (3) to apply the current theories of ion-molecule reactions to determine the success of these theories in describing low-energy negative ion reactions.

CHAPTER II

ION-MOLECULE REACTIONS

This study is primarily concerned with gaseous ions and their reactions with neutral molecules. Previous studies of ion-molecule reactions in the gas phase have provided a basis for the experimental methods used here, and theories of ion-molecule reactions have been utilized in evaluating the experimental data obtained in this study. Therefore a discussion of the history of ion-molecule reaction studies and the concurrent development of theoretical descriptions of ion-molecule reactive collisions is presented here to facilitate the later discussion of experimental results and conclusions.

I. HISTORY OF ION-MOLECULE REACTIONS

Gas-phase ion-molecule reactions have been known since the beginning of mass spectrometry, dating from the observation of the "X_3" ion in the mass spectrum of hydrogen by Sir J. J. Thomson (1) in 1913. His suggestion that this substance must be the H_3^+ ion was confirmed in 1916 by Dempster (20), and the mechanism of formation of this secondary ion was correctly proposed by Hogness and Lunn (21) in 1925 to be

$$H_2^+ + H_2 \rightarrow H_3^+ + H \qquad (11)$$

In 1936 Eyring, Hirschfelder, and Taylor (22) derived a theoretical rate constant for the reaction. Theoretical consideration of the interaction of an ion with a molecule in the gas phase had in fact preceded the initial observation of this phenomenon by Thomson, since Langevin (23)

had formulated an expression for ion-molecule collision processes as early as 1905. Hogness and Harkness (24) in 1928 detected I_3^+ and I_3^- in the mass spectrum of iodine vapor, marking the first observation of a negatively-charged ion-molecule reaction product. These early experiments established that the abundance of the secondary ion is dependent on the concentration of the reactant neutral species, and experimentors found that mass spectra obtained at low sample pressures did not exhibit these troublesome secondary ions which often interfered with chemical analyses. Thus with the development of improved vacuum systems and because of lack of interest in gas-phase ion chemistry, the study of ion-molecule reactions was set aside for some twenty years.

Positive Ion-Molecule Reactions

More recent investigations stem from observation of the CH_5^+ ion in the high-pressure mass spectrum of methane as a result of the reaction

$$CH_4^+ + CH_4 \rightarrow CH_5^+ + CH_3 \qquad (12)$$

Although this process was discovered by Eltenton (25) in 1940, it was the announcement in 1952 of the work of Tal'rose and Lyubimova (26) of the Soviet Union which regenerated interest in gas-phase ion chemistry. A very large number of experiments on the positive ion chemistry of hydrocarbons followed, and theories of ion-molecule reactions were developed to explain the kinetics of the reactions observed. Although a detailed discussion of the theory of ion-molecule reactions will follow, mention of the historical development of the theory is worthwhile at this point.

The early work of Langevin (23) was developed by Gioumousis and Stevenson (27) into a theory which demonstrated quite good agreement with

experimental results. Franklin, Field, and Lampe (28,29), through their extensive investigations of the ion chemistry of hydrocarbon systems, contributed a substantial body of information, both experimental and theoretical, toward the understanding of the reactions of ions with gases. Significant efforts from many other researchers quickly followed those of the groups mentioned, and today the field of ion-molecule reactions enjoys widespread interest due to the established importance of gas-phase ion chemistry. Particular emphasis has been given the study of positive ion reactions, and an important development in this area is Field and Munson's (30) use of ion-molecule reaction chemistry to supplement the low-pressure mass spectra of organic molecules under the terminology "Chemical Ionization Mass Spectrometry."

Negative Ion-Molecule Reactions

Investigations involving negative ions have evolved slowly, and very few reactions of negative ions were reported before 1960. Prior to this the previously-mentioned work of Hogness and Harkness (24) and studies by Muschlitz (31), Melton and Ropp (32), and Henglein and Muccini (33) constituted the entire body of information known about negative ion-molecule reactions. Reactions reported by Henglein and Muccini (33)

$$O^- + NO_2 \rightarrow NO_2^- + O \qquad (13)$$

$$SO^- + SO_2 \rightarrow SO_2^- + SO \qquad (14)$$

and those reported by Fehsenfeld, Ferguson, and Schmeltekopf (34)

$$O^- + O_3 \rightarrow O_3^- + O \qquad (15)$$

$$O_2^- + O_3 \rightarrow O_3^- + O_2 \qquad (16)$$

$$O_3^- + CO_2 \rightarrow CO_3^- + O_2 \quad (17)$$

$$CO_3^- + O \rightarrow O_2^- + CO_2 \quad (18)$$

$$CO_3^- + NO \rightarrow NO_2^- + CO_2 \quad (19)$$

$$O_3^- + NO \rightarrow NO_3^- + O \quad (20)$$

are typical of a large number of reactions investigated in the 1960's as the role of negative ion chemistry in the ionosphere became more evident. Extensive investigations of the chemical reactions of negative ions of oxygen have been reported, including those by Paulson (35,36), by Fehsenfeld, Schmeltekopf, Dunkin, and Ferguson (37), by Rutherford and Turner (38), and by Moruzzi and Phelps (39). The flowing afterglow technique described by Ferguson, Fehsenfeld, and Schmeltekopf (34) has proved particularly advantageous for the study of atmospheric reactions, and investigations using this technique have demonstrated the importance of negative ions in atmospheric chemistry.

Although the majority of studies of negative ion-molecule reactions has been directed toward areas of atmospheric interest, research in other negative-ion systems has been reported. Steiner (4) has shown that negative ions are formed in gaseous discharges and that reactions of such ions may serve to control the energy distribution in certain stars. Chalcote and Jensen (3) have discussed negative ion-molecule reactions as important processes in hydrocarbon flames, showing that reactions such as the hydrogen atom extraction process

$$C_2^- + C_2H_2 \rightarrow C_2H^- + C_2H \quad (21)$$

occur to produce the product ions observed. Melton (5) has recently demonstrated the occurrence of negative ions in radiation chemistry from

experiments on the radiolysis of water vapor by 100 eV electrons, an observation which suggests the possible importance of negative ions in other radiation systems.

Studies of the gas-phase solvation of negative ions by Kebarle, Searles, Zolla, Scarborough, and Arshadi (40) have shown that negative ions are held to the solvent molecule in the gas phase by ion-dipole forces, forming clusters by the step-wise reactions

$$Cl^- + CHCl_3 \rightarrow (CHCl_3)Cl^- \quad (22)$$

$$(CHCl_3)Cl^- + CHCl_3 \rightarrow (CHCl_3)_2Cl^- \quad (23)$$

$$(CHCl_3)_2Cl^- + CHCl_3 \rightarrow (CHCl_3)_3Cl^-, \text{ etc.} \quad (24)$$

Tiernan and Hughes (8) have utilized gas-phase reactions of organic anions to determine gas-phase acidities of a series of alcohols based on the relative rates of the forward reaction

$$CH_3O^- + CH_3CH_2OH \rightarrow CH_3CH_2O^- + CH_3OH \quad (25)$$

and the analogous reverse reaction

$$CH_3CH_2O^- + CH_3OH \rightarrow CH_3CH_2OH + CH_3O^- \quad (26)$$

Results of experiments such as those of Kebarle, Searles, Zolla, Scarborough, and Arshadi (40) and of Tiernan and Hughes (8) can be expected to provide information about solvent effects on ion chemistry.

Dillard and Franklin (41,42) and Dillard, Franklin, and Seitz (43) have studied the gas-phase negative ion reactions

$$S^- + COS \rightarrow S_2^- + CO \quad (27)$$

$$S_2^- + COS \rightarrow S_3^- + CO, \text{ etc.} \quad (28)$$

$$NH_2^- + CS_2 \rightarrow SCN^- + H_2S \quad (29)$$

$$NH_2^- + CS_2 \rightarrow HS^- + HNCS \quad (30)$$

$$NH_2^- + COS \rightarrow NH_2S^- + CO \quad (31)$$

$$NH_2^- + COS \rightarrow HS^- + HNCO \quad (32)$$

$$NH_2^- + COS \rightarrow OCN^- + H_2S \quad (33)$$

$$O^- + CNCl \rightarrow OCN^- + Cl \quad (34)$$

$$O^- + CNCl \rightarrow CN^- + OCl \quad (35)$$

$$NH_2^- + CS_2 \rightarrow CS_2^- + NH_2 \quad (36)$$

and have measured rate constants of about the same magnitude (10^{-10} cm^3/molecule·sec) as those determined for positive ion-molecule reactions. Kraus, Muller-Duysing and Neuert (44) earlier observed reaction 36 and other charge-transfer reactions

$$CS^- + SO_2 \rightarrow SO_2^- + CS \quad (37)$$

$$NH_2^- + SO_2 \rightarrow SO_2^- + NH_2 \quad (38)$$

MacNeil and Thynne (45,46), and Craddock, Harland, and Thynne (45) have recently reported secondary negative ions in the mass spectra of nonmetal fluorides and have proposed that the reactions proceed by the ion-molecule reactions

$$F_2^- + BF_3 \rightarrow BF_4^- + F \quad (39)$$

$$SiF_3^- + SiF_4 \rightarrow SiF_5^- + SiF_2 \quad (40)$$

$$GaF_3^- + GeF_4 \rightarrow GaF_5^- + GeF_2 \quad (41)$$

Estimates of the rate constants for these reactions in the range (10^{-10} cm^3/molecule·sec) are determined by comparison of the rate of reaction 27 measured by Dillard and Franklin (41). As a

part of the work presented here Rhyne and Dillard (48,49) have reported rate data for fluoride ion transfer reactions of the type

$$SF_6^- \; AF_n \rightarrow \left[AF_{n+1}\right]^- + SF_5 \qquad (42)$$

which will be discussed in detail later.

II. THEORY OF ION-MOLECULE COLLISIONS AND REACTIONS

Theories of ion-molecule reactions have been developed through considerations of positive ion-neutral molecule systems, and the question of whether these same principles apply to negative ion-neutral systems is not yet resolved. Ion-molecule reaction theory as developed by Lampe, Franklin, and Field (28,29) and by Gioumousis and Stevenson (27) has been applied to both positive and negative ion systems with about equal success, although the relatively small store of negative ion data still leaves questions unanswered. Melton (50) has questioned the applicability of the Gioumousis-Stevenson theory to negative ion systems because of the reduced likelihood of each collision resulting in reaction for the negative ion case. Ferguson (51) has noted that, although very few negative ion-atom interchange reactions are known, there does not seem to be any fundamental difference between positive and negative ion reactions. The rates measured for negative ion-atom interchange are typical of those measured for many positive ion reactions. Dillard and Franklin (41) have measured reaction rates for negative ion reactions in carbonyl sulfide which are of the same order of magnitude as similar positive ion reactions (52).

Since there is no conclusive evidence why the theory of positive ion-molecule reactions should not be applied to negative ion systems, this theory is utilized to describe the kinetics of the reactions observed in this study.

Phenomenological Reaction Cross Section

Primary ions are formed in the electron beam and are moved toward the ion exit slit upon experiencing the field of the repeller electrode. In moving from the electron beam toward the ion exit slit these ions may undergo collision and reaction with neutral molecules to form secondary ions, which in turn travel toward the exit slit. Since only a small number of molecules are ionized, the gas concentration, n, in the ion source may be taken as constant. The diminution of the primary ion current $(i_p)_o$ in the electron beam by collision to form secondary ions is analogous to the attenuation of a photon beam traversing an abosrbing medium. The measured primary ion current, i_p, is given by

$$i_p = (i_p)_o \, e^{-dnQ} \tag{43}$$

where Q is the phenomenological reaction cross section and is the analog of the molal extinction coefficient of the Beer-Lambert Law. The quantity d is the distance from the electron beam to the ion exit slit and n is the concentration of gas in the ion source.

If the primary ion reacts to give only one type of secondary ion, the measured secondary ion current, i_s, is

$$i_s = (i_p)_o - i_p \tag{44}$$

Substituting into equation 43 gives

$$i_p = (i_s + i_p) \, s^{-dnQ} \tag{45}$$

and rearranging and solving for Q yields the expression

$$Q = \frac{1}{nd} \ln\left(1 + \frac{i_s}{i_p}\right) \tag{46}$$

so that when $i_s/i_p \ll 1$, the phenomenological reaction cross section is given by

$$Q_r = \frac{i_s}{i_p} \left(\frac{1}{nd}\right) \tag{47}$$

which is the result obtained by Gioumousis and Stevenson (27). These workers have shown that the phenomenological reaction cross section is related to a bimolecular rate constant, k, by the expression

$$k = Q_r \left(\frac{eEd}{600\ m_i}\right)^{1/2} \tag{48}$$

where e is the electronic charge, E is the repeller field strength, and m_i is the primary ion mass.

Lampe, Franklin, and Field (29) have evaluated the specific reaction rate constant of an ion-molecule reaction as

$$k = \frac{i_s}{i_p} \left(\frac{1}{nt}\right) \tag{49}$$

where n is the concentration of neutral and t is the ion residence time in the reaction chamber. The residence time is given by

$$t = \left(\frac{2dm_i}{eE}\right)^{1/2} \tag{50}$$

where m_i is the primary ion mass, e is the electronic charge, E is the repeller field, and d is the ion path length in the ion source.

Reaction Cross Section from Collision Theory

From studies of the mobilities of ions in gases Langevin (23) in 1905 derived the classical collision cross section for the interaction of an ion of charge q and a neutral molecule of polarizability α. The long-range attraction potential energy between these two particles is described

by

$$P.E.(r) = -\frac{q^2}{2r^4} \tag{51}$$

The collision cross section for an orbiting collision between these two particles is given by Gioumousis and Stevenson (27) as

$$Q_c = \frac{2\pi e}{g}\left(\frac{\alpha}{\mu}\right)^{1/2} \tag{52}$$

where g is the relative velocity of the ion and μ is the reduced mass of the reactants. For Maxwellian velocity distributions for both ion and neutral, a rate constant is defined by Gioumousis and Stevenson (27) by the relationship

$$k_c = Q_c\left(\frac{eEd}{2m_i}\right)^{1/2} \tag{53}$$

and substitution yields the equation for the energy-independent collision rate constant

$$k_c = 2\pi e\left(\frac{\alpha}{\mu}\right)^{1/2} \tag{54}$$

which is numerically equal to the reaction rate constant if the probability of each collision being a reactive collision is taken as unity.

Gioumousis and Stevenson (27) were first to apply the Langevin orbiting collision cross section to ion-molecule reactions of positive ions observed in the laboratory, and their calculations of reaction cross sections based on Langevin's orbiting complex suggested that many ion-molecule collisions have a reaction probability approaching unity since the agreement with experiment was quite good, though not universal. Boelrijk and Hamill (53) proposed a modification of the theory to allow for the physical size of the colliding species, and a number of results have been

explained in terms of this description (54-57).

Light (58) has developed an extension of the simple orbiting picture which has been applied to ion-molecule reactions by Wolf (59). The phase-space theory of Light predicts the relative weights of competing exothermic reaction channels, with the most exothermic channels being markedly favored. This leads to the same general result as does the orbiting picture in that exothermic reactions are predicted to be fast. Ferguson (51) has pointed out that the failure of both theories in explaining slow reactions is probably due to their lack of consideration of true potential curves for the interacting species.

Electron Density Rearrangement Model

Schaefer and Henis (60) have proposed an electron density rearrangement model for qualitatively predicting the magnitude of the reaction cross sections for low-energy ion-molecule reactions. This model is restricted to systems which are exothermic and in which the reactants have a relative kinetic energy of less than about 1 eV and are not vibrationally excited. This allows use of a two-state approximation for describing the course of the reactions, and the process of predicting the relative magnitude of the reaction cross section is reduced to a determination of the change in electron density around the reaction centers.

The general negative ion-molecule reaction

$$A^- + BC \rightarrow AB^- + C \qquad (55)$$

in considered in terms of the relative electronegativities at the reaction centers A and B. If the electronegativity of A is larger than B, then little change in electron density will be necessary around center B upon

proceeding to the AB^- ion since the electronegative A moiety will command a larger share of the electron density in the product ion. However, if the electronegativity of B is much larger than that of A, then formation of the product ion will require a net shift of electron density to B at or near the time of reaction. The authors (60) thus predict that for the situation requiring little effective rearrangement of electron density the reaction will be enhanced and a large reaction cross section ($Q > 1\ A^2$/molecule) will probably be observed. Likewise, if the relative values of the electronegativities of A and B are such that extensive rearrangement occurs, then a small cross section is expected for the reaction. A later application of this theory to the negative ion systems investigated in this study will illustrate the utility of this model in qualitatively predicting the relative reactivity of ion-molecule reaction systems.

The relationships developed by Gioumousis and Stevenson (27) and Lampe, Franklin, and Field (29) will be utilized to evaluate reaction rate constants and reaction cross sections for the systems studied here, and the energy dependence of the cross sections determined will be discussed in light of the predictions of these researchers.

The usefulness of negative ion-molecule reactions in determining reactivity of free ions and in explaining the behavior of ions in solution has been alluded to earlier. In order to determine the extent to which negative ion-molecule reactions can be used for these purposes, negative ion-molecule reactions involving a series of inorganic nonmetal fluorides have been studied, and a description of the experimental techniques and apparatus used in these investigations is presented in the following chapter.

CHAPTER III

EXPERIMENTAL APPARATUS AND TECHNIQUES

The study of gaseous ion chemistry requires equipment capable of producing ions and detecting ionic species, as well as facilities for handling gases. Many types of apparatus have been developed for experiments in this field, including drift tubes (61), flowing afterglow systems (34), crossed beam systems (62,63), ion cyclotron resonance spectrometers (64,65), tandem mass spectrometers (66), and mass spectrometers utilizing high energy radiation as sources of ionizing energy (67). The apparatus chosen for this study was a single-source mass spectrometer utilizing electron impact as the ionizing medium.

I. MASS SPECTROMETER AND RELATED APPARATUS

The mass spectrometer was an Hitachi Perkin-Elmer RMU-7 double-focusing instrument capable of analyzing and detecting both positive and negative ions. Figure 2 shows a schematic outline of the ion-optical system of the spectrometer. The Nier-Johnson design utilizes a 45° electrostatic sector for kinetic energy focusing and a 90° magnetic sector for mass analysis. Although the instrument can be operated at very high resolving power ($M/\Delta M = 20,000$), the high resolution capability of the spectrometer was not used because the ions of interest did not require high resolving power for identification.

Ions are formed in the ion source of the mass spectrometer by electrons emitted from a rhenium filament. A potential of appropriate sign (e.g., a negative potential for negative ions) applied to the

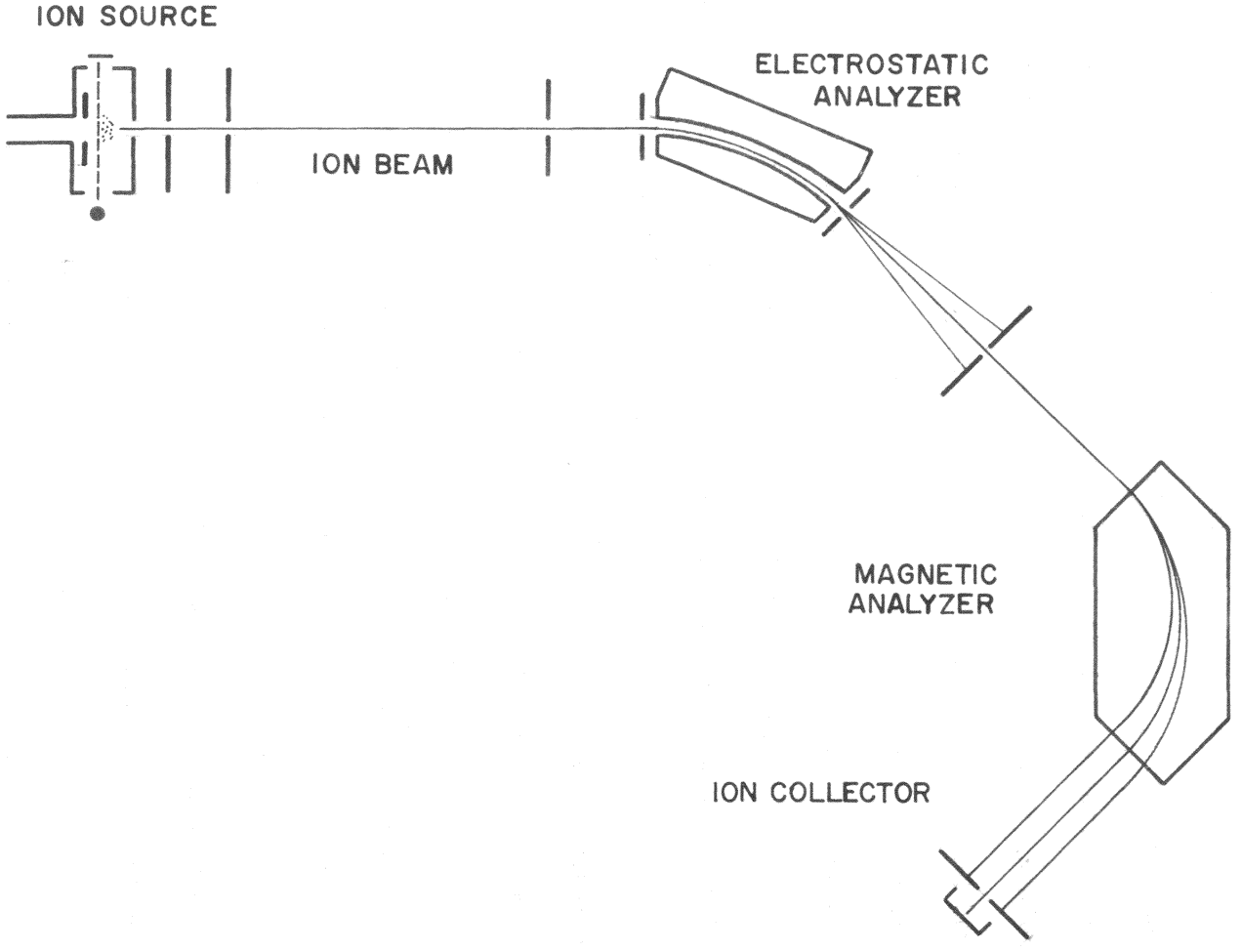

FIGURE 2. NIER–JOHNSON DOUBLE–FOCUSING
ION OPTICAL SYSTEM

repeller electrode pushes the ions out of the ionization chamber through the ion exit slit. The ions then pass through a region in which they are collimated by a lens system and are accelerated into the analyzer region of the spectrometer. The electrostatic analyzer does not separate ions according to their m/q ratio, but rather it is a velocity analyzer which allows ions of a given energy to travel to the magnet. This condition, in combination with the magnetic-sector mass analyzer, achieves the double-focusing condition in which ions of a given m/q ratio and homogeneous in kinetic energy are brought to the collector slit. The ion current is measured by a Faraday cup collector or a ten-stage electron multiplier calibrated for negative ions by the Faraday cup, and the signal is output to a Hitachi QPD 53 strip-chart recorder, a Honeywell 1706 Visicorder, or a PDP8/I digital computer.

Generation of a gas-phase ion in the mass spectrometer requires the collision of an electron with a molecule. In order to detect the existence of that ion, it must pass from the ion source to the collector without being destroyed by collision with an ion or neutral species, and this is accomplished by greatly reducing the total number of molecules present (e.g., by operating the instrument at reduced pressures). The mean free path of an ion is described as that distance which the ion may travel (on the average) without experiencing a collision with another particle. Since the ions must travel a distance of 159.2 cm in passing from the ion source to the collector, a mean free path of at least this magnitude is required to insure that no ions are lost in transit. Therefore the spectrometer must be operated at a pressure of 5×10^{-6} Torr or less since ions studied in these experiments have mean free paths of about

200 cm at this pressure.

Modifications for High Pressure Studies

The occurrence of ion-molecule reactions in a mass spectrometer involves the reactive collision of a primary ion, formed in the electron beam, with a molecule of the reactant gas while the two are still in the ionization chamber. Both primary and secondary ions are then analyzed in the mass spectrometer to give peaks at their respective m/q values. Since it is necessary that the ions pass from the ion source to the collector without undergoing collision, a pressure of less than 5×10^{-6} Torr is required in the analyzer region of the spectrometer. Reactive collisions must occur only in the ionization chamber, before the ion is accelerated into the analyzer region, if the mass analysis of secondary ions is to be accomplished under the same focusing conditions as primary ions. In order to provide a high-pressure region where collisions may occur and still maintain the low pressures required for mass analysis in the analyzer region of the instrument, it was necessary to differentially pump the ionization chamber envelope region with respect to the analyzer region of the spectrometer.

This was accomplished by construction of the high pressure ion source illustrated in Figure 3 and the differential pumping apparatus shown in Figure 4. The ion source region is separated from the analyzer region by a partition with a slit through which the ion beam enters the analyzer region. The envelope surrounding the ion source is pumped by a high speed (320 liters/second) oil diffusion pump which effectively removes gases which diffuse out of the ionization chamber. The ionization chamber is stainless steel and is constructed to minimize leaks into the envelope

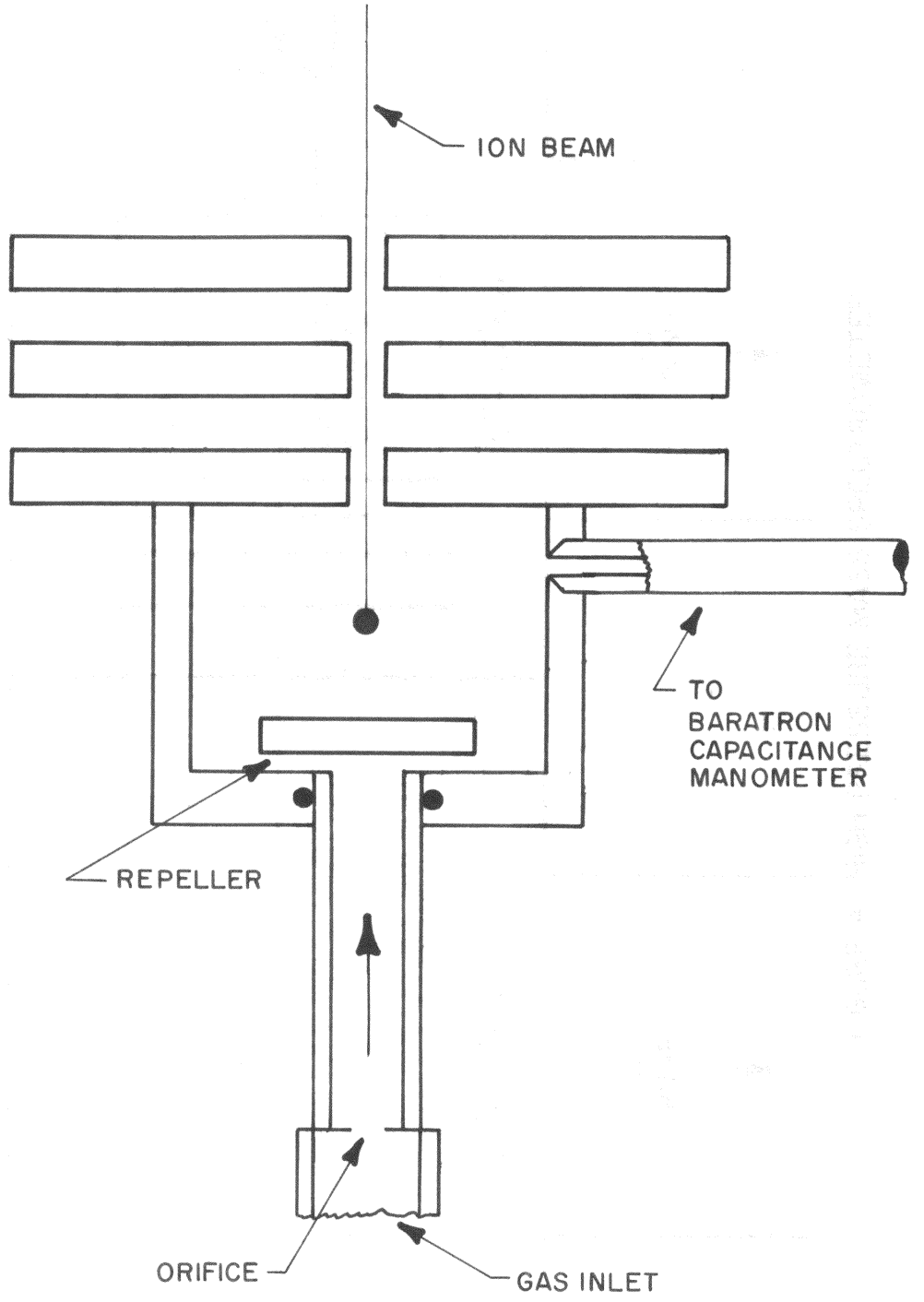

FIGURE 3. HIGH PRESSURE ION SOURCE

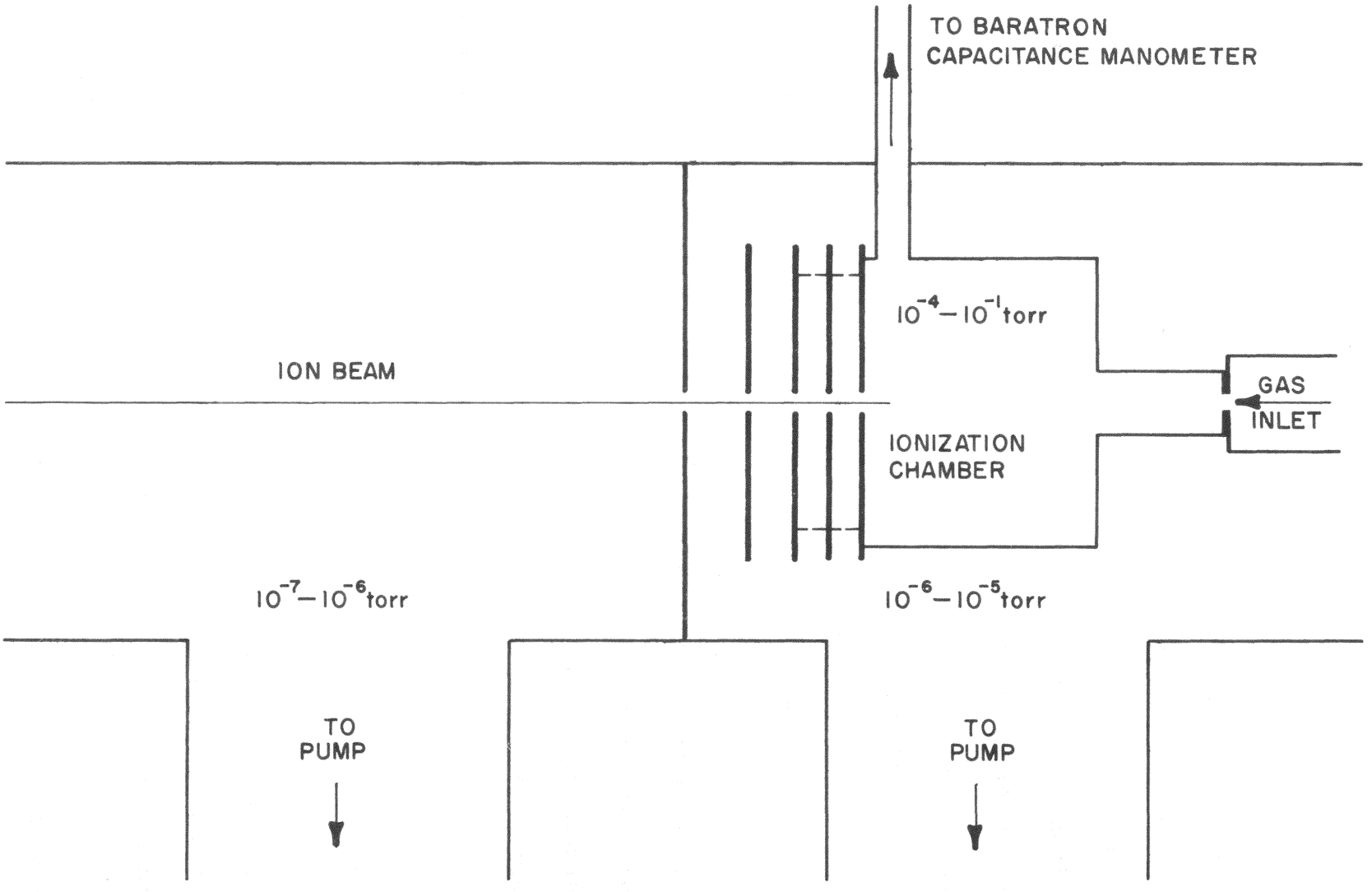

FIGURE 4. HIGH PRESSURE MASS SPECTROMETER

region. The gas inlet tube is fitted to the ion source block by a Viton O-ring so that gases cannot leak around the tube. The electron entrance slit (4.0 x 0.25 mm) and the ion exit slit (8.0 x 0.25 mm) are reduced in size from that normally used in this spectrometer. The electron target is electrically insulated from the ionization chamber by a Teflon gasket which also serves to prevent gas leakage through the electron exit slit. These changes limit diffusion of gases out of the ion source to the electron entrance slit and the ion exit slit. To facilitate the rapid removal of gases from the filament region, a filament grid of stainless steel mesh was used and the ion source assembly was positioned with the filament at the throat of the pumping system. Any ionic and/or neutral decomposition products resulting from pyrolysis on the filament are thus quickly removed from the ion source region.

The repeller electrode is a single electrode located 4.0 mm from the ion exit slit and 2.5 mm from the electron beam. Thus an ion formed in the electron beam travels 1.5 mm to reach the ion exit slit, and for a typical repeller field strength of 5 volts/cm the ion falls through a potential difference of 0.75 volt. To prevent field penetration into the ionization chamber from the lens and ion acceleration electrodes, the ion exit slit was covered with 80-90% transmittance stainless steel mesh. In an experiment to be discussed later, the reaction cross section for the reaction of Ar^+ with H_2 was measured as a function of repeller voltage, and the excellent agreement with previous studies indicates that field penetration into the ion source is insignificant and that measurements at low repeller voltages are valid.

The ion source may be operated at temperatures from 55° to 300° as

measured by a thermocouple attached directly to the ionization chamber. It is generally assumed that the gaseous sample is in thermal equilibrium with the ion source (68) and on this basis the temperature of the gas is taken as equal to the ion source temperature. Increasing the ion source temperature has two principal effects on mass spectra (68): (1) the intensities of all ions decreases and (2) the relative intensity of the parent ion decreases markedly. Investigation of the ratio of SF_6^-/SF_5^- ion currents as a function of temperature (69) has shown that the SF_6^- ion current is considerably diminished at higher temperatures. In order to minimize the influence of temperature on these studies, experiments were conducted at a common temperature of about 100°.

To extend the lifetime of the ion source and to reduce the probability of secondary electron formation on exposed metal surfaces, the ionization chamber surfaces and the repeller electrode were coated with a thin layer of colloidal carbon by painting these surfaces with Dag Dispersion #154. During the experiments no effects due to thermal decomposition of the compounds were detected, nor was there any evidence of deposits on the surfaces of the ion source due to reaction and/or decomposition.

When the nonmetal fluorides were introduced into the mass spectrometer, the ion source required extensive conditioning before consistent mass spectra could be obtained. This behavior has been reported by other workers (70) in investigations of inorganic fluorides, and presumably the erratic behavior results from reaction of the gas with the filament and other metal surfaces in the instrument. Until these surfaces are passivated, the ion signals vary unpredictably and the measured ion current

is not reproducible even over a short time span. Passivation of the instrument is accomplished by extended contact with the nonmetal fluoride, and the gas was allowed to flow through the instrument until consistent ion current measurements were obtained.

The length of time required for conditioning the instrument varied with the compound studied, with the phosphorus, boron, and silicon fluorides requiring about 1-2 hours. POF_3 required a conditioning period of about 3 hours, and PSF_3 and the arsenic fluorides required from eight to twelve hours before reproducible spectra were obtained.

Once the ion source was conditioned for a particular gas, subsequent experiments required no conditioning period unless a different compound was introduced into the instrument or unless the instrument was cleaned by evacuation at elevated temperature.

Determination of Pressure in the Ionization Chamber

The pressure in the ionization chamber was measured with an MKS Baratron Model 144 capacitance manometer which operates in the region of 10^{-5} to 1 Torr. The Baratron pressure head was connected to one side of the ionization chamber by about 10 mm of a 6 mm diameter stainless steel cone attached to a Kovar metal-to-glass tubing section. The glass tubing passes out of the ion source housing envelope through a Cajon Ultra-Torr O-ring fitting. A second Kovar metal-to-glass tube is attached to a 0.5" stainless steel bellows and copper tubing section which is welded directly to the pressure head coupling. The total length of tubing from the ion source to the pressure head is about one foot.

The pressure head of the Baratron contains a taut titanium metal diaphragm which separates the sample volume, at the pressure to be

measured, from a reference volume held at a constant pressure which is lower than that of the sample. Changes in the position of the metal diaphragm (caused by a change in pressure differential) are detected as a change in the capacitance across the diaphragm. Unlike McLeod gauge measurements, the Baratron pressure measurements are independent of the nature of the sample gas and accurate pressure readings for condensible vapors may be obtained.

The Baratron was calibrated for ion source pressure measurements using a gas of known absolute cross section for ionization by electrons of a specific energy (71). The positive ions formed in this gas are collected at the repeller electrode by applying a negative potential to the repeller, and the voltage drop across a precision resistor (681 KΩ $\pm$ 1%) is related by Ohm's law to the number of ions collected at the repeller electrode. The pressure of the gas can then be calculated using the relationship (50)

$$N_m = \frac{N_i}{Q_i N_e l_e} \tag{56}$$

where N_m is the number of neutral molecules per cubic centimeter, N_i is the number of ions collected per second, N_e is the number of electrons collected per second at the target, l_e is the electron beam path length, and Q_i is the absolute ionization cross section for the sample gas. The voltage drop across the resistor was measured by a Triplett Model 60 volt-ohmmeter with an input impedence of 11 megohm.

Another method used in calibrating the Baratron gauge was the comparison of pressure readings taken with the Baratron and McLeod gauge. Both pressure measuring devices were attached to the vacuum line manifold.

The pressure was measured with each device and readings compared.

The use of each of these calibration techniques revealed experimental difficulties with the reference vacuum supplied to the Baratron gauge. These experiments were conducted with the reference being merely an evacuated tube closed off by means of a vacuum stopcock. Results of the above two experiments demonstrated that this reference volume was not maintaining a constant pressure, and the apparatus was modified to include a separate pumping system which constantly evacuates the reference volume, giving more reproducible behavior for the Baratron gauge. Final calibration of the pressure measurements was then accomplished using the known cross sections for previously studied positive ion-molecule reactions.

Gases were introduced into the mass spectrometer from the dual inlet system shown in Figure 5. The gas storage bulbs provide a reservoir volume of approximately three liters for each gas, and a reservoir pressure of about 20-50 Torr provided a constant gas flow into the ion source for up to eight hours. Gases were delivered through two identical glass leaks into a common line connected to the mass spectrometer. Gas flow was controlled by Nupro stainless steel fine metering valves, and the partial pressure of each gas was measured using the Baratron gauge. The ionization chamber pressure was maintained in the 0.1-10 micron range in these experiments to reduce scattering of the electron beam. The ion source envelope pressure was maintained at about 10^{-6} - 10^{-5} Torr and the pressure in the analyzer region of the spectrometer was always less than about 2.0×10^{-6} Torr, as measured by an ionization gauge attached to the analyzer tube.

Examination of the compounds used in this work raises questions

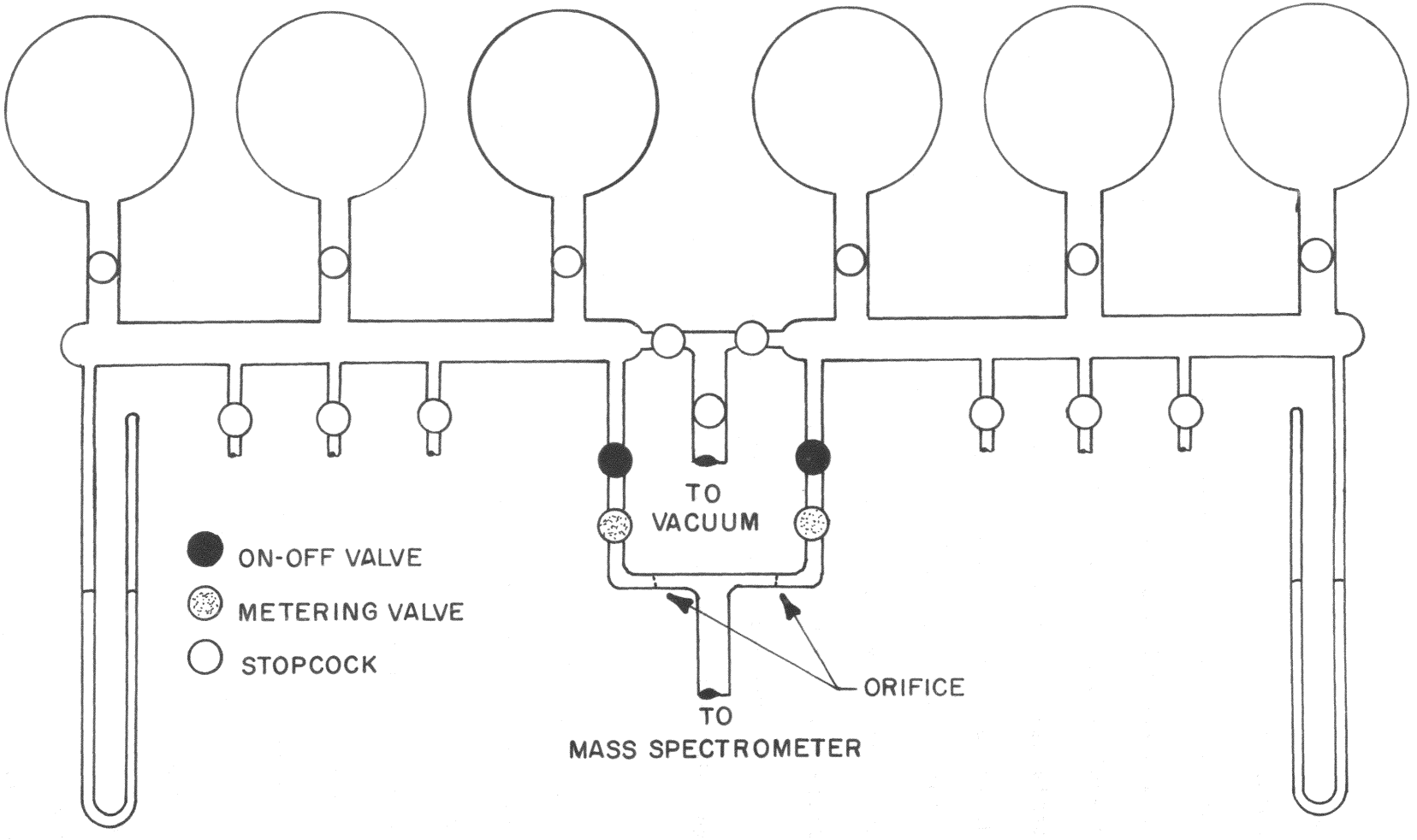

FIGURE 5. MASS SPECTROMETER DUAL INLET SYSTEM

concerning experimental difficulties encountered because of the dangerous and/or corrosive nature of these materials. With the single exception of sulfur hexafluoride, all of the compounds studied are to some extent toxic and sensitive to residual moisture, and PSF_3 is spontaneously flammable in air. Precautions were taken to prevent contamination of the laboratory with these gases during purification and transfer, and the pumping systems were vented to the hood exhaust. Vacuum lines in which these chemicals were handled were maintained moisture-free either by flaming the glass repeatedly during evacuation or by wrapping the vacuum line with heating tape which maintained the glass at about 100° during pumpdown. The mass spectrometer inlet system was kept dry by constant heating except when samples were being introduced into the spectrometer, and no peaks due to water were observed in the mass spectra nor was there any observable hydrolysis of the fluorides while in the inlet system.

Modifications of Electronic Circuits

In order to improve the precision with which the repeller electrode voltage and the electron energy could be controlled, the electronic circuits supplying these voltages were modified. Figure 6 shows the improved repeller electrode voltage supply in which the voltage source is a 67.5 V dry cell battery. A ten-turn potentiometer is used to select the voltage applied to the repeller electrode, and the available dynamic range is +8.0 to -8.0 volts relative to the ionization chamber.

Since contact potentials due to surface effects in the ion source can cause a shift in the effective repeller voltage experienced by the ions formed in the electron beam, zero volts on the repeller electrode was established by monitoring the SF_6^- ion current as the repeller voltage

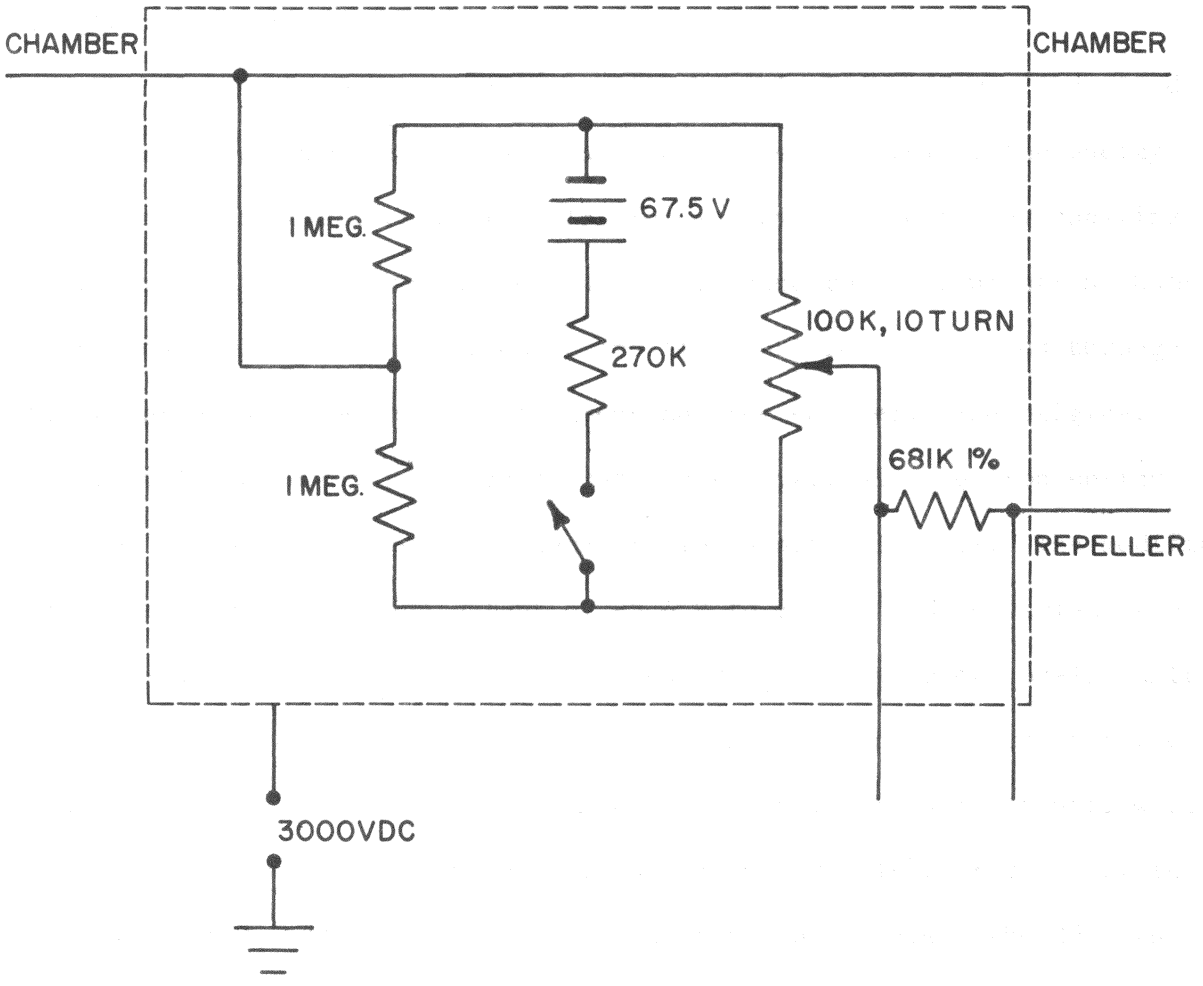

FIGURE 6. MODIFIED REPELLER VOLTAGE SUPPLY CIRCUIT

was changed from two to zero volts. As the repeller voltage reaches 0 volt, the measured ion current drops sharply since ions are no longer pushed out of the ion source into the accelerating region. The linearity of the voltage supply was confirmed by measuring the voltage supplied to the repeller over the entire range. The circuit was found to vary by less than five per cent from the expected output based on a calculated change of 1.60 volt/turn.

The electron energy control circuit shown in Figure 7 was installed in the mass spectrometer to enable a more precise control of the energy of the impacting electrons. The electron energy is selected by applying a negative voltage to the filament with reference to the ionization chamber so that the electrons formed at the filament are accelerated through the potential drop between the filament and the chamber. The original chamber voltage supply provided a continuously variable electron energy range of 0-150 V, selected by a ten-turn 10 KΩ potentiometer. The modified circuit provides a voltage output of -5.4 V to 20.8 V and is varied by a 10 KΩ 25-turn potentiometer which has less than one per cent non-linearity over the entire range. The voltage source is a bank of mercury batteries. A rotary switch allows the selection of either the original circuit, which is used for electron energies higher than about 20 volts, or the modified control circuit, which is used for low-energy experiments. The 25-turn potentiometer provides much smaller increments in the voltage range (1.08 volt/turn, compared to about 15 volt/turn in the original circuit) and the high linearity of the potentiometer and constant output of the mercury cells provide a scale of electron energy which is more reproducible and more precise than is available with the original circuit. The negative

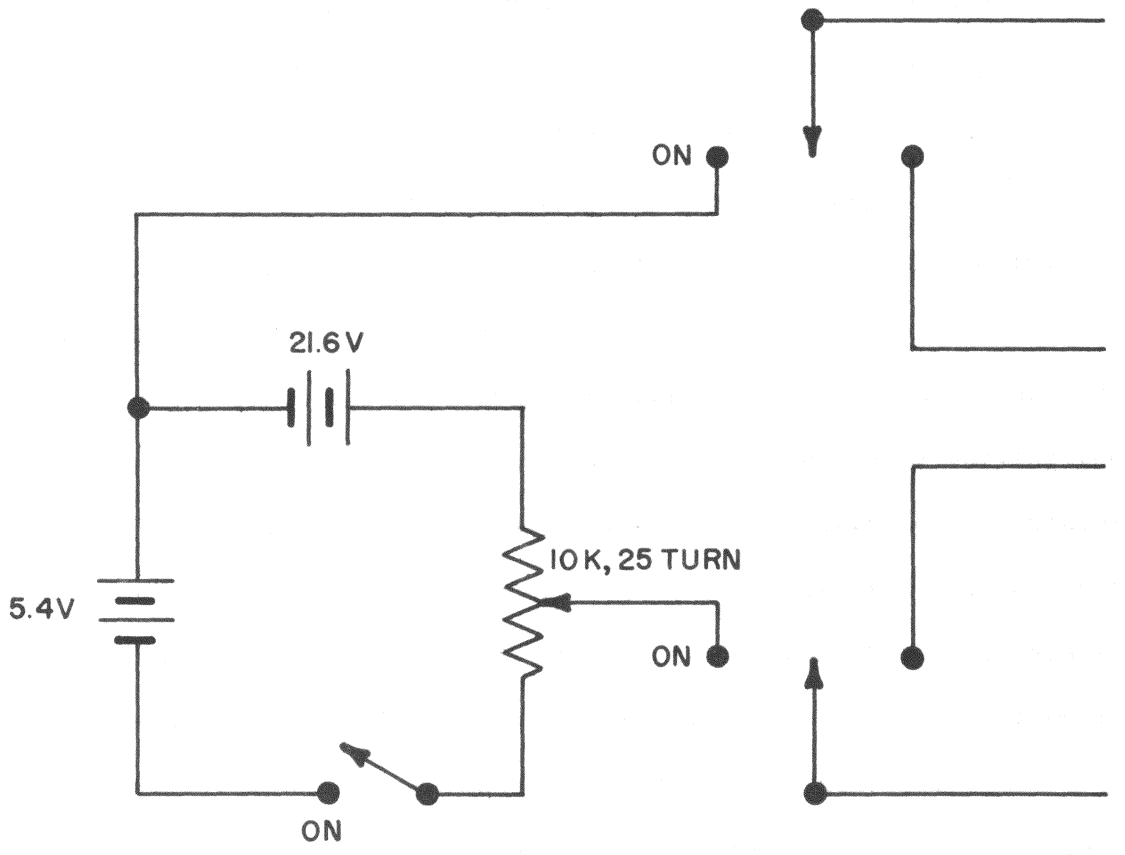

FIGURE 7. MODIFIED ELECTRON ENERGY SUPPLY CONTROL CIRCUIT

portion of the voltage range was included so that ionization efficiency curves for resonant electron capture processes could be measured over the entire resonance region.

Examination of the electron capture ionization efficiency curves for SF_6^- and SF_5^- shown in Figure 8 suggests that the ions are not formed at a single electron energy, but rather are formed by a distribution of electron energies. Ionizing electrons are produced from a heated filament and have appreciable thermal energies which are described by the Maxwellian distribution law. This distribution of thermal energies is imparted to the SF_6^- ions formed by resonance electron capture so that the SF_6^- ionization efficiency curve reflects the width of the thermal energy distribution on the electron beam (16).

The emission regulator circuit of the mass spectrometer maintains a constant level of electron emission under normal operation by varying the current supplied to the filament. Although this is desirable for obtaining mass spectra at high electron energies, it is necessary to maintain a constant filament current when studying low energy (near 0 eV) processes such as the formation of SF_6^- by resonant electron capture. Variation in the filament current during the measurement of ionization efficiency curves causes erratic changes in the SF_6^- ion current due to changes in the thermal energy distribution of the electron beam and in early experiments such behavior prompted the modification of the emission regulator circuit as shown in Figure 9. A mercury cell supplies a voltage to the tube grid so that no electrons are passed to the collector and the circuit is prevented from regulating the filament current as if there were a high level of emission. This circuit is of value for electron energies

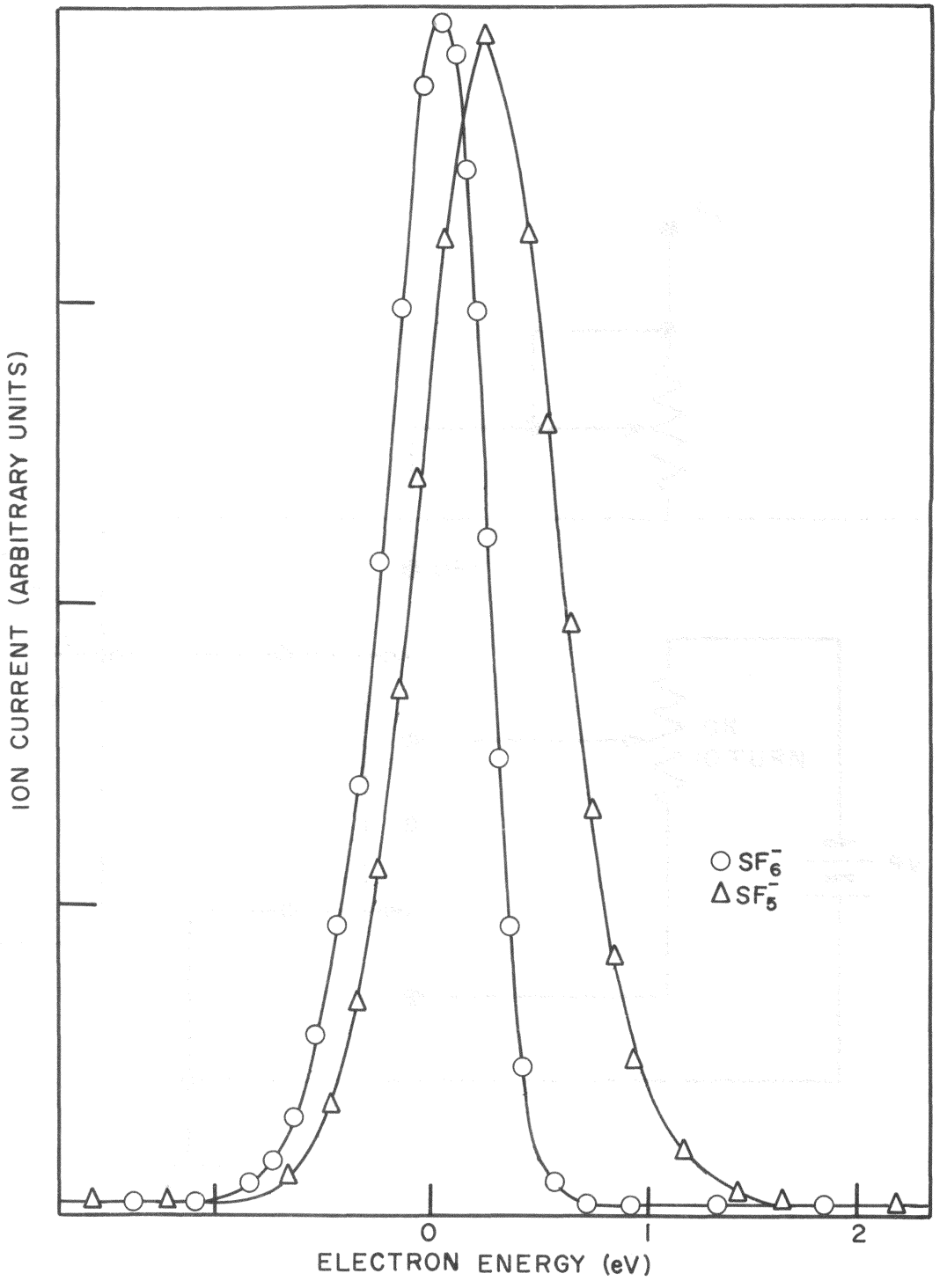

FIGURE 8. ELECTRON CAPTURE IONIZATION EFFICIENCY CURVES FOR SF_5^- AND SF_6^-

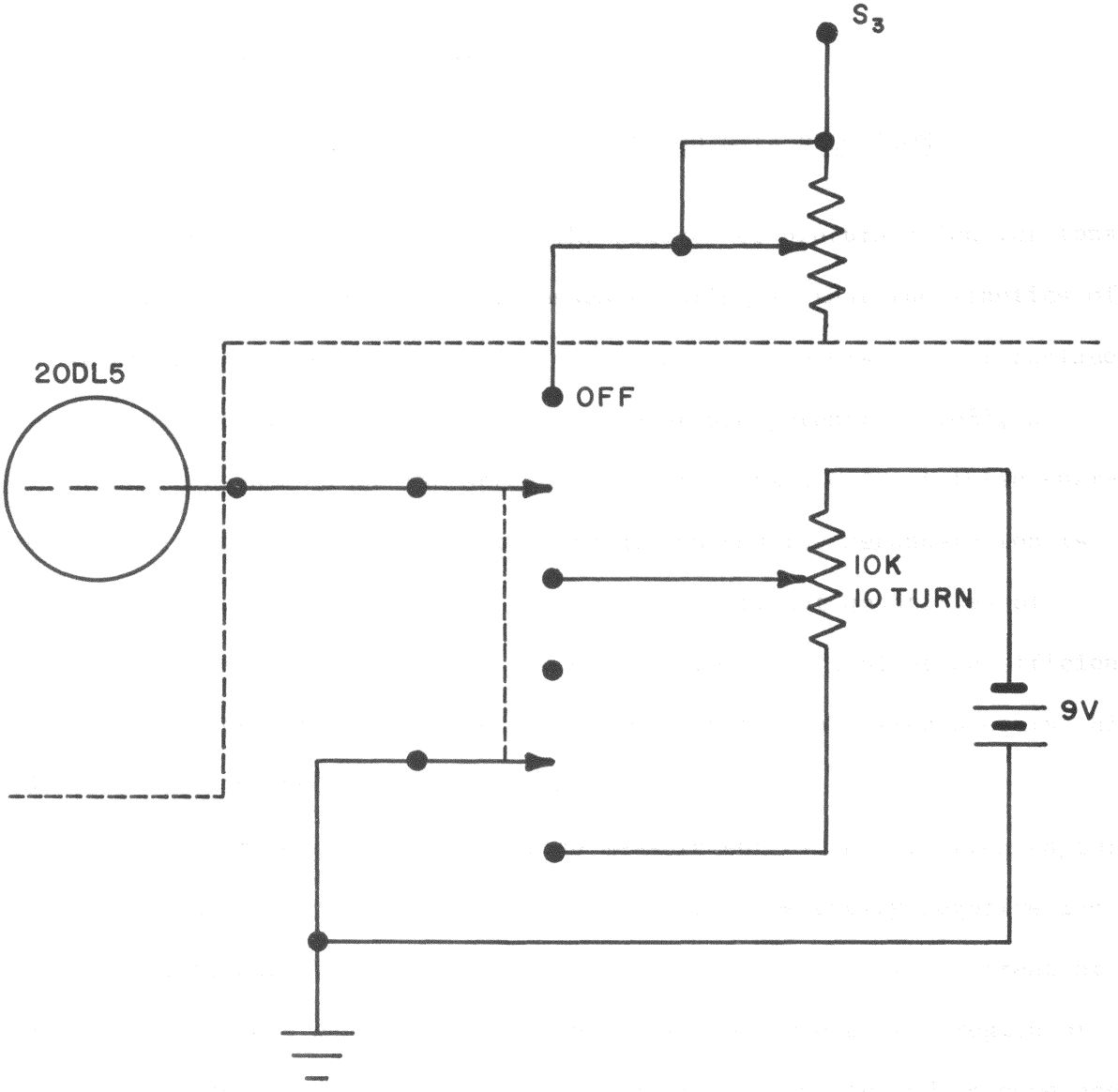

FIGURE 9. MODIFIED EMISSION STABILIZER CONTROL CIRCUIT

of 10-25 volts and for lower electron energies at high filament current. It has been found that for experiments conducted in the resonance capture region, a low filament current (about 2.8-3.0 A) is sufficient condition to prevent operation of the emission regulator circuit and thus provide a constant filament current. Under these conditions the emission stabilizer circuit is not used.

II. COMPUTERIZED DATA ACQUISITION AND DATA REDUCTION

Experimental identification of the primary or precursor ion (or ions) is necessary to understand the processes occuring so that the kinetics of the reaction may be evaluated using the proper parameters. The technique used in this study is that of matching appearance potentials (68), a method which assumes that the secondary ion is formed only at those energies at which the precursor ion is formed. Unless the secondary ion is formed by an endothermic process requiring significant quantities of kinetic or vibrational energy in the primary ion, the ionization efficiency curves of the primary and secondary ions will match, allowing unequivocal identification of the reaction process.

This procedure requires a precise measurement of the electron capture ionization efficiency curves for all ions in the low energy negative ion mass spectrum, and this is accomplished by monitoring the ion current of the respective ions as the electron energy is varied over the region of interest. Secondary ions are often of very low intensity and in some cases the signal-to-noise ratio even approaches unity. In order to measure these low intensity ion signals and to obtain ionization efficiency curves with the precision necessary for identification of the precursor ion, the mass

spectrometer was interfaced with a laboratory computer and the ion current signal was time averaged to give improved signal-to-noise ratios. In addition to improving the signal-to-noise ratio, the computerized data acquisition process has advantages which should not be overlooked. Measurement of ionization efficiency curves is accomplished quickly and with a higher degree of accuracy than is possible using the potentiometric recorder. The data are stored in the computer memory and can be operated on by software routines such as least-squares smoothing. Also, the ionization efficiency curves may be stored in the disk memory, enabling the instant recall of a particular curve for comparison with a newly determined one. Upon completion of the experiments, the accumulated data sets may be plotted on an X-Y recorder, and the data are output on punched paper tape as a permanent record.

Laboratory Computer

The computer used in this study was a Digital Equipment Corporation PDP-8/I with a core memory of 8192 twelve-bit data words. Bulk data storage devices available are a 32 K Type DF32 random access disk file and a Tennecomp TP-1351 magnetic tape data storage unit. The computer is equipped with a photoelectric high speed paper tape reader and a high speed paper tape punch, and graphical data are displayed on a Tektronix Type RM 503 oscilloscope and are plotted on a Hewlett-Packard Model 2D-2AM X-Y recorder.

The mass spectrometer was interfaced to the computer through a Digital Equipment Corporation AX08 Laboratory Peripheral Unit as shown in Figure 10. This unit has nine-bit signed digital-to-analog (DAC) and analog-to-digital (ADC) converters which handle digital information in

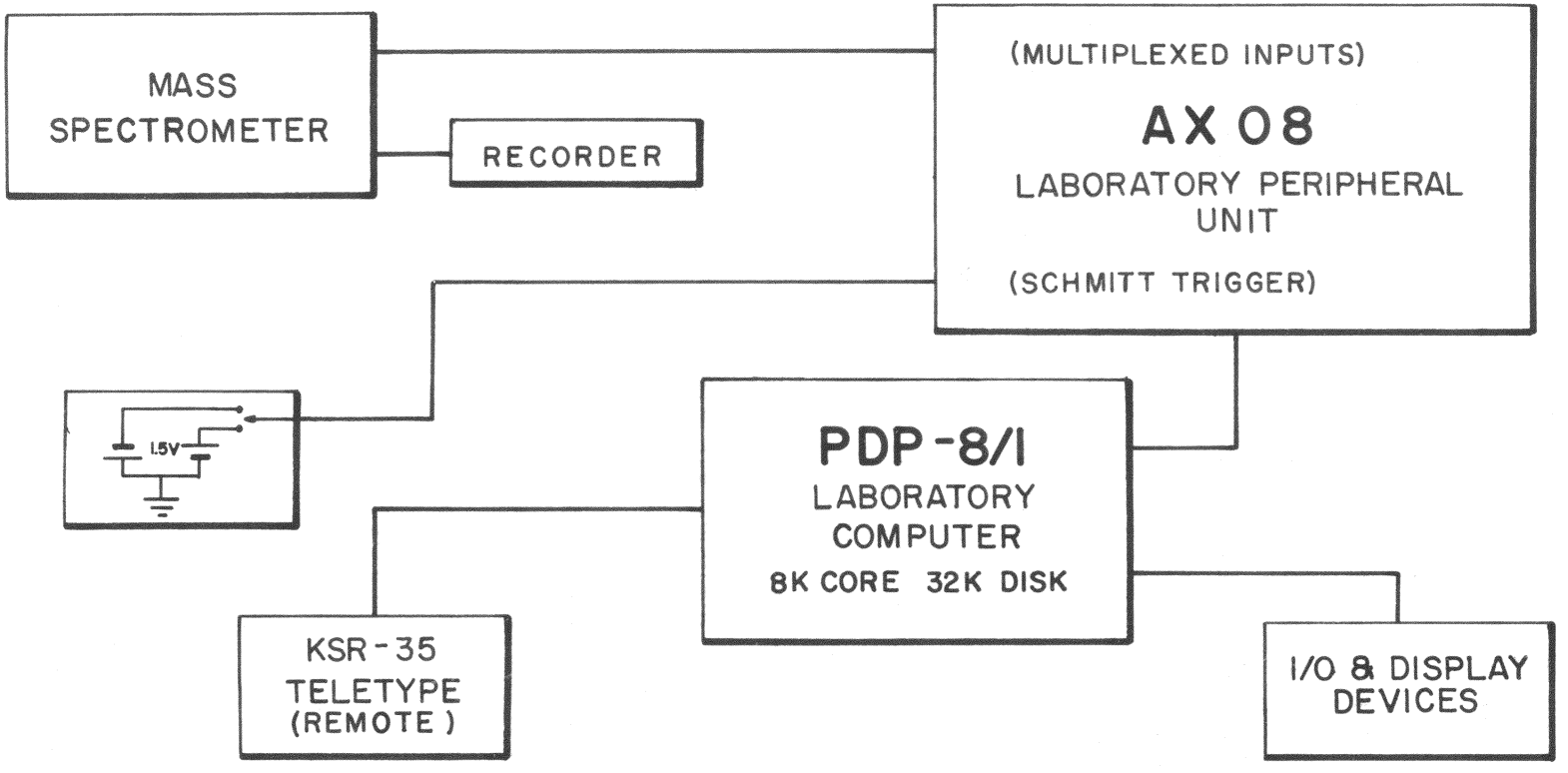

FIGURE 10. MASS SPECTROMETER - COMPUTER INTERFACE

the range -256 to +256 (Y axis) and 0 to 512 (X axis). Ion signals are input to software-selected multiplex channels which accept analog signals with dynamic ranges of ± 1.0 V, ± 125 mV, ± 16 mV, or ± 2 mV. The multiplexed input feeds a sample-and-hold register which in turn provides access to the ADC unit. The analog-to-digital conversion requires about 17 μsec for completion, so that the maximum sampling rate is about 58 kHz. The data acquisition was facilitated through use of the MADCAP IV (72) data acquisition program written by G. W. Dulaney and modified for use in this study by the author. This program is designed to sample and digitize the analog signal 2048 times, compute the average digital value, and store this value in core for later plotting and display. The program will take any number of data points up to the limit of core storage (about 1000 points), and the data acquisition is terminated by typing CTRL/C on the teletype. All other characters are ignored.

The data acquisition process is initiated by a pulse sent to a Schmitt trigger sensor in the AX08 which detects a change in the applied voltage level from a positive value to a voltage more negative than the reference level. This is accomplished by the arrangement of 1.5 V dry cells shown in Figure 10. Since no current is passed in the process of changing the voltage level, two size AA dry cells suffice as a voltage supply and the voltage level is switched from +1.5 V to -1.5 by closing the push-button switch shown in the diagram.

The ionization efficiency curves measured in this study were obtained through use of MADCAP IV, and since a large number of curves are ordinarily measured for any given experiment, MADCAP IV was modified to utilize disk files for on-line storage and allow remote operation of the computer

through the KSR-35 teletype. The electron energy was varied in increments of 0.05 eV, and the ionization efficiency curves were measured several times to insure that no instrumental artifacts were present in the curves. When necessary, the data sets were smoothed by an eleven-point least squares parabolic fit smoothing routine. Unless otherwise specified, all ionization efficiency curves presented here were measured at a repeller potentional of 2 V, and the ion currents for all ions were arbitrarily scaled to the same height for display purposes.

Calculations of the per cent ion current, reaction rate constants, and reaction cross sections were carried out using the laboratory computer and the FOCAL language programs listed in Appendix A. These studies were conducted at low electron energies where SF_6^- is formed via resonance electron capture, and the ion currents for all primary and secondary ions formed at this electron energy were measured using the Hitachi QPD 53 recorder. These measurements and the temperature, pressure, and repeller voltage were then combined using the relationship described in Appendix A to calculate the per cent ion current, the reaction rate constant, and the reaction cross section.

University Computing Center

In addition to the laboratory computer, an IBM System 360 (Model 65 and Model 50) computer was utilized for calculation of isotopic abundances of various ions which were observed in this study. These calculations were carried out using a FORTRAN IV program obtained from R. W. Kiser and R. E. Sullivan and modified for use on the Virginia Polytechnic Institute Computing Center System 360. Use was also made of a statistical program available at the VPI Computing Center for regression analysis of the cross

section data obtained for the reactions studied. This program is the "Biomedical Computer Programs" (73), BMD-05R, developed at the University of California at Los Angeles.

III. MATERIALS

The compounds used in these experiments were purchased from commercial sources with the exception of thiophosphoryl fluoride which was prepared using a method cited in the literature. Before use, all compounds were examined for purity by mass spectrometric analysis. Purification methods, where necessary, are described below. Table 1 lists the compounds of interest in these experiments. Several of the compounds listed are impurities found in the sample gases, and the boiling point and freezing point data (74) pertinent to these compounds and to the purification procedures followed are also tabulated here.

Sulfur hexafluoride and phosphorus pentafluoride were purchased from Matheson Gas Products and were used without further purification since mass spectrometric analysis revealed no detectable impurities. Phosphorus trifluoride and phosphoryl trifluoride, products of the Ozark-Mahoning Company, were also found to be of sufficient purity to be used as supplied by the manufacturer. The limit of detectability of impurities in these compounds is less than about 0.5% of the total sample. In 1:1 mixtures of SF_6 and nonmetal fluorides the secondary ions observed in these studies are formed in abundance approximately 0.01 that of SF_6^-, so that an impurity level of 0.5% is insignificant with respect to the measurements of secondary ion current.

Silicon tetrafluoride was obtained from Matheson Gas Products. Mass

TABLE I

COMPOUNDS OF INTEREST

Compound	Melting Point, °C	Boiling Point, °C	Principal Impurity
SF_6	-50.8	-63.8[a]	none
PF_3	-151.5	-101.15	none
PF_5	-93.8	-84.6	none
SiF_4	-90	-95[a]	hydrous oxide
BF_3	-127.1	-101.0	$BFCl_2$, BF_2Cl
POF_3	-68	-39.8	none
PSF_3	-148.8	-52.3	$PSFCl_2$, PSF_2Cl
AsF_3	-5.97	57.13	SiF_4
AsF_5	-79.8	-53.2	$AsOF_3$
$AsOF_3$	-68.3	25.6	
PSF_2Cl	-155.2	-6.3	
$PSFCl_2$	-96	-64.7	

[a]Sublimation temperature at 760 mmHg

spectrometric analysis revealed oxygen-containing impurities which presumably were formed by hydrolysis of the tetrafluoride, a reaction which is known of occur (75) slowly to produce hydrous oxides of silicon. These impurities were successfully removed by repeated trap-to-trap vacuum distillation of the tetrafluoride using a benzyl acetate slush bath (-52°) (76).

Boron trifluoride was also a Matheson product, and it contained impurities which were removed by trap-to-trap vacuum distillation before use. The principal impurities contained chlorine and were likely the mixed chloride-fluorides of boron, $BClF_2$ and BCl_2F, which are present in mixtures of BF_3 and BCl_3 due to hologen exchange (77,78).

Arsenic trifluoride and arsenic pentafluoride were obtained from the Ozark-Mahoning Company. The trifluoride is a liquid at room temperature and about 2 ml of liquid was transferred to 500 ml sample bulb prior to introduction into the mass spectrometer. The mass spectrum revealed the presence of significant amounts of SiF_4 and repeated distillations failed to remove this impurity. In fact, SiF_4 was not successfully removed from the sample until the AsF_3 was transferred under vacuum to a Hoke stainless steel cylinder and then repeatedly trap-to-trap distilled using a chloroform slush bath (-63°). Once the SiF_4 had been removed from the sample, no problems due to its recurrence were encountered even though vaporized samples were still introduced into the mass spectrometer through a glass inlet system. Apparently, the liquid AsF_3 etched the glass surface and caused the formation of the SiF_4.

The mass spectrum of arsenic pentafluoride contained ions which suggested the presence of arsenyl fluoride (79), $AsOF_3$, as an impurity. Although this compound has a much higher boiling point than AsF_5 the

much broader liquid range of $AsOF_3$ places the melting points of the two compounds quite close together and complicates the separation process. Repeated passes of the material through a U-tube cooled by a chloroform slush (-63°) resulted in gradual removal of $AsOF_3$ until the remaining AsF_5 was found to be of satisfactory purity for use in these studies.

Thiophosphoryl fluoride was prepared according to the procedure of Tullock and Coffman (80). One mole of NaF (Matheson, Coleman and Bell) was stirred in a three-necked round bottom flask containing about 100 ml of tetramethylene sulfone (tetrahydrothiophene -1, 1-dioxide, Eastman Organic Chemicals) as solvent. About 0.25 mole of thiophosphoryl chloride (Alfa Inorganics, Inc.) was slowly added from an addition funnel, and the system was evacuated and heated to about 150°. Impure PSF_3 was condensed in a trap cooled by liquid nitrogen (-195°) as it evolved from the solution, and the mixture was transferred to a vacuum line for subsequent purification. Principal impurities detected by mass spectrometric analysis were the mixed halides PSF_2Cl and $PSFCl_2$. The latter impurity was readily removed by trap-to-trap distillation using a chloroform slush (-63°), but the PSF_2Cl presented a more difficult problem since its boiling point is higher than that of the desired component and in addition its freezing point is lower. PSF_3 was almost entirely removed by many very slow passes through a trap cooled by a 1-nitropropane slush (-108°). This process was extremely tedious and resulted in loss of quantities of the desired compound, so another method of purification was used which gave more satisfactory results.

A quantity of the crude PSF_3 was sealed in a dry Pyrex tube along with NaF and the system was maintained at 100° for about three weeks. Analysis

of the gaseous residue revealed a quantitative yield of PSF_3 from PSF_2Cl, and this product was used in the experiments. Before measurements of the reactions of interest could be carried out with confidence, it was necessary to conduct several preliminary experiments to determine the degree of accuracy of kinetic data measured using this instrument.

IV. PRELIMINARY EXPERIMENTS

Preliminary experiments were conducted to evaluate the performance of the instrumentation and to serve as a calibration for pressure measurements. Comparisons of measured rate constants and cross sections with accepted literature values were utilized to establish the accuracy and repeatability of measurements obtained using the apparatus constructed for this study.

Evaluation of Experimental Apparatus

The performance of the high pressure ion source described earlier was evaluated by the measurement of reaction rates and cross sections for the well-characterized processes

$$CD_4^+ + CD_4 \rightarrow CD_5^+ + CD_3 \quad (57)$$

$$Ar^+ + H_2 \rightarrow ArH^+ + H \quad (58)$$

$$O^- + N_2O \rightarrow NO^- + NO \quad (59)$$

Reaction 57 has been extensively studied (28,56,81-86) and the rate constant for the formation of CD_5^+ was reported by Harrison, Ivko, and Shannon (85) to be 6.3×10^{-10} cm^3/molecule-sec at a repeller field strength of 10.5 volt/cm. Experiments with the high pressure mass spectrometer used for the present study yielded a rate constant of 7.1×10^{-10}

cm^3/molecule-sec for reaction 57. This measurement was conducted using a repeller field strength of 10 volt/cm.

The reaction of Ar^+ with hydrogen has also been investigated by many researchers (56,87-92). Stevenson and Schissler (89) have measured the reaction cross section for reaction 58 at various repeller voltages. A similar investigation of the Ar^+-H_2 reaction was carried out with the instrument used in this study and the results are compared with the data of Stevenson and Schissler. Figure 11 shows the variation of reaction cross section with $(d\ E)^{-1/2}$ as determined by Stevenson and Schissler (85) and by the author. The quantity (dE) is the product of repeller field strength (E) and the distance the primary ion travels in the ion source (d), and the reaction cross section is seen to vary as a linear function of $(\text{ion energy})^{-1/2}$.

The excellent agreement with accepted values for the experimental data obtained for these systems demonstrates that the high pressure mass spectrometer constructed for this study is capable of yielding reliable kinetic data for positive ion-molecule reaction systems. Since the experiments of interest in this study involve negative ions, reaction 59 was studied to determine the capabilities of the spectrometer for negative ion-molecule reaction studies.

Paulson (35,36) has studied reaction 59 and has reported a rate constant of 3.4×10^{-11} cm^3/molecule-sec for a repeller potential of 4.0 volts. Measurements by the author for reaction 59 yielded a rate constant of 3.14×10^{-11} cm^3/molecule-sec at the same repeller field strength used by Paulson. This agreement confirmed that the high pressure mass spectrometer is suitable for the study of negative ion-molecule reactions.

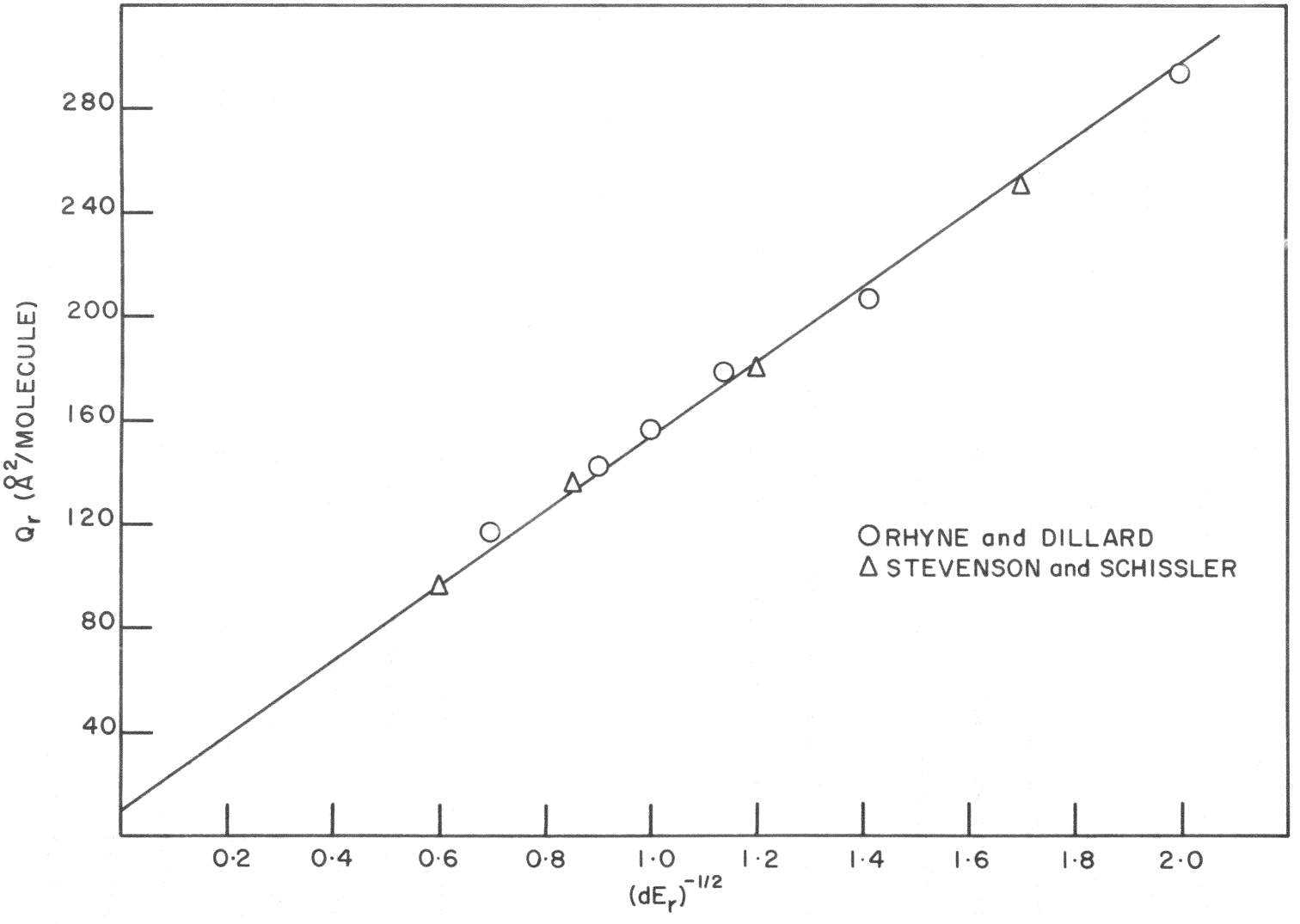

FIGURE 11. REACTION CROSS SECTION AS A FUNCTION OF ION ENERGY FOR THE REACTION $Ar^+ + H_2 \rightarrow ArH^+ + H$

Correction for Autodetachment of SF_6^-

The primary reactant ion in the SF_6^- -nonmetal fluoride systems studied here has been the subject of many mass spectrometric investigations, and Compton, Christophorou, Hurst, and Reinherdt (93) and others (94,95) have observed that SF_6^- is a "temporary negative ion" which spontaneously decomposes by loss of an electron. Since measurements of reactions involving SF_6^- as the primary ion are dependent on the number of SF_6^- ions present at the ion source exit slit, the measured ion current must be corrected for any loss of primary ions along the path from the ion source to the collector.

Two processes may contribute to the destruction of SF_6^- in the analyzer region of the spectrometer: collisional detachment

$$SF_6^- + M \rightarrow SF_6 + M + s \qquad (60)$$

and autodetachment

$$SF_6^- \rightarrow SF_6 + s^- \qquad (61)$$

Collisional detachment by a process such as reaction 60, where M is a bath molecule (either SF_6 or nonmetal fluoride), is probably not a significant pathway for destruction of SF_6^- in the low-pressure region of the mass spectrometer. The rate of collisional detachment for SF_6^- by xenon has been measured by Hasted and Beg (96) to be 2×10^{-15} cm^3/sec. Since it is likely that collision detachment by SF_6 or a nonmetal fluoride would not differ significantly from that by Xe, it is apparent that the collisional detachment process is insignificant. In addition, it is observed that for SF_6 alone, the SF_6^- ion current is a linear function of pressure of SF_6 over the pressure range used in these studies, and this

confirms that SF_6^- is not removed in the ion source by reaction 60 when M is SF_6. Similar behavior with nonmetal fluorides can reasonably be expected, and in all calculations it has been assumed that no SF_6^- has been lost due to collisional detachment.

Autodetachment, however, is a significant process for the loss of SF_6^- in the analyzer region of the spectrometer. The autodetachment half-life for SF_6^- has been measured by various methods as 10 μsec (94), 26 μsec (93), and 500 μsec (95). Klots (97) has evaluated these differences and has suggested that variation in ion source temperature and electron energy distributions contribute to this variation in lifetime measurements. Fehsenfeld (69) has studied the SF_6^-/SF_5^- ion current ratio as a function of temperature and has shown that the SF_6^- ion current decreases markedly at higher temperatures.

Since the measurement by Compton, Christophorou, Hurst, and Reinhardt (93) was obtained using experimental conditions similar to those of this study, their value of 26 μsec for the autodetachment lifetime was used for correction of the SF_6^- ion current. The SF_6^- ion flight time between acceleration and collection is of the order of 20 μsec in the mass spectrometer. A correction factor established from the autodetachment lifetime, the ion path length, and the ion accelerating voltage was applied to the measured SF_6^- ion current. The correction factors are 2.087 and 2.465 for accelerating voltages of 3.75 and 2.5 kV, respectively. Since the ion flight time varies with accelerating voltage, the appropriateness of the correction factor may be evaluated by comparison of reaction cross sections measured at different accelerating voltages while holding other experimental conditions constant. With the SF_6^- ion current corrected for

autodetachment the cross sections should show no dependence on accelerating voltage. Table II lists reaction cross sections for BF_4^- formation at two accelerating voltages and a series of repeller potentials. It is observed that consistant reaction cross sections are obtained at the accelerating voltages employed in these experiments, and the measured cross sections are found to be independent of the accelerating voltage. On the basis of the data in Table II the correction factor applied to the measured SF_6^- ion current is deemed reasonable.

If the correction factor applied here is inaccurate, then the calculated rate constants and cross sections will reflect the error in the correction for autodetachment. Overestimation of the correction factor will yield rate constants and cross sections smaller than the true values, whereas undercorrection for loss of SF_6^- due to autodetachment will give rate constants and cross sections which are too large. However, since the correction factor is not changed throughout this study, any error inherent in the calculated rate constants and cross sections does not affect the conclusions drawn from comparisons of relative values of rates and cross sections.

With the exception of AsF_5^- and SF_6^-, all other ions are even-electron ions with completed electron structures, and there is no reason to suspect that these ions might be destroyed by autodetachment in the low pressure region of the mass spectrometer. Therefore no correction factor was applied to the measured ion current for these ions. AsF_5^- may be lost by an autodetachment process since it is a radical anion like SF_6^-. However, since no facilities were available for confirming whether AsF_5^- is a temporary negative ion, no correction was applied to the AsF_5^- ion current,

TABLE II

REACTION CROSS SECTIONS FOR THE REACTION

$$SF_6^- + BF_3 \rightarrow BF_4^- + SF_5$$

AS A FUNCTION OF ACCELERATING VOLTAGE

Repeller Voltage (V)	Reaction Cross Section (A^2/molecule) Accelerating Voltage (KV)	
	3.75	2.50
2.0	74.5	73.9
2.5	56.4	57.3
3.0	54.4	56.7
3.5	46.0	46.9
4.0	47.5	51.2

and the abundance of AsF_5^- was taken as that measured at the collector. If AsF_5^- is indeed a temporary negative ion then the rate constants and cross sections calculated for formation of this ion are lower than the actual rates and cross sections.

CHAPTER IV

EXPERIMENTAL RESULTS

Investigations of the reactions of negative ions in solution have demonstrated the importance of negative ion-molecule reactions in explaining the chemical behavior of systems containing negative ions. The reactions of gaseous SF_6^- with nonmetal fluorides have been investigated in this study to provide information about the chemistry of negative ions and the mechanisms by which negative-ion reactions occur both in the gas phase and in solution.

Phosphorus pentafluoride was chosen as the neutral reactant in initial studies of fluoride ion transfer from SF_6^- since the expected product ion, PF_6^-, is well known in solution (17,18,19). Although PF_3 apparently does not accept a fluoride ion in solution to form PF_4^- (17), this molecule was studied to determine whether the PF_4^- ion might be formed in the gas phase.

I. PHOSPHORUS PENTAFLUORIDE AND PHOSPHORUS TRIFLUORIDE

The dominant negative ions observed in the mass spectra of PF_5 and PF_3 at low pressure were the F^- ion and the series of phosphorus-containing ions formed by successive loss of fluorine atoms. No parent negative ions were observed at any electron energy, and the fragment negative ions were observed at electron energies greater than about 10 eV. MacNeil and Thynne (45) have studied the negative ion mass spectrum of PF_3 and the lowest appearance potential for negative ion formation reported by these workers is 10.3 eV for PF_2^-.

In gaseous mixtures of SF_6 and PF_5 or PF_3 at low electron energies and high pressures in the mass spectrometer the secondary ions PF_6^- and PF_4^- are observed. These ions are not present at low electron energies in the low pressure negative ion mass spectra of either phosphorus fluoride-SF_6 mixtures or in the high pressure mass spectrum of pure PF_5 of PF_3. Therefore it appears that these ions are formed via negative ion-molecule reactions involving phosphorus-containing ions and/or negative ions produced from SF_6.

Ion-Molecule Reactions

Since no parent negative ions or fragment negative ions were observed at low electron energies for either PF_5 or PF_3, the formation of secondary ions by processes such as

$$PF_5^- + PF_5 \rightarrow PF_6^- + PF_4 \quad (62)$$

$$PF_3^- + PF_3 \rightarrow PF_4^- + PF_2 \quad (63)$$

$$PF_4^- + PF_5 \rightarrow PF_6^- + PF_3 \quad (64)$$

$$PF_2^- + PF_3 \rightarrow PF_4^- + PF \quad (65)$$

is eliminated. At low electron energies when a mixture of SF_6 and PF_5 or PF_3 was introduced into the ion source PF_6^- or PF_4^-, respectively, was detected. Since no other PF_x^- ions were detected, formation of the secondary ions by reactions involving fluorine atom abstraction from SF_6 such as reaction 66 is eliminated.

$$PF_5^- + SF_6 \rightarrow PF_6^- + SF_5 \quad (66)$$

The most abundant negative ions formed from sulfur hexafluoride are SF_6^- and SF_5^- (16) which have maxima in the electron capture ionization

efficiency curves at 0.08 and 0.16 eV, respectively. The fluoride ion has also been detected at near 0 eV, with the abundance of F^- being no greater than about 0.01 that of SF_6^- (98). Since the secondary ions are formed in abundance about 0.01 that of SF_6^- it is unlikely that F^- is the primary ion.

The secondary ions PF_6^- and PF_4^- appear in the energy region where the SF_6^- and SF_5^- are abundant. Ion molecule reactions which may explain the occurrence of the secondary ions are (using PF_5 as the example)

$$SF_6^- + PF_5 \xrightarrow{k_1} PF_6^- + SF_5 \tag{67}$$

$$SF_5^- + PF_5 \xrightarrow{k_1} PF_6^- + SF_4 \tag{68}$$

$$SF_6^- + PF_5 + M \xrightarrow{k_2} PF_6^- + SF_5 + M \tag{69}$$

$$SF_5^- + PF_5 + M \xrightarrow{k_2} PF_6^- + SF_4 + M \tag{70}$$

Reactions 67 and 68 are bimolecular processes involving the formation of the secondary ion and neutral SF_5 or SF_4, respectively, while reactions 69 and 70 are three-body processes involving collisional stabilization of the secondary negative ion.

The number of primary ions present will always be small compared to the number of neutral molecules, and reactions 67 and 68 may be treated as pseudo-first order reactions and reactions 69 and 70 become pseudo-second order. Expressions 71 and 72 represent the pressure dependence of the ion current ratio, $i_s/(i_s + i_p)$, for the first and second order dependence, respectively, at constant SF_6 pressure

$$\frac{i_s}{i_s + i_p} = k_1 t\ (PF_5) \tag{71}$$

$$\frac{i_s}{i_s + i_p} = k_2 t\ (PF_5)\ (M) \tag{72}$$

where (PF_5) is the concentration of PF_5 and (M) is the concentration of a bath molecule, either SF_6 or PF_5, which is involved in collisional stabilization. If it is assumed that SF_6 and PF_5 are equally efficient as bath molecules, a plot of ion current ratio as a function of PF_5 pressure at constant SF_6 pressure should lead to an identification of the order of the reaction. A plot of ion current ratio as a function of PF_5 pressure is given in Figure 12 and the observed pressure variation is in agreement with the prediction of equation 71, confirming that the process observed is a simple bimolecular reaction. Similar results were obtained for the SF_6-PF_3 system.

The primary reactant ion, SF_6^- or SF_5^-, was identified by the method of matching ionization efficiency curves. Figure 13 shows the electron capture ionization efficiency curves for SF_6^-, SF_5^-, and PF_6^-, determined for a mixture of SF_6 and PF_5 in the mass spectrometer. The correspondence of the ionization efficiency curves for PF_6^- and SF_6^- identifies reaction 67 as the process leading to the formation of PF_6^-. Similar results were obtained for PF_4^-, indicating that the secondary ions are formed by transfer of a fluoride ion from SF_6^- to the nonmetal fluoride according to the general reaction

$$SF_6^- + AF_n \rightarrow \left[AF_{n+1}\right]^- + SF_5 \qquad (73)$$

Reaction Rate Constants and Reaction Cross Sections

Having identified the process by which the secondary ions are formed, the kinetics of the fluoride ion transfer were investigated. The ion current of all ions in the low energy mass spectrum were measured as a function of repeller voltage and at various partial pressures of nonmetal fluoride and SF_6. Reaction rate constants and cross sections were

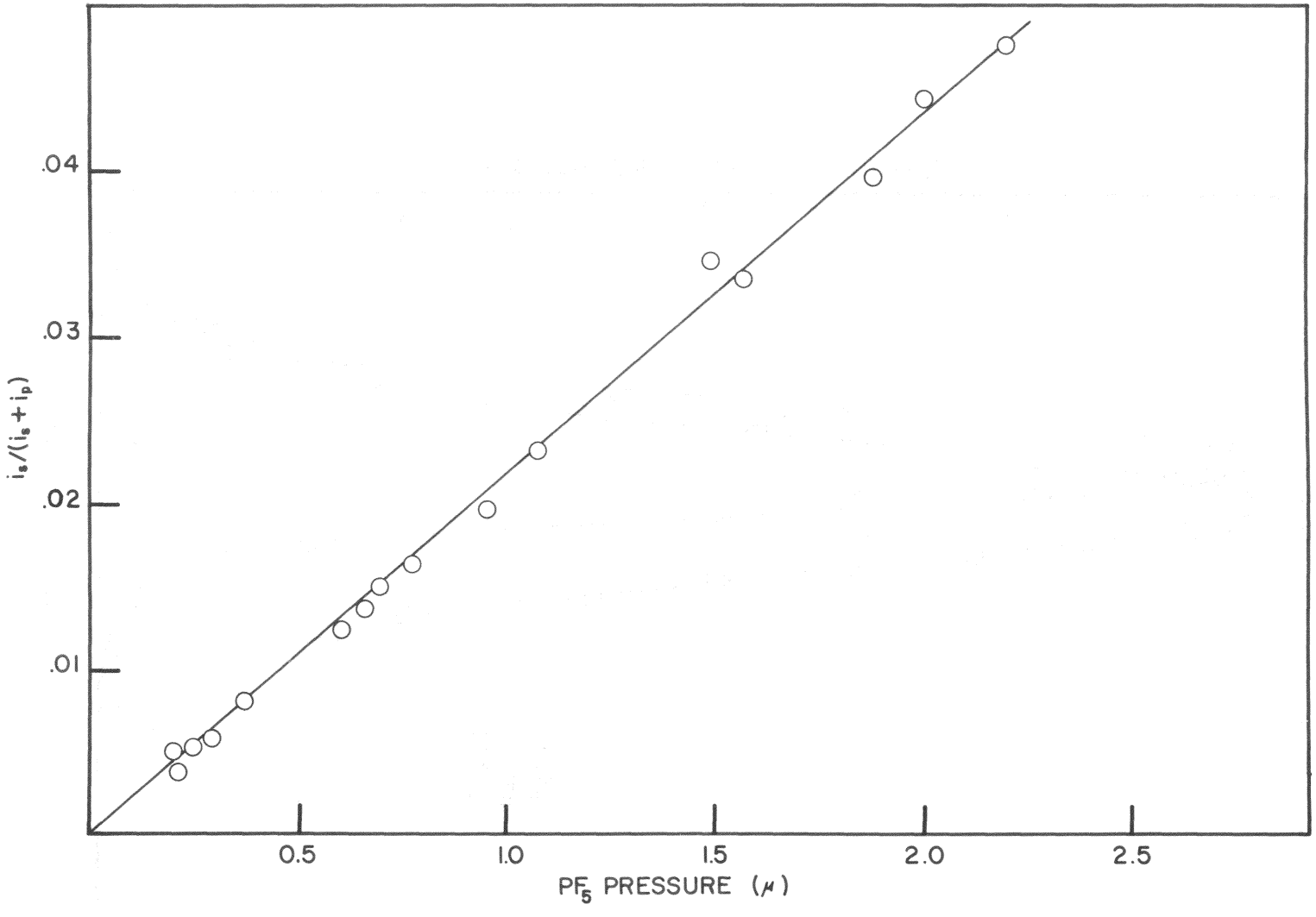

FIGURE 12. ION CURRENT RATIO AS A FUNCTION OF PF_5 PRESSURE

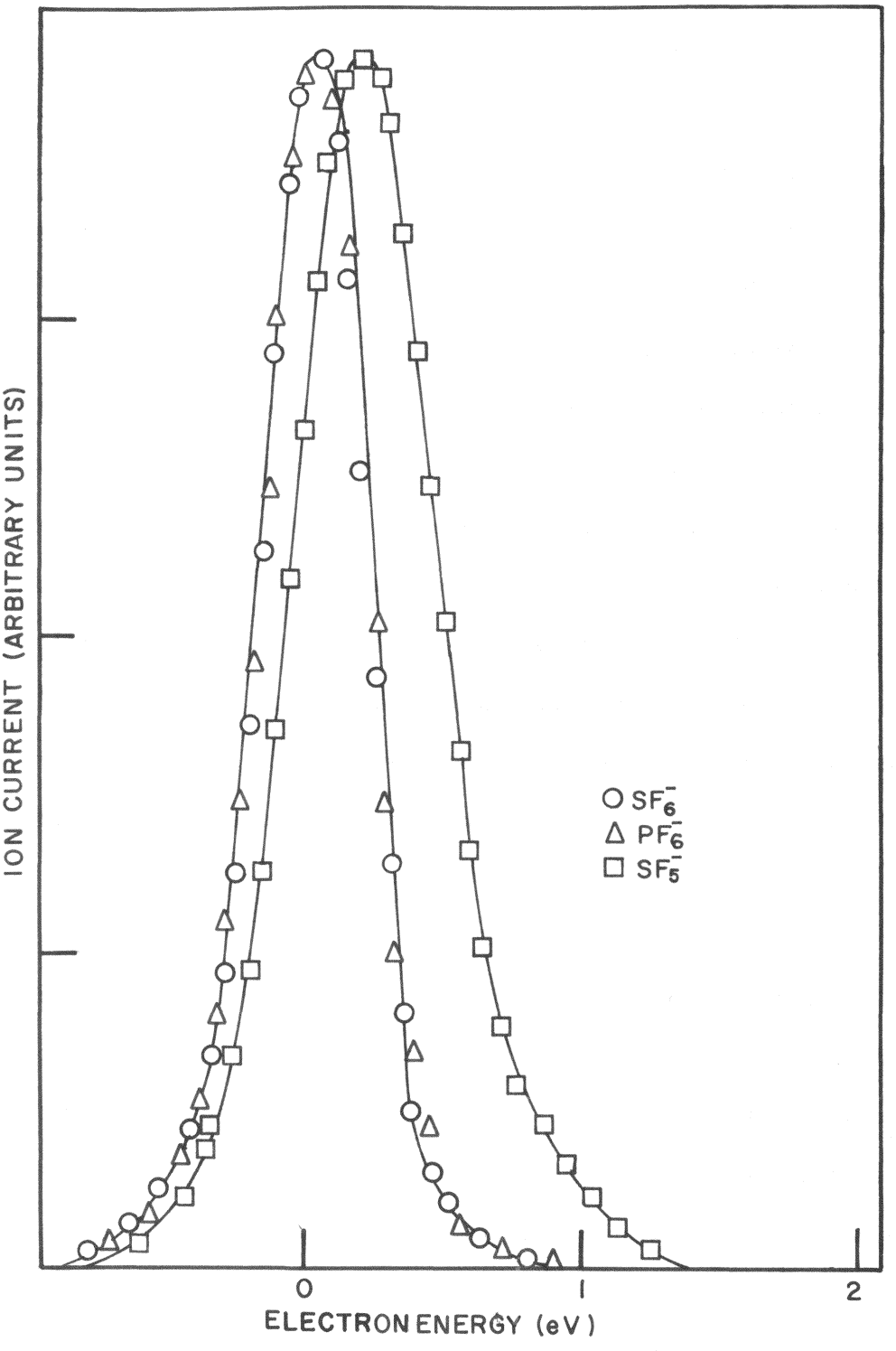

FIGURE 13. IONIZATION EFFICIENCY CURVES FOR SF_6^-, SF_5^- AND PF_6^-

calculated using the relationships discussed earlier employing the computer program listed in Appendix A. Values obtained are presented in Tables III and IV.

The rate constant for fluoride ion transfer to PF_5 to form PF_6^- at a repeller field of 2.0 volts is 1.59×10^{-10} cm^3/molecule-sec, indicating that this reaction is much faster than are typical free radical reactions. This extremely fast rate of reaction is characteristic of ion-molecule reactions and is a factor which dictates their consideration as important processes in any system containing gaseous ions.

The observation of fluoride ion transfer to the phosphorus fluorides suggested a general reaction which would enable studies of many inorganic systems which might produce fluoro-anions. Since the BF_4^- and SiF_5^- anions are well known in condensed phases (18,19,99,100), boron trifluoride and silicon tetrafluoride were chosen as reactants for subsequent studies of negative ion-molecule reactions with SF_6^-.

II. BORON TRIFLUORIDE AND SILICON TETRAFLUORIDE

The low-pressure negative ion mass spectra of BF_3 and SiF_4 exhibit no molecular ion formation, and no negative ions were formed at electron energies less than approximately 10 eV. When BF_3 is introduced into the mass spectrometer the negative ions BF_2^- and F^- dominate the spectrum and F_2^- is observed in low abundance. This is in agreement with the previously reported (45) negative ion mass spectrum of BF_3. Silicon tetrafluoride also forms only fragment negative ions in the mass spectrometer, and again no ions were observed below 10 eV. MacNeil and Thynne (46) have observed the formation of the negative ions F^-, SiF_3^-, and F_2^- in SiF_4 at

TABLE III

REACTION RATE CONSTANTS FOR THE FORMATION OF SECONDARY IONS AS A FUNCTION OF REPELLER VOLTAGE FOR THE REACTIONS

$$SF_6^- + PF_5 \rightarrow PF_6^- + SF_5$$

$$SF_6^- + PF_3 \rightarrow PF_4^- + SF_5$$

Repeller Voltage	Rate Constant (X 10^{10} cm^3/molecule-sec.) Secondary Ion	
(V)	PF_6^-	PF_4^-
1.5	1.48	0.167
2.0	1.59	0.143
2.5	1.59	0.145
3.0	1.57	0.116
3.5	1.64	0.111
4.0	1.64	0.112

TABLE IV

REACTION CROSS SECTIONS FOR THE FORMATION OF SECONDARY IONS AS A FUNCTION OF REPELLER VOLTAGE FOR THE REACTIONS

$$SF_6^- + PF_5 \rightarrow PF_6^- + SF_5$$

$$SF_6^- + PF_3 \rightarrow PF_4^- + SF_5$$

Repeller Voltage	Cross Section (A^2/molecule) Secondary Ion	
(V)	PF_6^-	PF_4^-
1.5	34.4	3.88
2.0	31.9	2.88
2.5	28.5	2.60
3.0	25.7	1.89
3.5	24.9	1.68
4.0	23.3	1.59

low pressures, with no ions detected below 10 eV.

Ion-Molecule Reactions

The high pressure negative ion mass spectra of BF_3 and SiF_4 exhibit fragment negative ions formed only at electron energies greater than about 10 eV. No molecular negative ions (i.e., BF_3^- of SiF_4^-) were detected in either the spectra of the pure gases or spectra of mixtures with SF_6. MacNeil and Thynne (45,46) have observed the formation of the secondary ions BF_4^- and SiF_5^- in pure BF_3 and SiF_4, respectively, by the ion-molecule reactions 74 and 75 at high pressures.

$$F_2^- + BF_3 \rightarrow BF_4^- + F \qquad (74)$$

$$SiF_3^- + SiF_4 \rightarrow SiF_5^- + SiF_2 \qquad (75)$$

The appearance potentials for the primary and secondary ions in these reactions are all reported to be 10.5 eV, measured relative to the formation of O^- from CO at 0.65 eV. These workers report no ion formation at less than 10 eV, and in this study no ions containing boron or silicon were detected at low electron energies when pure BF_3 or SiF_4 was introduced into the mass spectrometer at high pressures.

When SF_6 was added to BF_3 or SiF_4 in the ion source at high pressures the secondary ions BF_4^- and SiF_5^-, respectively, were detected at near 0 eV electron energies where ions from SF_6 are abundant. Since no BF_x^- or SiF_x^- ions were detected at low electron energies in pure BF_3 or SiF_4, ion-molecule reactions involving negative ions formed from BF_3 or SiF_4 are excluded from consideration for the formation of secondary ions at near-zero electron energies.

Examination of the electron capture ionization efficiency curves

shown in Figure 14 for ions detected at low electron energies in mixtures of SF_6 and BF_3 indicates that formation of the secondary ion BF_4^- occurs by fluoride ion transfer according to reaction 73. SF_6^- is identified as the primary ion by the matching ionization efficiency curves for SF_6^- and the secondary ion BF_4^-. Ionization efficiency curves obtained for ions in the SF_6-SiF_4 system show that the secondary ion SiF_5^- is also formed via fluoride ion transfer from SF_6^-.

The plot of ion current ratio as a function of SiF_4 pressure shown in Figure 15 confirms that SiF_5^- is formed by a simple bimolecular process. The linear dependence on pressure of neutral reactant is the expected behavior for a pseudo-first order reaction as predicted by equation 67. The ion current ratio for BF_4^- likewise exhibits a linear dependence on BF_3 pressure. Therefore it is concluded that the secondary ions BF_4^- and SiF_5^- are formed by a fluoride ion transfer process involving bimolecular collision with SF_6^- according to the reactions

$$SF_6^- + BF_3 \rightarrow BF_4^- + SF_5 \qquad (76)$$

$$SF_6^- + SiF_4 \rightarrow SiF_5^- + SF_5 \qquad (77)$$

Reaction Rate Constants and Reaction Cross Sections

The reaction rate constants and cross sections for the formation of secondary ions by reactions 76 and 77 were calculated from the measured parameters using the computer program listed in Appendix A. Rate constants and cross sections for a series of repeller voltages are presented in Table V and VI. The magnitude of the reaction cross section indicates that both BF_3 and SiF_4 accept a fluoride ion more readily than do the phosphorus fluorides.

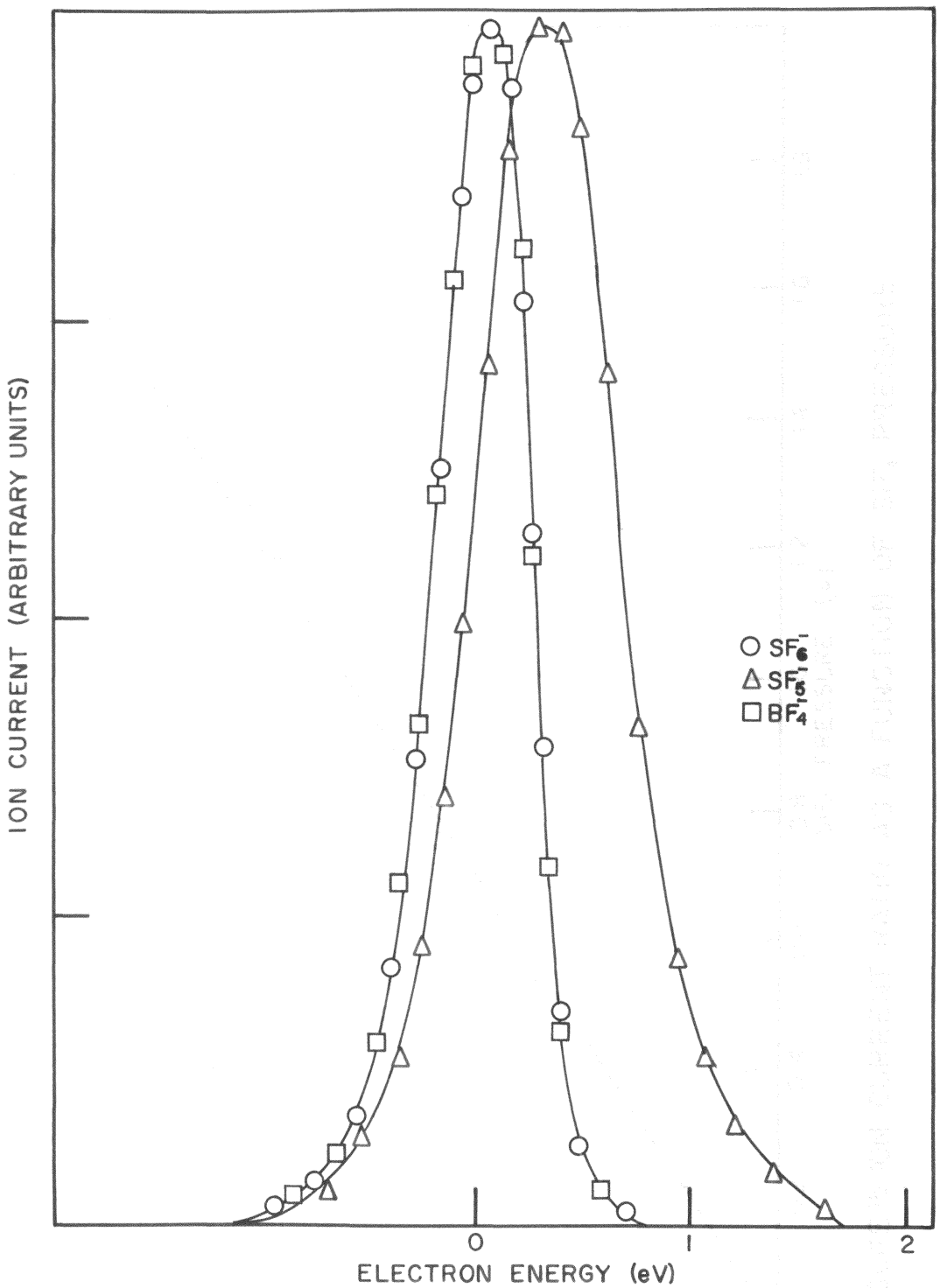

FIGURE 14. IONIZATION EFFICIENCY CURVES FOR SF_6^-, SF_5^- AND BF_4^-

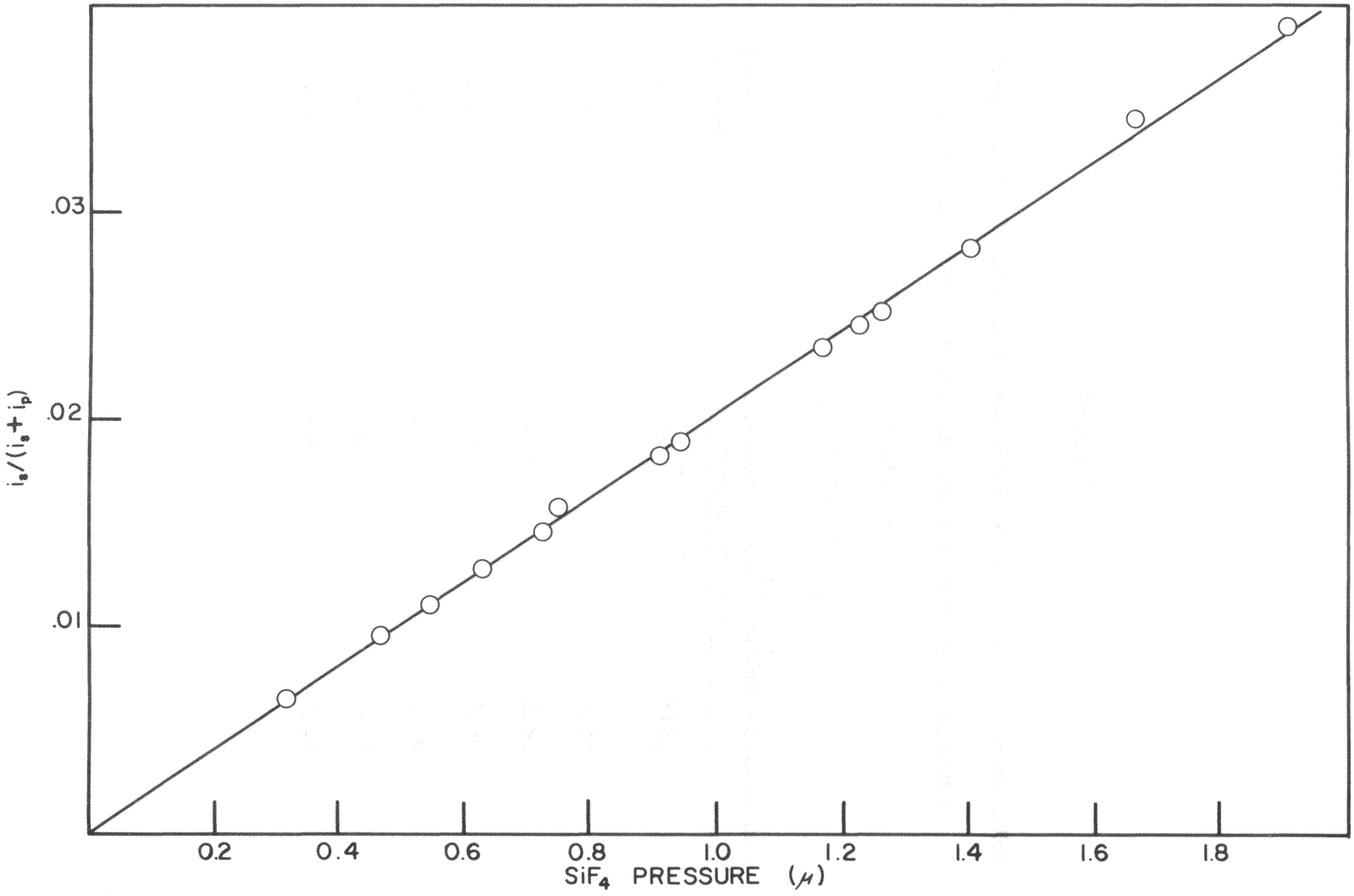

FIGURE 15. ION CURRENT RATIO AS A FUNCTION OF SiF_4 PRESSURE

TABLE V

REACTION RATE CONSTANTS FOR THE FORMATION OF SECONDARY IONS AS A FUNCTION OF REPELLER VOLTAGE FOR THE REACTIONS

$$SF_6^- + BF_3 \rightarrow BF_4^- + SF_5$$

$$SF_6^- + SiF_4 \rightarrow SiF_5^- + SF_5$$

Repeller Voltage	Rate Constant (X 10^{10} cm^3/molecule-sec.) Secondary Ion	
(V)	BF_4^-	SiF_5^-
1.5	3.17	2.97
2.0	3.68	2.81
2.5	3.19	2.90
3.0	3.45	3.06
3.5	3.09	3.11
4.0	3.60	3.44

TABLE VI

REACTION CROSS SECTIONS FOR THE FORMATION OF SECONDARY IONS AS A FUNCTION OF REPELLER VOLTAGE FOR THE REACTIONS

$$SF_6^- + BF_3 \rightarrow BF_4^- + SF_5$$

$$SF_6^- + SiF_4 \rightarrow SiF_5^- + SF_5$$

Repeller Voltage	Cross Section (A^2/molecule) Secondary Ion	
(V)	BF_4^-	SiF_5^-
1.5	73.6	68.8
2.0	73.9	56.5
2.5	57.3	52.1
3.0	56.7	50.1
3.5	46.9	47.2
4.0	51.2	48.8

In order to determine the effects of hetero atoms on the rates of fluoride ion transfer processes, the reactions of SF_6^- with phosphoryl fluoride, POF_3, and thiophosphoryl fluoride, PSF_3, were studied. The hetero atom effectively replaces two fluorine atoms in the bonding sphere of pentavalent phosphorus, so that POF_3 and PSF_3 have different coordination numbers than PF_5. The substituted phosphorus fluorides also differ from PF_5 with respect to structure, polar character, and polarizability, and an examination of the rates of fluoride ion transfer to these molecules should reveal the effects of these differences on reactivity.

III. PHOSPHORYL FLUORIDE AND THIOPHOSPHORYL FLUORIDE

When pure POF_3 and PSF_3 were introduced into the mass spectrometer at low pressure, only the F^- ion was observed at electron energies greater than 10 eV. No ions were detected in the low energy region near 0 eV at low pressures, and similar behavior was observed for the high pressure negative ion spectra at low energies. Upon addition of SF_6 to the nonmetal fluoride in the mass spectrometer, secondary ions were observed in the electron energy region where SF_6^- and SF_5^- are formed by resonance electron capture. This behavior is analogous to that already described for the fluorides of phosphorus, boron, and silicon.

Ion-Molecule Reactions

Since the secondary ions POF_4^- and PSF_4^- are not observed in the high pressure mass spectra of pure POF_3 and PSF_3, an ion-molecule reaction with ions formed from SF_6 is suggested. Figure 16 shows ionization efficiency curves for the ions observed at low electron energies for mixtures of SF_6

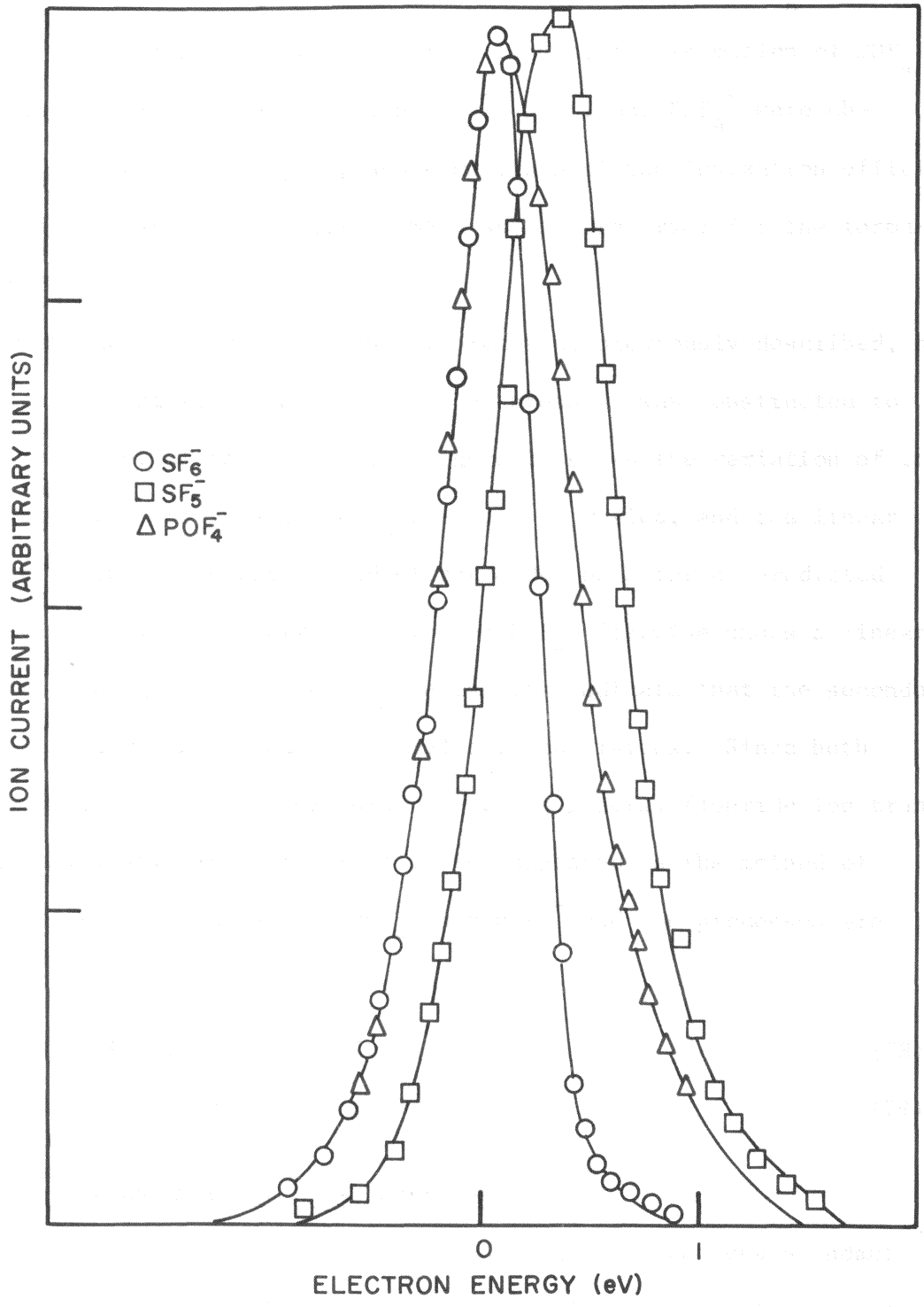

FIGURE 16. IONIZATION EFFICIENCY CURVES FOR SF_6^-, SF_5^- AND POF_4^-

and POF_3, and the matching ionization efficiency curves for SF_6^- and POF_4^- confirms that SF_6^- is the precursor ion for the formation of POF_4^-. For mixtures of SF_6 and PSF_3 the ions SF_6^-, SF_5^-, and PSF_4^- were observed at low electron energies, and comparison of the ionization efficiency curves for these ions identified SF_6^- as the precursor for the formation of PSF_4^-.

As with the fluoride ion transfer processes previously described, a plot of ion current ratio as a function of pressure was constructed to identify the order of the reaction. Figure 17 shows the variation of ion current ratio for PSF_4^- as the PSF_3 pressure is varied, and the linear dependence is in accord with pseudo-first order behavior as predicted by equation 71. The ion current ratio for POF_4^- likewise shows a linear dependence on POF_3 pressure, and these results indicate that the secondary ions are formed via bimolecular ion-molecule collisions. Since both systems involve SF_6^- as the precursor ion, the general fluoride ion transfer process illustrated by reaction 73 is suggested as the method of formation of the secondary ions POF_4^- and PSF_4^- and the processes are given as

$$SF_6^- + PSF_3 \rightarrow PSF_4^- + SF_5 \qquad (78)$$

$$SF_6^- + POF_3 \rightarrow POF_4^- + SF_5 \qquad (79)$$

Reaction Rate Constants and Cross Sections

The secondary ions formed in POF_3 and PSF_3 are much less abundant than those formed in BF_3, SiF_4 and PF_5, indicating that the tendency to accept a fluoride ion is less than that for the fluorides of boron, silicon, and phosphorus.

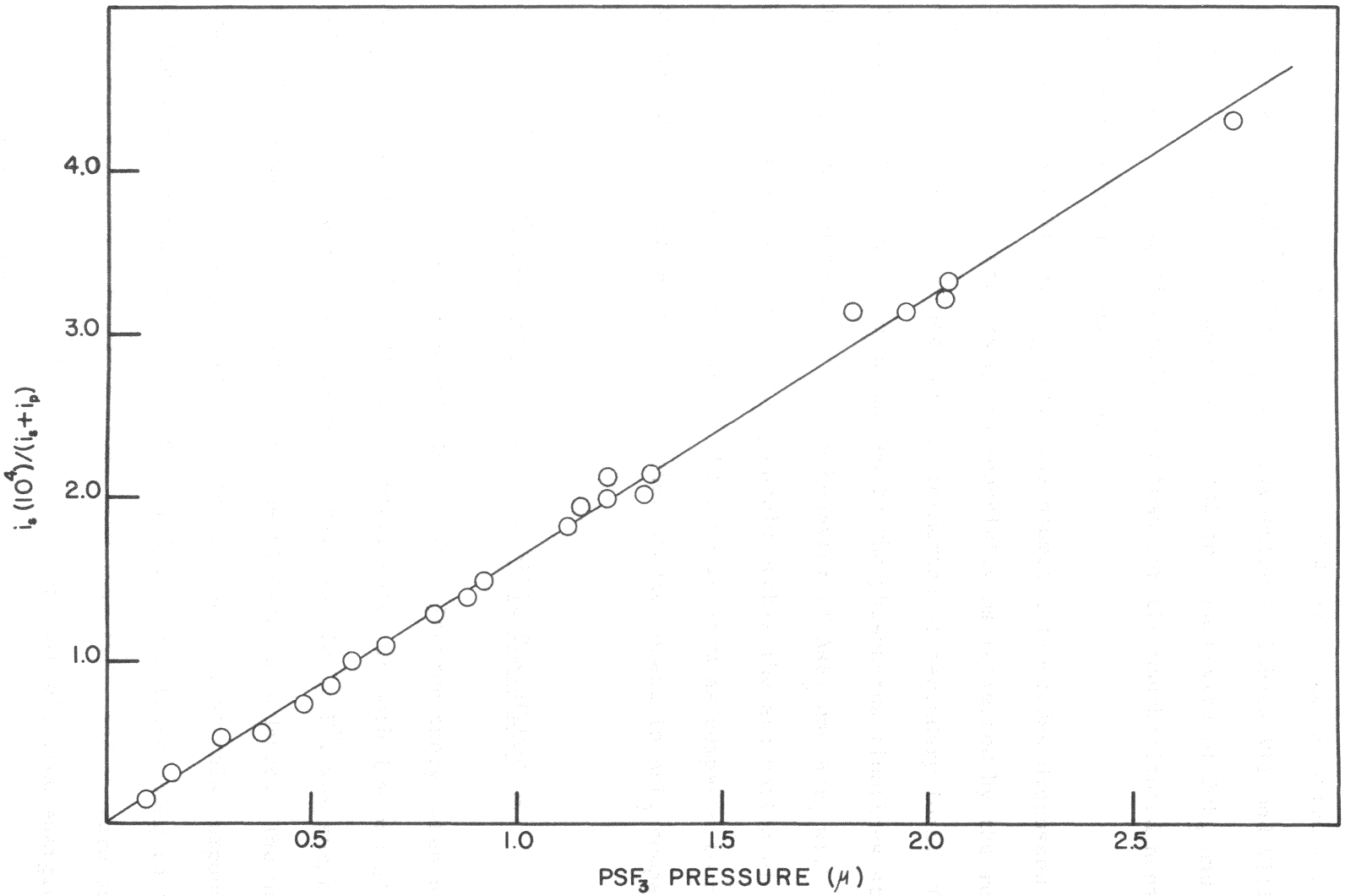

FIGURE 17. ION CURRENT RATIO AS A FUNCTION OF PSF_3 PRESSURE

The reaction rate constants and cross sections measured for the formation of POF_4^- and PSF_4^- are presented in Tables VII and VIII, and an examination of the data shows that the reactivity of POF_3 and PSF_3 toward SF_6^- is significantly less than for the unsubstituted nonmetal fluorides previously discussed.

The reactions of SF_6^- with the nonmetal fluorides discussed thus far have shown a large range in reactivity as reflected by the reaction cross sections determined for the formation of secondary ions. The fluorides of arsenic are analogous to the phosphorus fluorides studied initially, and comparisons of the behavior of AsF_3 and AsF_5 with the phosphorus fluorides PF_3 and PF_5 should enable the evaluation of the effect of the increased size of the arsenic atom as compared to phosphorus and the influence of increased dipole moment in AsF_3 compared to PF_3.

IV. ARSENIC TRIFLUORIDE AND ARSENIC PENTAFLUORIDE

No negative ions were detected at any electron energy when pure AsF_3 was introduced into the mass spectrometer at both low and high pressure. The absence of fragment ions, especially F^-, was surprising since PF_3 formed several fragment ions of large abundance. The negative ion mass spectrum of AsF_5 was also surprising in that this compound formed a parent negative ion, AsF_5^-, and an ion corresponding to the molecular ion plus a fluorine atom. The ions AsF_4^- and F^- were observed in the low pressure mass spectrum of AsF_5 at high electron energies, and the AsF_4^- ion was detected at near 0 eV.

TABLE VII

REACTION RATE CONSTANTS FOR THE FORMATION OF SECONDARY IONS AS A FUNCTION OF REPELLER VOLTAGE FOR THE REACTIONS

$$SF_6^- + POF_3 \rightarrow POF_4^- + SF_5$$

$$SF_6^- + PSF_3 \rightarrow PSF_4^- + SF_5$$

Repeller Voltage	Rate Constant (X 10^{10} cm^3/molecule-sec.) Secondary Ion	
(V)	POF_4^-	PSF_4^-
1.5	0.200	0.0185
2.0	0.274	0.0205
2.5	0.238	0.0230
3.0	0.226	0.0246
3.5	0.227	0.0266
4.0	0.213	0.0268

TABLE VIII

REACTION CROSS SECTIONS FOR THE FORMATION OF SECONDARY IONS AS A FUNCTION OF REPELLER VOLTAGE FOR THE REACTIONS

$$SF_6^- + POF_3 \rightarrow POF_4^- + SF_5$$

$$SF_6^- + PSF_3 \rightarrow PSF_4^- + SF_5$$

Repeller Voltage	Cross Section (A^2/molecule) Secondary Ion	
(V)	POF_4^-	PSF_4^-
1.5	4.64	0.429
2.0	5.50	0.412
2.5	4.28	0.413
3.0	3.71	0.404
3.5	3.45	0.404
4.0	3.02	0.381

Ion-Molecule Reactions

When AsF_5 is introduced into the ion source at high pressure the ions AsF_4^-, AsF_5^-, and AsF_6^- are formed at near 0 eV electron energy. Examination of the ionization efficiency curves shown in Figure 18 for AsF_4^-, AsF_5^-, and AsF_6^- reveals that all are formed at the same electron energy and the widths of all resonance curves are approximately equal. The reaction for the formation of AsF_4^- is the dissociative electron capture process

$$AsF_5 + e^- \rightarrow AsF_4^- + F \tag{80}$$

similar to the reaction for formation of SF_5^-. Two possibilities exist for the formation of AsF_5, either resonance electron capture

$$AsF_5 + e^- \rightarrow AsF_5^- \tag{81}$$

or the charge-transfer ion-molecule reaction

$$AsF_5 + AsF_4^- \rightarrow AsF_5^- + AsF_5 \tag{82}$$

The AsF_6^- ion may be formed by the reactions

$$AsF_4^- + AsF_5 \rightarrow AsF_6^- + AsF_3 \tag{83}$$

or

$$AsF_5^- + AsF_5 \rightarrow AsF_6^- + AsF_4 \tag{84}$$

Figure 19 shows the variation with pressure of the per cent of total ion current for AsF_4^-, AsF_5^-, and AsF_6^-. The primary ion AsF_4^- is observed to decrease slightly in per cent abundance with an increase in pressure of

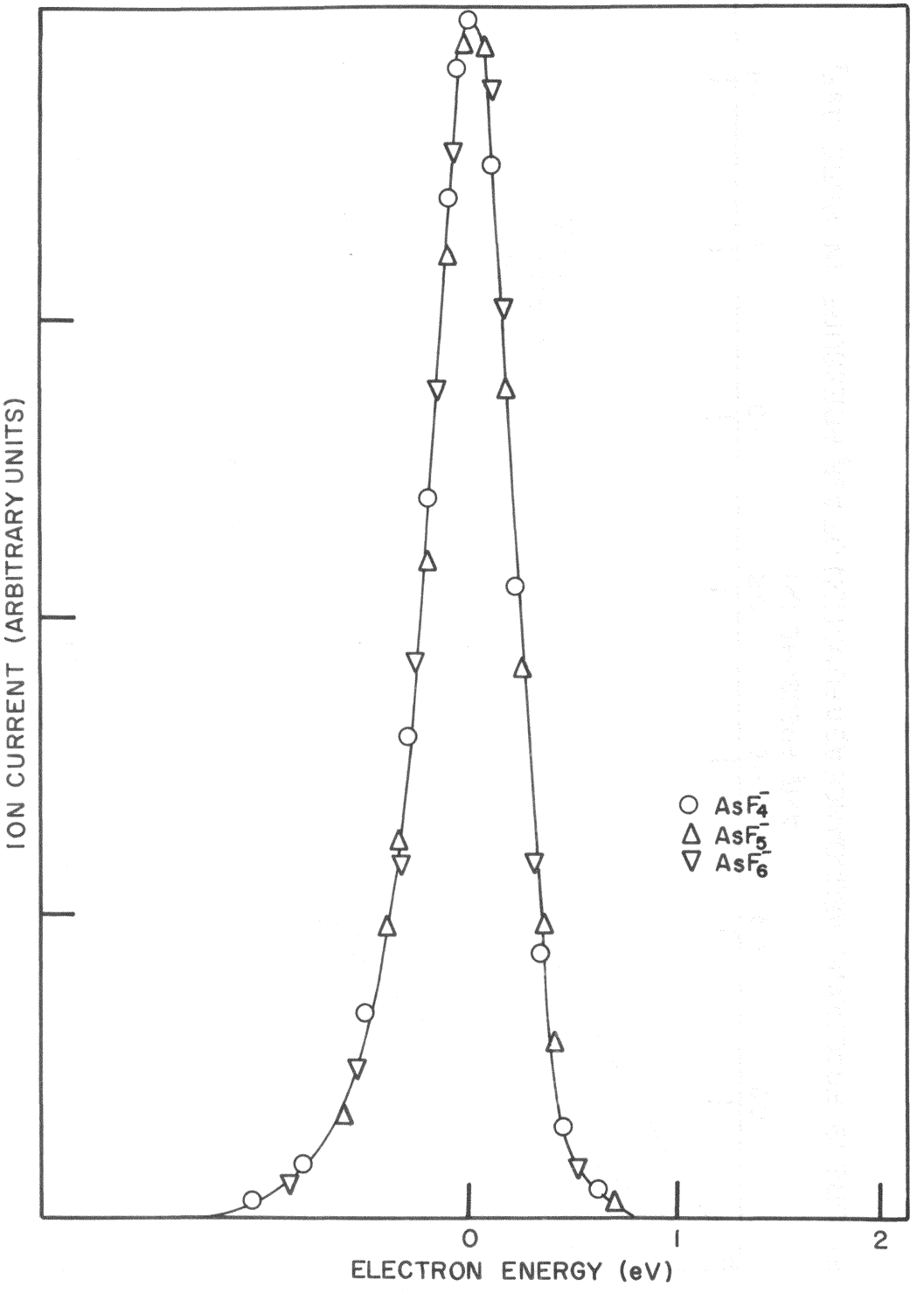

FIGURE 18. IONIZATION EFFICIENCY CURVES FOR IONS FORMED IN PURE AsF_5

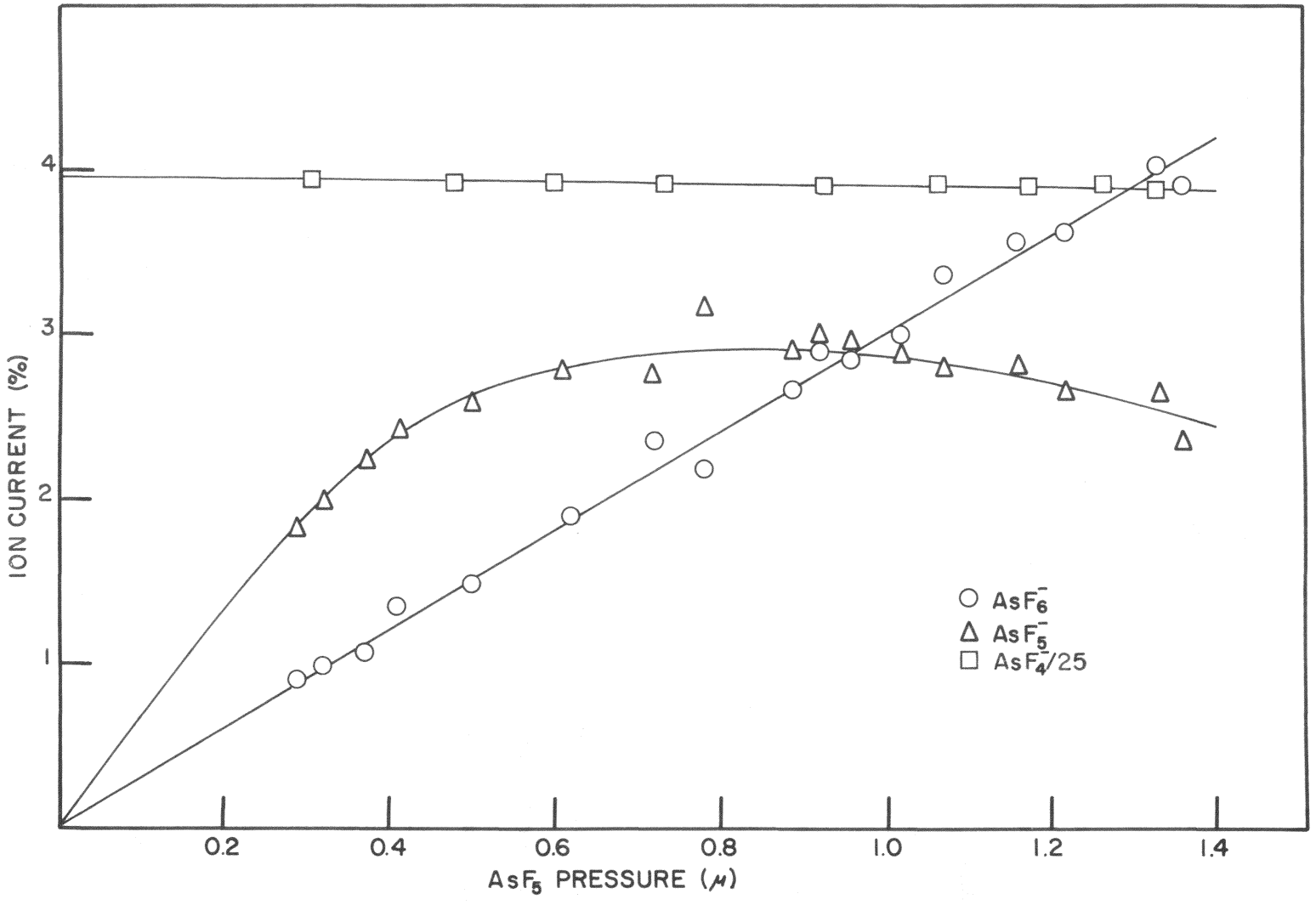

FIGURE 19. FRACTIONAL ABUNDANCE AS A FUNCTION OF AsF_5 PRESSURE IN PURE AsF_5

AsF_5, while both AsF_5^- and AsF_6^- increase with increasing AsF_5 pressure. Examination of the variation of per cent ion current for AsF_5^- as a function of AsF_5 pressure suggests that AsF_5^- is a secondary ion, and since the ionization efficiency curve for AsF_5^- coincides with that of AsF_4^-, the molecular ion AsF_5^- is presumed to be formed by charge transfer according to reaction 82. At pressures exceeding 0.5μ of AsF_5 the per cent ion current levels off and proceeds to drop slowly, suggesting that the cross section for charge transfer decreases dramatically at these pressures and that AsF_5^- formed by charge transfer is destroyed by some process not operable at lower AsF_5 pressure. The mechanism for destruction of AsF_5^- is likely collisional detachment by AsF_5

$$AsF_5^- + AsF_5 \rightarrow 2\ AsF_5 + e^- \qquad (85)$$

although an ion-molecule reaction (reaction 84) is possible. Since the initial formation of AsF_5^- is pressure dependent (pseudo-first order) and corresponds to a biomolecular process, reaction 84 would demonstrate pesudo-second order kinetics and would require consecutive bimolecular reactive collisions if this were contributing to the formation of AsF_6^-. This process is not likely since much higher pressures are normally required for such behavior, and no change in slope of the curve for the formation of AsF_6^- is observed in the region where AsF_5^- is diminishing. If reaction 84 does contribute to the formation of AsF_6^-, the amount of AsF_6^- formed is insignificant to that resulting from other pathways of formation. Therefore reaction 84 is eliminated from consideration as a means of destruction of AsF_5^- and the loss of AsF_5^- is ascribed to collisional detachment (reaction 85). AsF_6^- is observed to be formed with a linear pressure

dependence over the entire range studied, and the correspondence of the ionization efficiency curve with that for AsF_4^- identifies reaction 83 as the process for formation of AsF_6^- in pure AsF_5.

Since secondary ions are observed in the high pressure negative ion mass spectrum of pure AsF_5, the identification of ion-molecule reactions with SF_6^- was made more difficult. When SF_6^- was added to AsF_5 in the mass spectrometer, the secondary ion AsF_6^- was observed to increase in abundance while AsF_4^- and AsF_5^- showed no corresponding increases. This behavior was determined by three experiments in which pure AsF_5 was introduced into the instrument and the ion currents for AsF_4^-, AsF_5^-, and then AsF_6^- were monitored as the SF_6 was added. This behavior suggested that the ion-molecule reaction

$$SF_6^- + AsF_5 \rightarrow AsF_6^- + SF_5 \qquad (86)$$

occurs in mixtures of SF_6 and AsF_5 and that charge transfer between SF_6^- and AsF_5 does not take place. The ionization efficiency curves for the formation of negative ions in the low energy region are presented in Figure 20 for mixtures of SF_6 and AsF_5. Since the SF_6^- curve is coincident with the curves for all ions containing arsenic, positive identification of reaction 86 to the exclusion of reaction 83 is not possible.

Figure 21 shows the variation of AsF_6^- ion current ratio in mixtures of SF_6 and AsF_5 as a function AsF_5 pressure. The points designated by squares are the calculated ratios for reaction 83 based on the measured rate constants for the ion-molecule reaction in pure AsF_5. The calculated AsF_6^- ion current due to reaction 83 was subtracted from the measured ion current and the ion current ratio due to reaction 86 was taken as

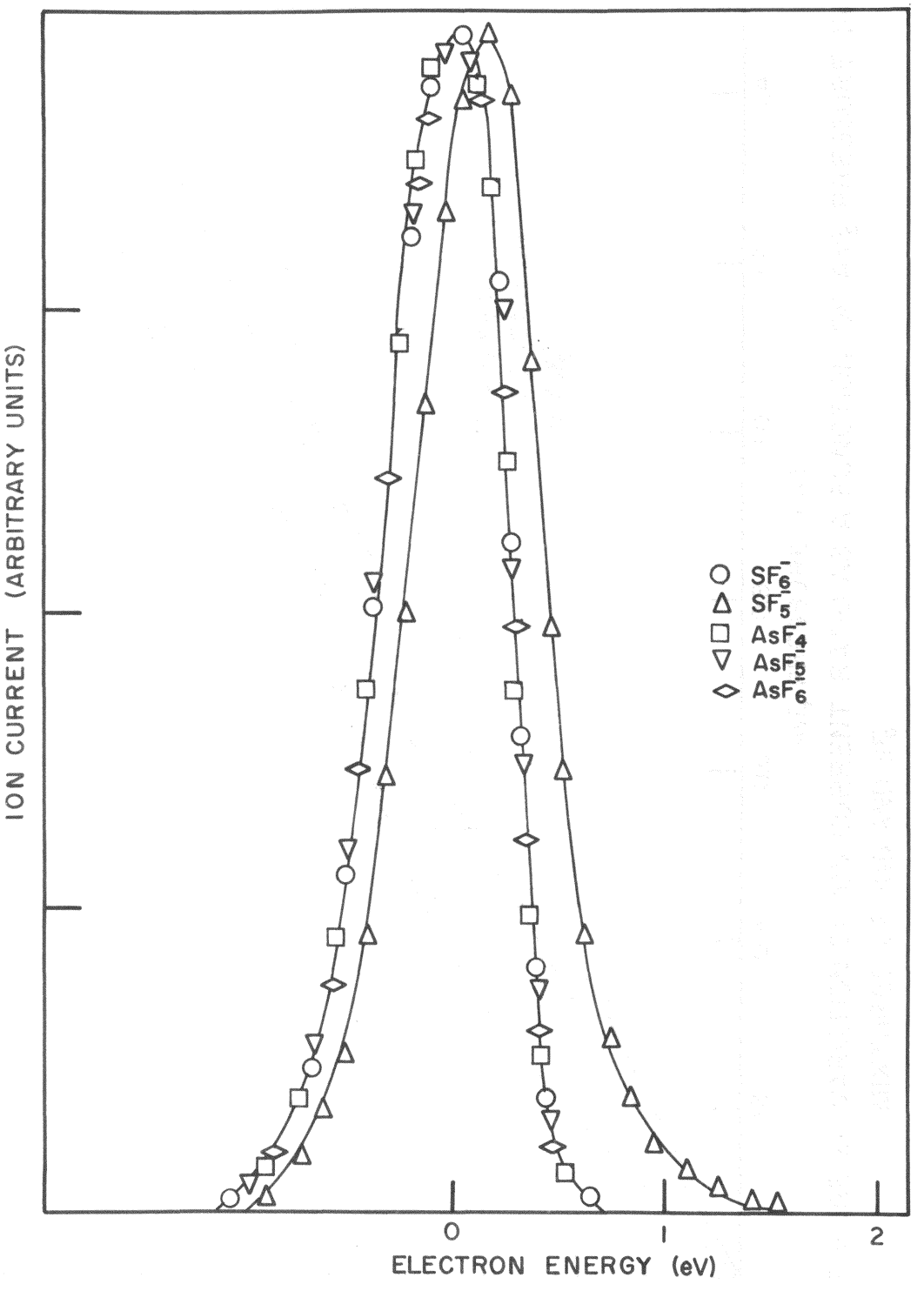

FIGURE 20. IONIZATION EFFICIENCY CURVES FOR IONS FORMED IN SF_6 - AsF_5 MIXTURES

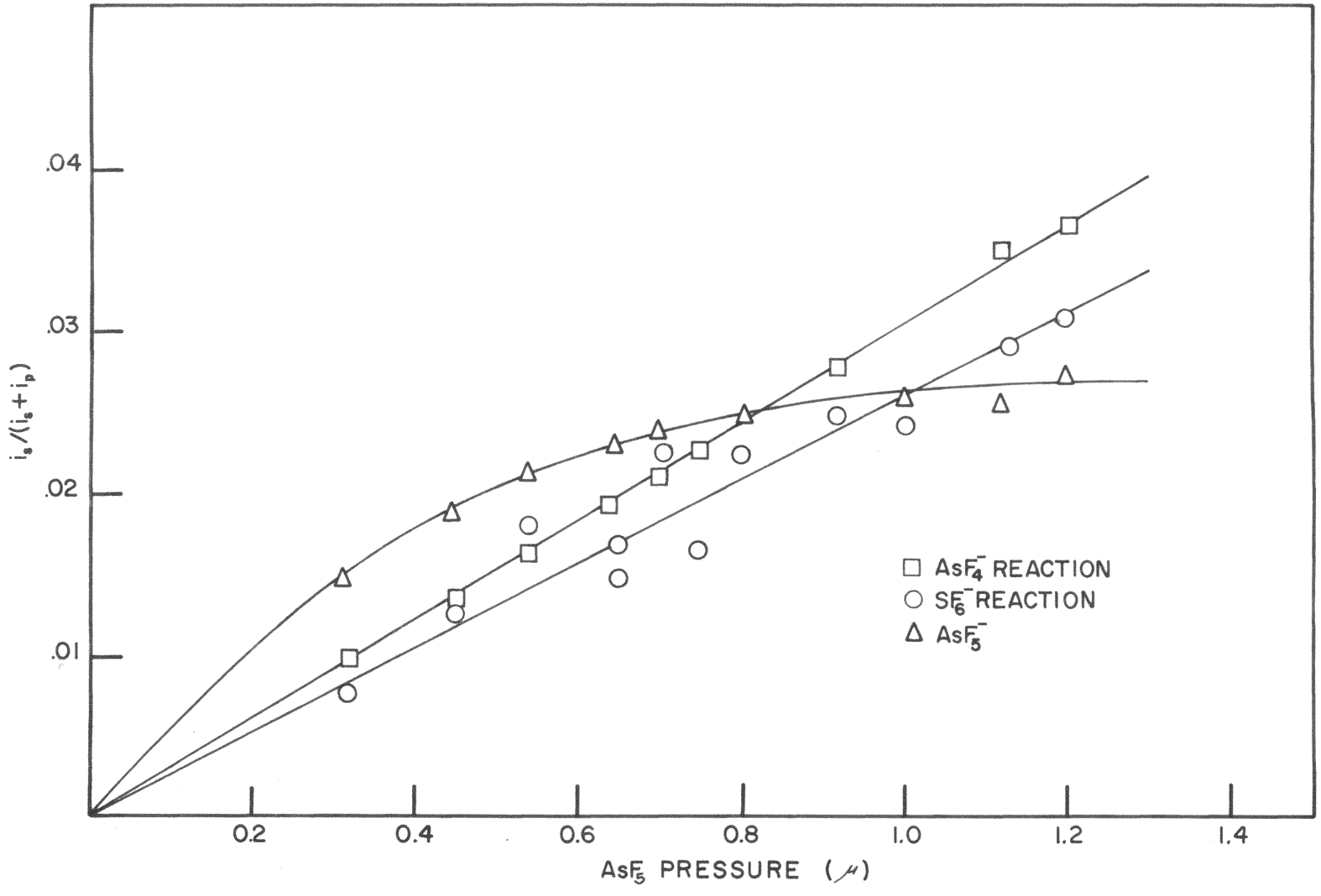

FIGURE 21. VARIATION OF ION CURRENT RATIO AS A FUNCTION OF AsF_5 PRESSURE IN MIXTURES OF AsF_5 AND SF_6

the difference. Although a direct measurement of the separate contributions to the formation of AsF_6^- would be preferable to this subtraction technique, the linear pressure dependence of AsF_6^- formation due to reaction 83 suggests that the data derived in this manner are valid.

When SF_6 was added to AsF_3 in the mass spectrometer, the secondary ion AsF_4^- was observed in the region where SF_6^- and SF_5^- are formed by resonance electron capture. The ionization efficiency curves for SF_6^-, SF_5^-, and AsF_4^- are presented in Figure 22, and SF_6^- is identified as the precursor for formation of the secondary ion AsF_4^-. Figure 23 shows the pressure dependence of the secondary ion formation, and, as with nonmetal fluorides previously discussed, the formation of AsF_4^- is pseudo-first order in pressure of AsF_3 and corresponds to the fluoride ion transfer reaction.

$$SF_6^- + AsF_3^- \rightarrow AsF_4^- + SF_5 \qquad (87)$$

Reaction Rate Constants and Cross Sections

In pure AsF_5 the formation of secondary ions was observed, and the reaction rate constants and cross sections for these reactions are presented in Tables IX and X. The large values measured for both the charge transfer reaction (reaction 82) and the fluoride ion transfer reaction (reaction 83) reflect the very strong acceptor properties of the AsF_5 molecule. The charge transfer reaction forming AsF_5^- is the only such reaction observed in these studies of nonmetal fluorides, and the magnitude of the cross section for AsF_5^- formation indicates that AsF_5 is an extremely reactive gas and that ion-molecule reactions are probably quite important in the gas-phase chemical behavior of arsenic pentafluoride.

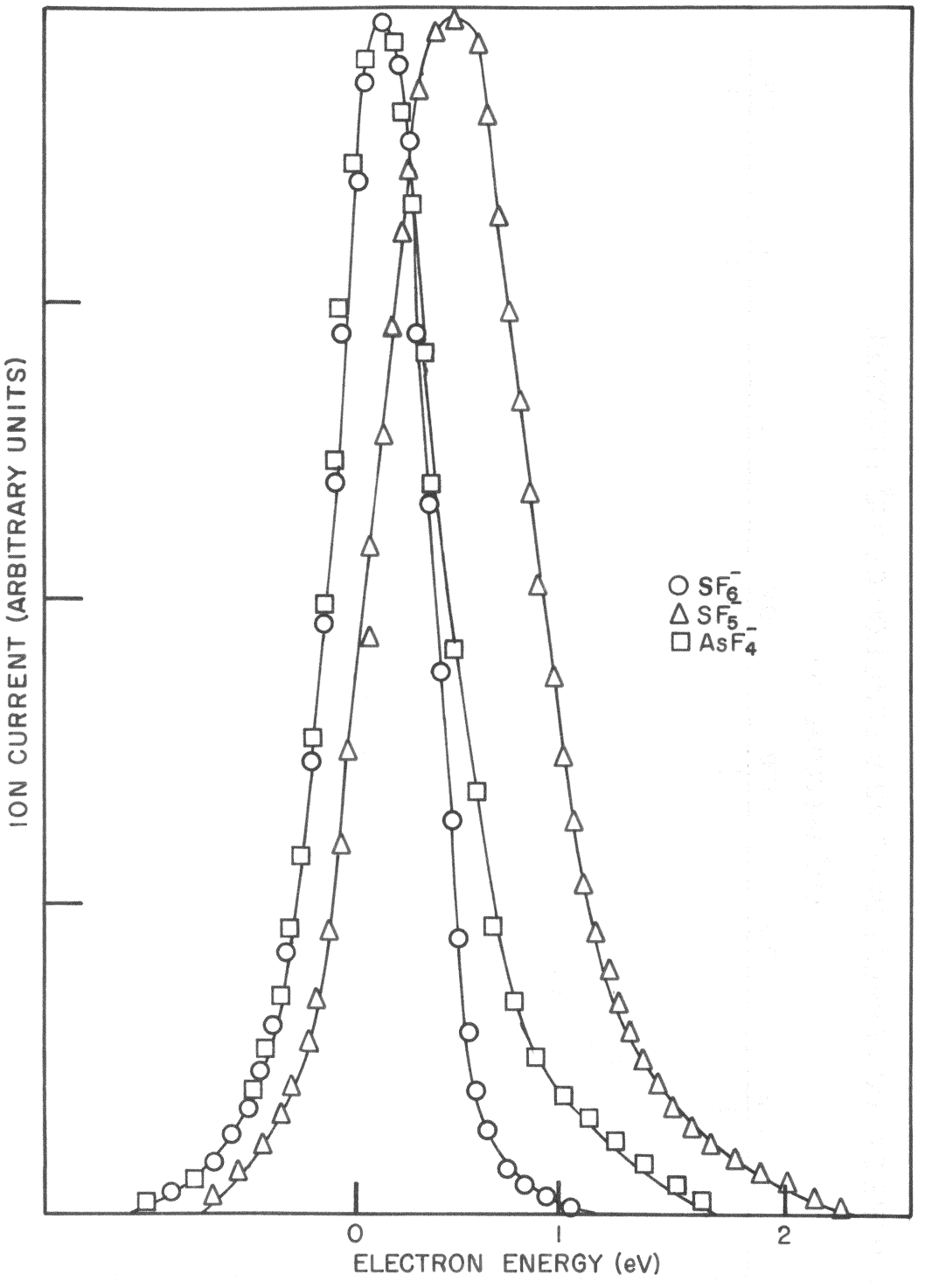

FIGURE 22. IONIZATION EFFICIENCY CURVES FOR SF_6^-, SF_5^- AND AsF_4^-

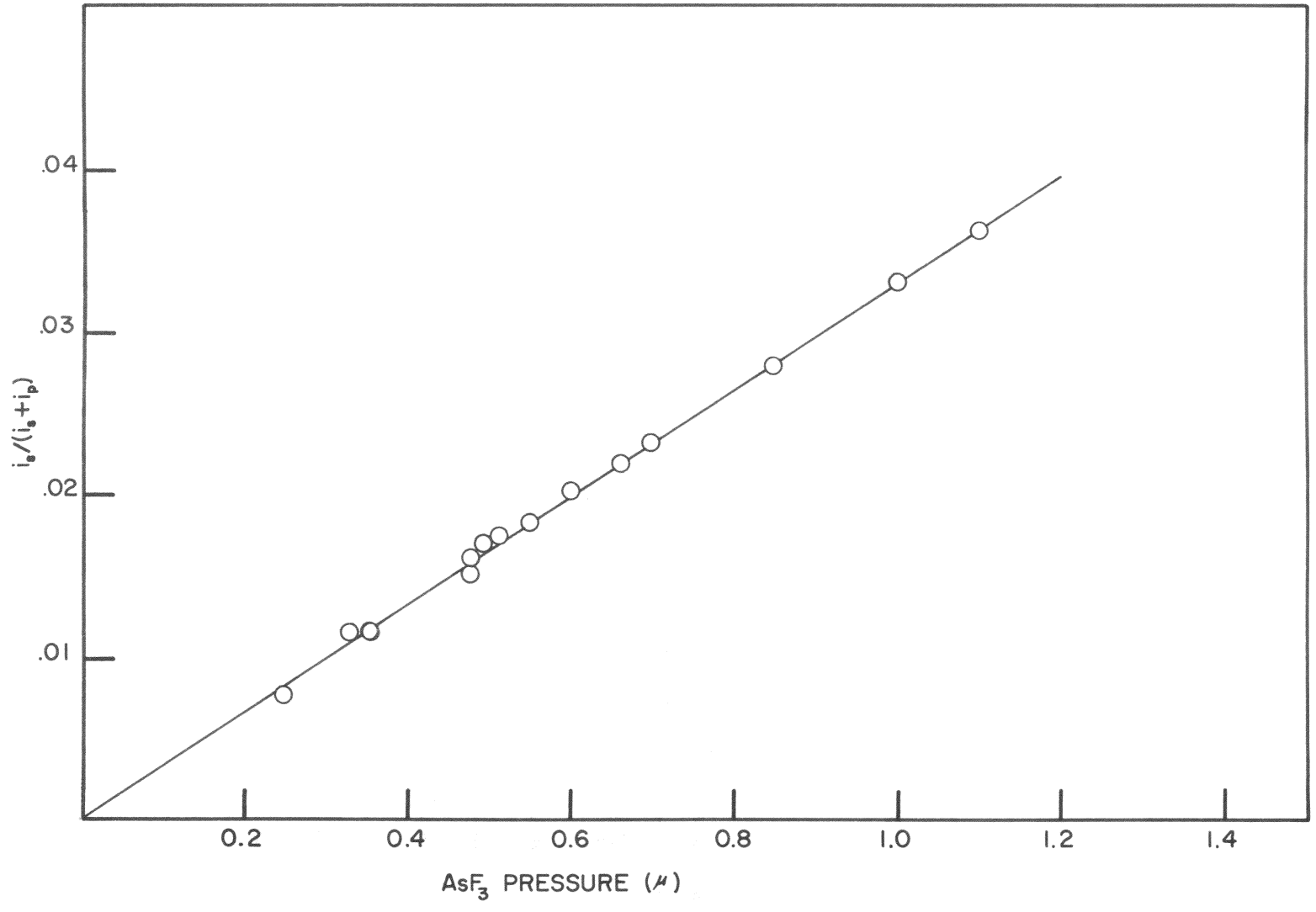

FIGURE 23. ION CURRENT RATIO AS A FUNCTION OF AsF_3 PRESSURE

TABLE IX

REACTION RATE CONSTANTS FOR THE FORMATION OF SECONDARY IONS IN PURE AsF_5 AS A FUNCTION OF REPELLER VOLTAGE FOR THE REACTIONS

$$AsF_4^- + AsF_5 \rightarrow AsF_5^- + AsF_4$$

$$AsF_4^- + AsF_5 \rightarrow AsF_6^- + AsF_3$$

Repeller Voltage	Rate Constant (X 10^{10} cm^3/molecule-sec.) Secondary Ion	
(V)	AsF_5^-	AsF_6^-
1.5	5.88	4.68
2.0	5.21	3.83
2.5	5.31	3.80
3.0	5.26	3.65
3.5	5.53	3.58
4.0	5.82	3.53

TABLE X

REACTION CROSS SECTIONS FOR THE FORMATION OF SECONDARY IONS IN PURE AsF_5 AS A FUNCTION OF REPELLER VOLTAGE FOR THE REACTIONS

$$AsF_4^- + AsF_5 \rightarrow AsF_5^- + AsF_4$$

$$AsF_4^- + AsF_5 \rightarrow AsF_6^- + AsF_3$$

Repeller Voltage	Cross Section (A^2/molecule) Secondary Ion	
(V)	AsF_5^-	AsF_6^-
1.5	138.7	110.5
2.0	105.6	78.2
2.5	97.0	66.8
3.0	87.8	60.5
3.5	85.8	55.4
4.0	84.1	51.1

The reaction rate constants and cross sections for the formation of secondary ions in mixtures of SF_6 and the arsenic fluorides are presented in Tables XI and XII. The values tabulated for the formation of AsF_6^- were calculated after subtracting the contribution to the AsF_6^- ion current due to reaction 82 as described in the preceding section.

TABLE XI

REACTION RATE CONSTANTS FOR THE FORMATION OF SECONDARY IONS AS A FUNCTION OF REPELLER VOLTAGE FOR THE REACTIONS

$$SF_6^- + AsF_3 \rightarrow AsF_4^- + SF_5$$

$$SF_6^- + AsF_5 \rightarrow AsF_6^- + SF_5$$

Repeller Voltage	Rate Constant (X 10^{10} cm^3/molecule-sec.) Secondary Ion	
(V)	AsF_4^-	AsF_6^-
1.5	4.34	3.12
2.0	4.22	2.76
2.5	4.38	2.20
3.0	4.49	2.10
3.5	4.59	2.15
4.0	4.61	2.13

TABLE XII

REACTION CROSS SECTIONS FOR THE FORMATION OF SECONDARY IONS AS A FUNCTION OF REPELLER VOLTAGE FOR THE REACTIONS

$$SF_6^- + AsF_3 \rightarrow AsF_4^- + SF_5$$

$$SF_6^- + AsF_5 \rightarrow AsF_6^- + SF_5$$

Repeller Voltage	Cross Section (A^2/molecule) Secondary Ion	
(V)	AsF_4^-	AsF_6^-
1.5	100.7	72.4
2.0	84.7	55.8
2.5	78.7	39.6
3.0	73.7	34.7
3.5	69.7	32.7
4.0	65.5	30.4

CHAPTER V

DISCUSSION OF RESULTS

The reaction rate constants and cross sections for the gas-phase negative ion-molecule reactions described here represent the first such data determined for systems of nonmetal fluorides. These data may be utilized to calculate ionic heats of formation of the secondary ions formed, and the reactivity of the neutral species is considered in light of the magnitude of the reaction cross section determined.

I. REACTION CROSS SECTION AS A FUNCTION OF ION ENERGY

The gas-phase ion-molecule reactions which occur in the mass spectrometer ion source involve collisions of primary ions with molecules to yield the reaction products. The primary ions are formed in the electron beam, 1.5 mm from the ion exit slit, and experience continuous acceleration in moving to the exit slit due to the effect of the repeller electrode field. The total ion energy is therefore the sum of its thermal energy, kinetic energy, and the energy imparted to the ion by acceleration in the repeller field. At repeller fields used in this study the thermal energy is negligible, and since SF_6^- is formed with no kinetic energy (16) by resonance electron capture, the only energy imparted to the ion is that due to the repeller field. Calculations of reaction rate constants require a knowledge of the primary ion energy, and in the calculation method used here the ion is assigned an average energy based on the repeller field strength.

Many efforts have been devoted to determine the dependence of

reaction cross section on the energy of the primary ion. Gioumousis and Stevenson (27) and Stevenson and Schissler (87,89) have proposed an $E^{-1/2}$ dependence and many simple systems have been found to exhibit this behavior. An example is the reaction of Ar^+ with H_2 discussed earlier in conjunction with Figure 11.

This behavior is by no means universally observed, however, and Field, Franklin, and Lampe (101) and Field and Lampe (83) have found that the reaction cross section varies with reciprocal ion energy (E^{-1} dependence) for many reactions involving primary positive ions formed in hydrocarbons. Thus for polyatomic ions and molecules having many internal degrees of freedom the energy dependence is not a simple $E^{-1/2}$ behavior. In a series of reports (53-57) Hamill and coworkers have stated that the energy dependence is observed to vary with the ion exit energy. At low repeller fields an $E^{-1/2}$ dependence is noted while at high repeller field strengths a transition to E^{-1} dependence is predominant. They suggest that at repeller fields greater than the energy at which this transition occurs, the impact parameters of neutral molecule collisions and the influence of short-range repulsive forces must be included in a complete description of the energy dependence of the reaction cross section. Two different cross sections are therefore important over the range of ion energies, a cross section for hard-sphere collisions and the collision cross section for Langevin orbiting collisions as developed by Gioumousis and Stevenson (27).

Futrell and Ryan (102) and Harrison, Myher, and Thynne (103) have utilized pulsed ion sources to investigate the reactions of thermal energy ions and the former have suggested that space charge effects and

discrimination effects may be responsible for the various energy dependences observed at low field strengths.

The investigations of the energy dependence of reaction cross sections described above have involved systems containing positive ions. The ion-molecule reactions observed in this study involve negative ions, and the energy dependence of these reactions was investigated to determine whether $E^{-1/2}$ or E^{-1} behavior is evident in these systems. Figures 24 and 25 show the variation of reaction cross section with E^{-n} (n = 1/2,1) for the formation of secondary ions by the reactions

$$SF_6^- + PF_5 \rightarrow PF_6^- + SF_5 \quad (88)$$

$$SF_6^- + SiF_4 \rightarrow SiF_5^- + SF_5 \quad (89)$$

The energy dependence of these cross section data is not characteristic of $E^{-1/2}$ behavior (see Figure 11, for example) and the dependence only roughly approximates an E^{-1} relationship. This suggests that for the fluoride ion transfer reactions studied here the Langevin orbiting collision model proposed by Gioumousis and Stevenson (27) is not a satisfactory description of the energetics of collision processes occurring in the ion source.

The energy dependence of these reactions may be determined by further measurements of reaction cross sections at higher repeller voltages so that the behavior at lower E^{-n} values may be examined. In this study the cross sections at repeller voltages higher than 4 volts were not considered reliable because a reaction forming secondary ions via reaction with SF_5^- contributed to the secondary ion current at high repeller potentials. In order to determine the energy dependence of the

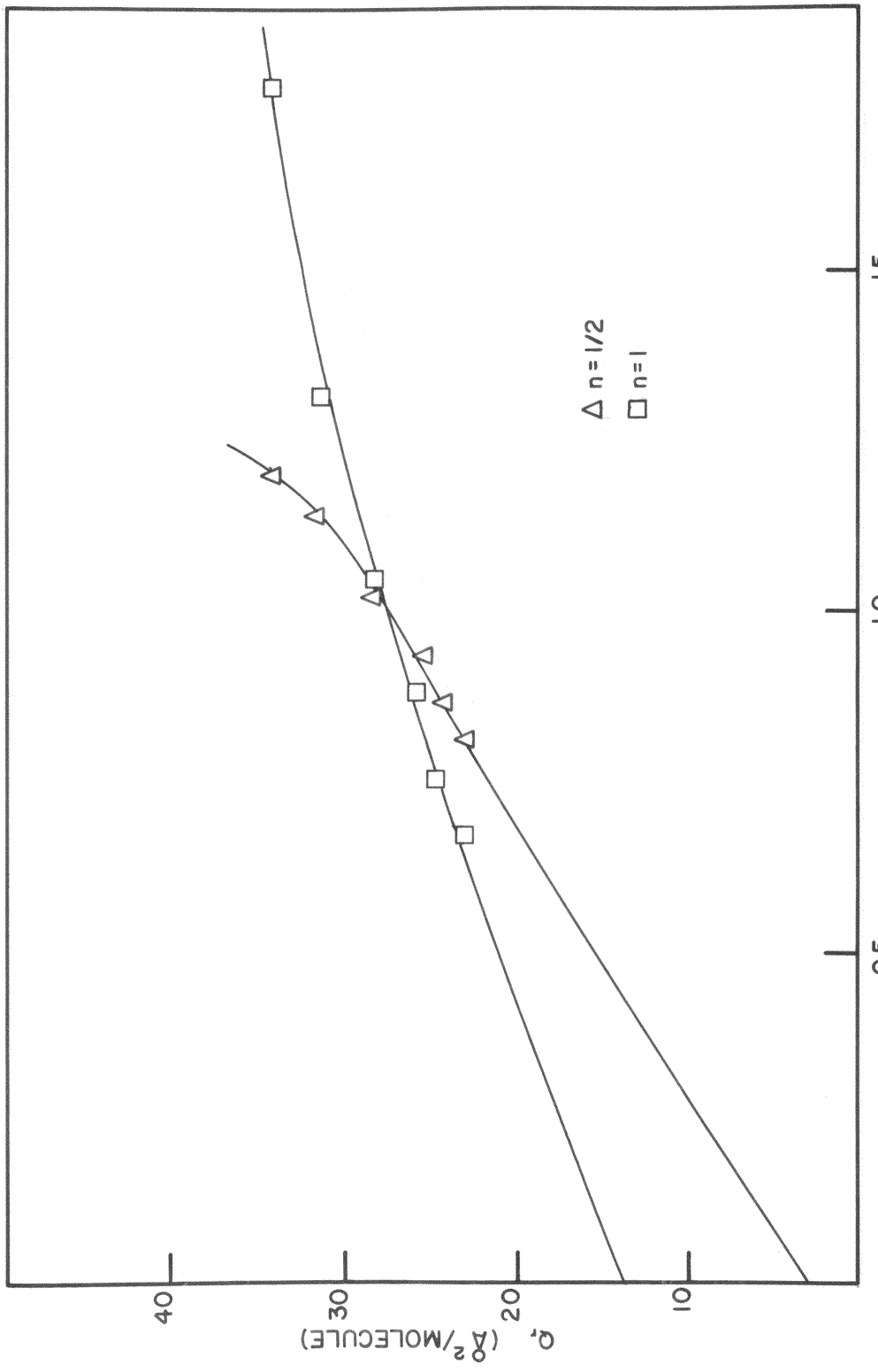

FIGURE 24. REACTION CROSS SECTION AS A FUNCTION OF $(E)^{-n}$ FOR PF_6^- FORMATION

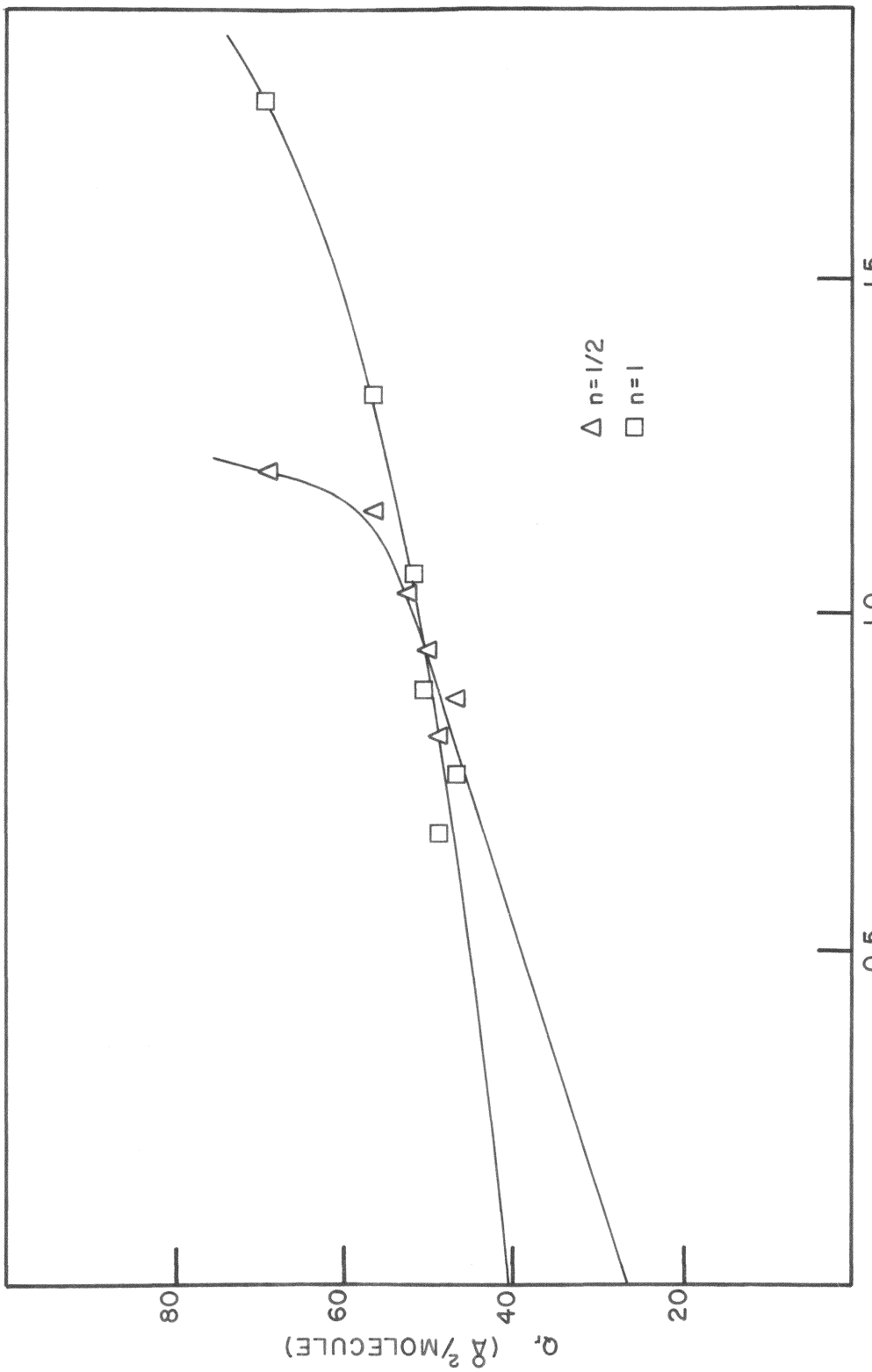

FIGURE 25. REACTION CROSS SECTION AS A FUNCTION OF $(E)^{-n}$ FOR SiF_5^- FORMATION

SF_6^- reaction it would be necessary to subtract the contribution from the endothermic reaction, and more extensive investigation of the reaction involving SF_5^- is required before this subtraction can be carried out. Determination of the reaction cross section for the SF_6^- reactions using the pulsed ion source methods described by Ryan and Futrell (102) and Harrison, Myher, and Thynne (103) also might provide information which would be useful in establishing the energy dependence.

Since the electron affinity of SF_6 has been estimated to be about 1.1 eV (93) or 0.75 eV<E.A. (SF_6)<1.47 eV (104), SF_6^- produced at near zero electron energies in this study must be formed with excess internal energy in the form of electronic and/or vibrational excitation. It is of course possible that this quantity of internal energy is sufficient to mask the $E^{-1/2}$ dependence of the cross section at low ion energies. Therefore studies of the temperature dependence of the reaction cross section would be of value in determining the energy dependence for these reactions.

The cross sections for the reactions studied here exhibit a decrease in magnitude with increasing ion energy, an effect which is characteristic of exothermic reactions. The reactions involving SF_6^- are therefore shown to be exothermic, and thermochemical calculations of the ionic heats of formation of the secondary ions may be carried out since ΔH (reaction)≥ 0 for these reactions.

II. THERMODYNAMIC CALCULATIONS

Heats of formation of primary ions observed and radical species predicted in this study may be calculated from a knowledge of the

appearance potential and the predicted reaction process. The heat of formation of the ion is calculated using the appearance potential of the ion and known heats of formation of neutral species. Heats of formation of the neutral radical species are evaluated for the appearance potential of an ion which has a known heat of formation. Tables XIII and XIV list the heats of formation of the neutral and ionic species of interest, respectively, in this study. From the near-zero appearance potential of SF_6^- (16) for the resonance electron capture process

$$SF_6 + e^- \rightarrow SF_6^- \tag{90}$$

the heat of formation of SF_6^- is taken to be equal to the heat of formation of SF_6, and therefore $\Delta H_f(SF_6^-) = -289$ kcal/mole. SF_5^- is formed at 0.16 eV by the process

$$SF_6 + e^- \rightarrow SF_5^- + F \tag{91}$$

and ΔH_f (SF_5^-) is calculated to be -304 kcal/mole.

The heat of formation of the SF_5 radical may be calculated from the reaction

$$SF_6 + e^- \rightarrow SF_5 + F^- \tag{92}$$

for which Curran (98) has determined the appearance potential of F^- and the total kinetic energy to be 0 and 0.23 eV, respectively. The heat of formation of SF_5 is given by

$$\Delta H_f(SF_5) = D(SF_5\text{-}F) + \Delta H_f(SF_6) - \Delta H_f(F) \tag{93}$$

where $D(SF_5\text{-}F)$ is the bond dissociation energy of the sulfur-fluorine

TABLE XIII

HEATS OF FORMATION OF GASEOUS NEUTRAL SPECIES OF INTEREST IN THIS STUDY

M (q)	ΔH_f(kcal/mole)	Reference
SF_6	-289	105
SF_5	-234	a
SF_4	-185.2	105
PF_5	-381.4	105
PF_3	-219.6	105
BF_3	-271.75	105
SiF_4	-385.98	105
POF_3	-289.5	105
PSF_3	-254	106
AsF_5	-295.5	107
AsF_4	-258	a
AsF_3	-220.04	105
F	18.88	105

[a]See Text

TABLE XIV

HEATS OF FORMATION OF GASEOUS IONS OF INTEREST IN THIS STUDY

Ion	Process	ΔH_f(kcal/mole)	Reference
SF_6^-	$SF_6 + s^- \rightarrow SF_6^-$	-289	a
SF_5^-	$SF_6 + s^- \rightarrow SF_5^- + F$	-304	a
PF_6^-	$SF_6^- + PF_5 \rightarrow PF_6^- + SF_5$	-436	a
	$SF_5^- + PF_5 \rightarrow PF_6^- + SF_4$	-466	a
PF_4^-	$SF_6^- + PF_3 \rightarrow PF_4^- + SF_5$	-275	a
BF_4^-	$SF_6^- + BF_3 \rightarrow BF_4^- + SF_5$	-327	a
	Lattice Calculations	-407	108,109
SiF_5^-	$SF_6^- + SiF_4 \rightarrow SiF_5^- + SF_5$	-441	a
	$SF_5^- + SiF_4 \rightarrow SiF_5^- + SF_4$	-466	a
	$SiF_3^- + SiF_4 \rightarrow SiF_5^- + SiF_2$	-583	110
POF_4^-	$SF_6^- + POF_3 \rightarrow POF_4^- + SF_5$	-345	a
PSF_4^-	$SF_6^- + PSF_3 \rightarrow PSF_4^- + SF_5$	-309	a
	$SF_5^- + PSF_3 \rightarrow PSF_4^- + SF_4$	-349	a
AsF_4^-	$AsF_5 + s^- \rightarrow AsF_4^- + F$	-308	a
	$SF_6^- + AsF_3 \rightarrow AsF_4^- + SF_5$	-273	a
AsF_5^-	$AsF_5 + s^- \rightarrow AsF_5^-$	-296	a
	$AsF_4^- + AsF_5 \rightarrow AsF_5^- + AsF_4$	-346	a
AsF_6^-	$AsF_4^- + AsF_5 \rightarrow AsF_6^- + AsF_3$	-384	a
	$SF_6^- + AsF_5 \rightarrow AsF_6^- + SF_5$	-351	a

[a]See Text

bond broken in the dissociation process. This quantity is related to the appearance potential of F^-, the electron affinity of F, and the total kinetic energy by

$$D(SF_5\text{-}F) = AP(F^-) + EA(F) - KE(Total) \quad (94)$$

so that on substitution of 94 into 93 equation 93 becomes

$$\Delta H_f(SF_5) = AP(F^-) + EA(F) + \Delta H_f(SF_6) - \Delta H_f(F) - KE(Total) \quad (95)$$

Expression 95 now yields $\Delta H_f(SF_5) = -234$ kcal/mole using the data reported by Curran (98), the electron affinity (111) of fluorine (3.45 eV), and the heats of formation of SF_6 and F listed in Table XIII.

The observed decrease in reaction cross section with increasing repeller voltage (and therefore, increasing ion energy) indicates that the formation of secondary ions by fluoride ion transfer from SF_6^- is an exothermic process. The general reaction for the formation of these secondary ions

$$SF_6^- + AF_n \rightarrow \left[AF_{n+1}\right]^- + SF_5 \quad (96)$$

and the thermochemical relationship

$$\Delta H(reaction) = \sum \Delta H(products) - \sum \Delta H(reactants) + U + W \quad (97)$$

(where $\Delta H(reaction) \geq 0$ for these reactions) may be used.

For these calculations, the heat of reaction is assumed to be equal to zero. Heats of formation of gaseous ions calculated from these mass spectrometric measurements may be larger than the true heat of formation due to excitation energy (U) and kinetic energy (W) in the product ion. Thus,

if ions are formed with kinetic energy or in excited states, the calculated heats of formation represent upper limits unless the excess energy involved in the process has been determined. In these studies no measurements of kinetic energy of the negative ions were conducted, and the thermodynamic values reported here must be considered as upper limits for the actual heats of formation.

These data are of value, however, since the heats of formation calculated here represent the first such enthalpy data for the fluoroanions and these values may serve as reasonable estimates for use in further studies of the thermochemistry of inorganic nonmetal fluorides.

In this study it has been shown that the dominant process for the formation of the $\left[AF_{n+1}\right]^-$ ions at low repeller potentials (low ion energy) is described by reaction 96, an exothermic ion-molecule reaction. However, all primary ions acquire kinetic energy from the repeller field as they are swept toward the ion exit slit and it is possible that the kinetic energy gained may be sufficient to initiate endothermic ion-molecule reactions. From the enthalpy differences of reactions 96 and 98

$$SF_6^- + AF_n^- \rightarrow \left[AF_{n+1}\right]^- + SF_5 \qquad (96)$$

$$SF_5^- + AF_n \rightarrow \left[AF_{n+1}\right]^- + SF_4 \qquad (98)$$

the reaction with SF_5^- is calculated to be endothermic by about 2.6 eV.

In the dissociative resonance process SF_5^- is formed with less than 0.1 eV kinetic energy (16), which is not sufficient to overcome the endothermicity of reaction 98. However, if the repeller potential is increased the kinetic of SF_5^- will also be increased and at kinetic energies greater than the endothermicity of the reaction, the formation of

secondary ions may be observed. From an examination of the ionization efficiency curves for SF_6^-, SF_5^-, and $\left[AF_{n+1}\right]^-$ at high repeller potentials, a shift in the high energy portion of the $\left[AF_{n+1}\right]^-$ curve should be observed.

In addition, the formation of AF_{n+1}^- by the endothermic process (reaction 98) should lead to an increase in the fractional abundance of $\left[AF_{n+1}\right]^-$ as the repeller potential is increased. Extrapolation of the rising portion of the fractional abundance curve gives an approximate value for the repeller potential (related to ion energy) at which the endothermic reaction becomes significant. A value for the heat of formation of the $\left[AF_{n+1}\right]^-$ ion can then be estimated from the endothermic reaction by utilizing the extrapolated value for the endothermicity and the heats of formation of the ionic and neutral species listed in Tables XIV and XIII.

Hexafluorophosphate (V): PF_6^-

The hexafluorophosphate (V) negative ion is formed by the reaction

$$SF_6^- + PF_5 \rightarrow PF_6^- + SF_5 \qquad (99)$$

By application of Hess's Law using neutral and ionic heats of formation in Tables XIII and XIV the heat of formation of PF_6^- may be calculated from expression 97,

$$\Delta H_f(PF_6^-) = \Delta H_f(SF_6^-) + \Delta H_f(PF_5) - \Delta H_f(SF_5) \qquad (97)$$

The value obtained is $\Delta H_f(PF_6^-) = -436$ kcal/mole.

Examination of the ionization efficiency curve for PF_6^- formation at 6 V (Figure 26) and the variation of PF_6^- fractional abundance for repeller voltages in the range 0.5 to 8.0 V suggest that additional processes may

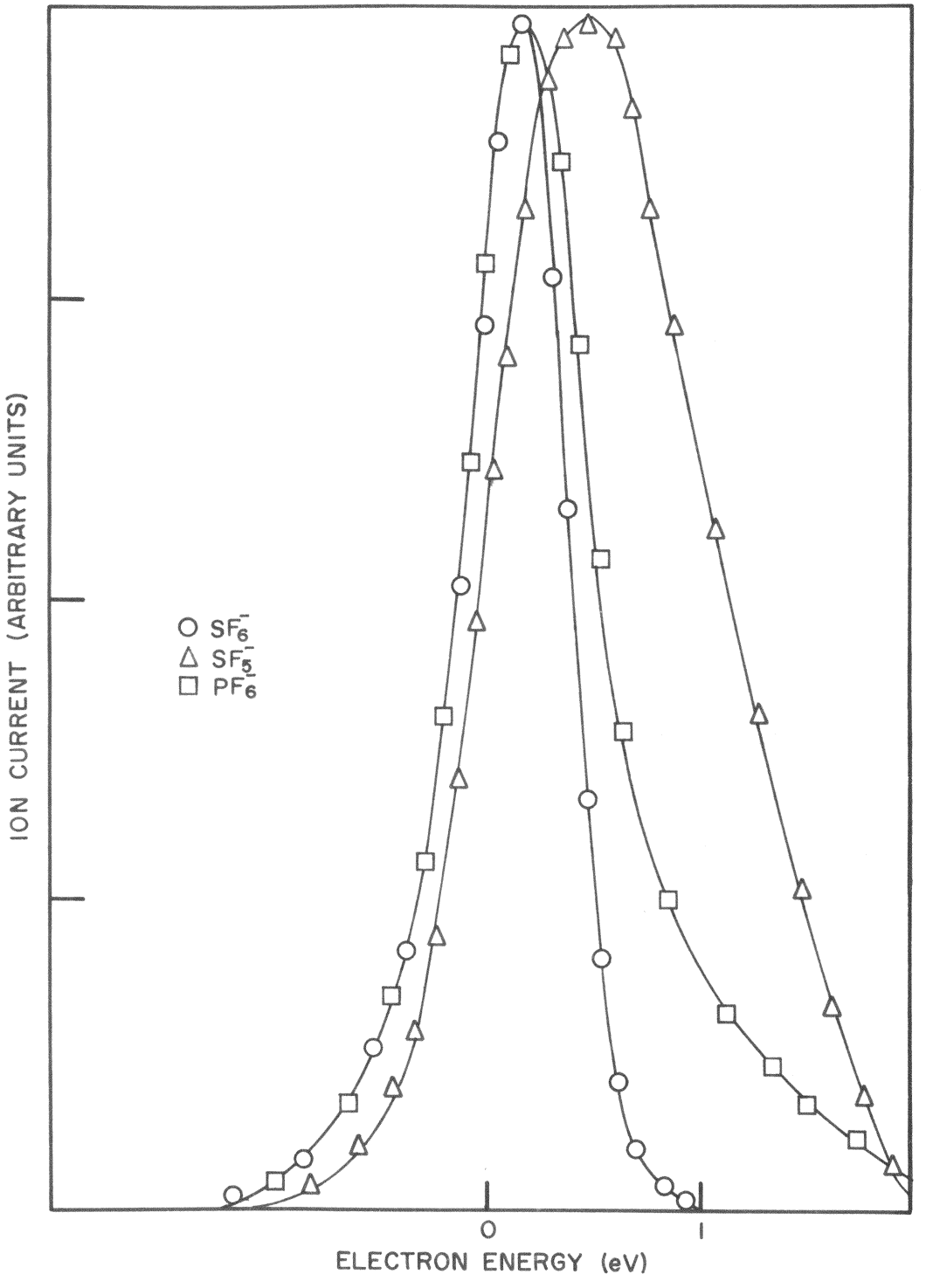

FIGURE 26. IONIZATION EFFICIENCY CURVES FOR SF_6^-, SF_5^- AND PF_6^- AT 6.0V REPELLER

produce PF_6^-.

The low energy portions of the SF_6^- and PF_6^- curves are identical within experimental reproducibility, but as the ion energy is increased the formation of PF_6^- ions is observed at higher electron energies. The production of the PF_6^- ions at these higher energies could occur in several ways. Two likely explanations are that an energetic or excited SF_6^- ion is involved (i.e., excited to some level not formed at near zero eV) or that SF_5^- is formed with sufficient kinetic energy at these repeller voltages to react with PF_5 neutrals via an endothermic process. Since the SF_6^- ionization efficiency curve is not altered at higher repeller potentials and the distribution on the electron beam is not distorted at higher repeller potentials, an excited SF_6^- ion is not responsible for the formation of PF_6^- ions high repeller voltages.

Additional evidence for the formation of PF_6^- by the endothermic process is presented in Figure 27 where the fractional abundance of PF_6^- is plotted vs. repeller potential. It is noted that the fractional abundance of PF_6^- decreases initially as would be expected for an exothermic ion-molecule reaction; however, at about 5.0 V repeller potential (1.80 eV ion energy) the abundance of PF_6^- increases dramatically. The onset energy for the formation of secondary ions at this ion energy approaches the endothermicity calculated for reaction 98.

Extrapolation of the curve for the endothermic process to zero fractional abundance corresponds to an ion energy of 1.5 eV for this process. A value for the heat of formation of PF_6^- may be estimated from the endothermic reaction, by utilizing the extrapolated value for the endothermicity of the reaction and the heats of formation listed in

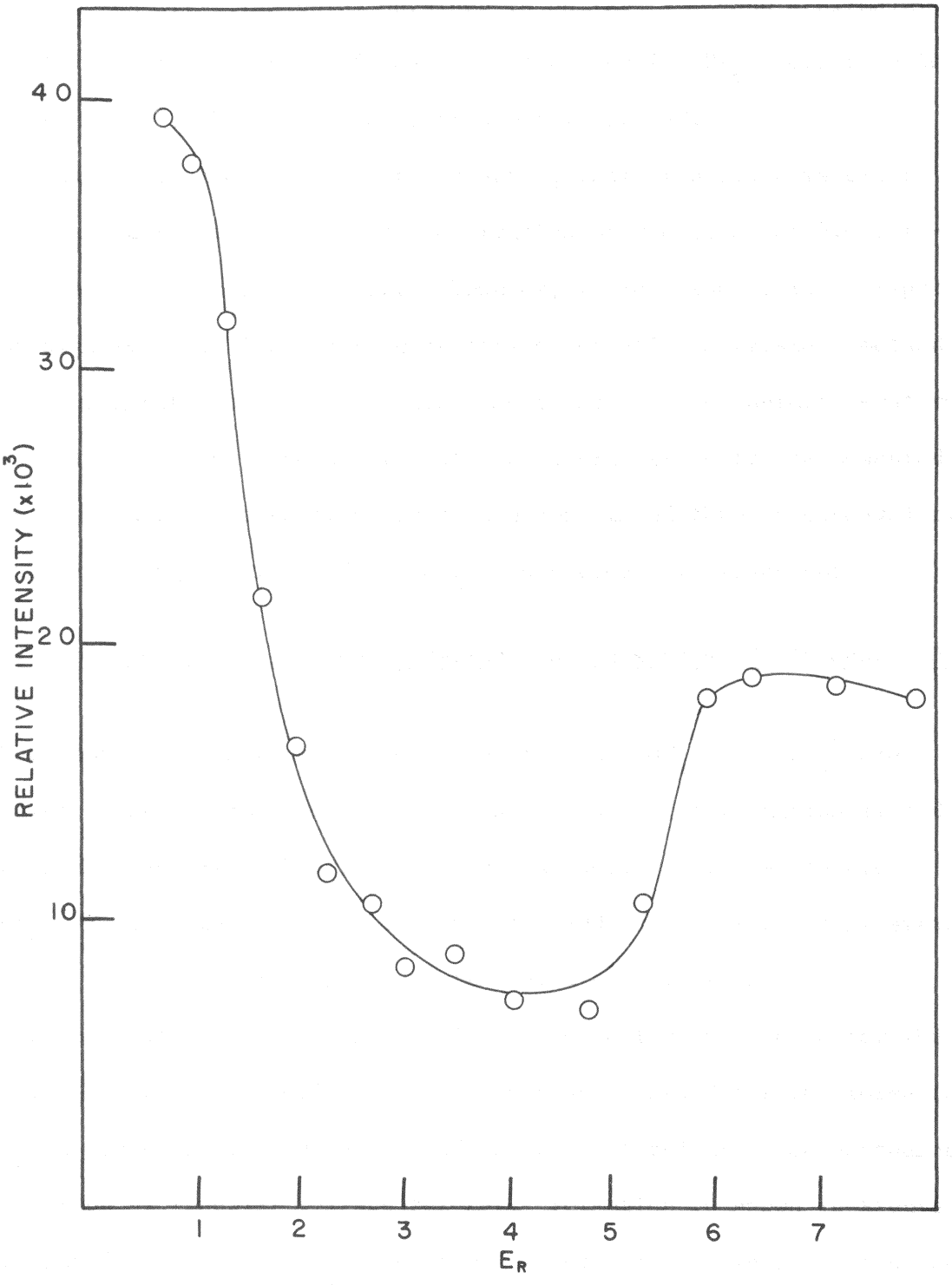

FIGURE 27. FRACTIONAL ABUNDANCE OF PF_6^- AS A FUNCTION OF REPELLER VOLTAGE

Tables XIII and XIV. The value obtained is $\Delta H_f(PF_6^-)$ = -466 kcal/mole. This differs from the heat of formation calculated for PF_6^- formed in the SF_6^- reaction by 30 kcal/mole, or approximately 1.3 eV.

In this study the energy of the reacting ions at a given repeller field is an average energy and the observation of the onset of 5.0 V repeller potential is a gross effect. However, if reaction 92 is of importance at high repeller field strengths this observation suggests a method of determining rate constants and cross sections for endothermic negative ion-molecule reactions. Separation of the contributions to the measured rate constant and cross section could be accomplished through deconvolution of the overlapping portions of the PF_6^- ionization efficiency curve.

Tetrafluorooxyphosphate (V) and Tetrafluorothiophosphate (V) Anions: POF_4^- and PSF_4^-

The heats of formation of the secondary ions POF_4^- and PSF_4^- are calculated using a form of equation 97 and the heats of formation listed in Tables XIII and XIV. Upper limits for the heats of formation are $\Delta H_f(POF_4^-)$ = -345 kcal/mole and $\Delta H_f(PSF_4^-)$ = -309 kcal/mole. No literature values are available for comparison with these calculations.

The observation of shift in the ionization efficiency curve for the secondary ion at high repeller voltage was also observed for the formation of PSF_4^- as is shown in Figure 28, and the plot of relative ion abundance as a function of repeller voltage for PSF_4^- formation is shown in Figure 29. Extrapolation of the rising portion of the curve to zero ion abundance may not be valid here since the maximum in the rising portion of the curve lies beyond the limits of the data available. The extrapolated value of repeller voltage (2.8 volts) indicates that the reaction occurs with an

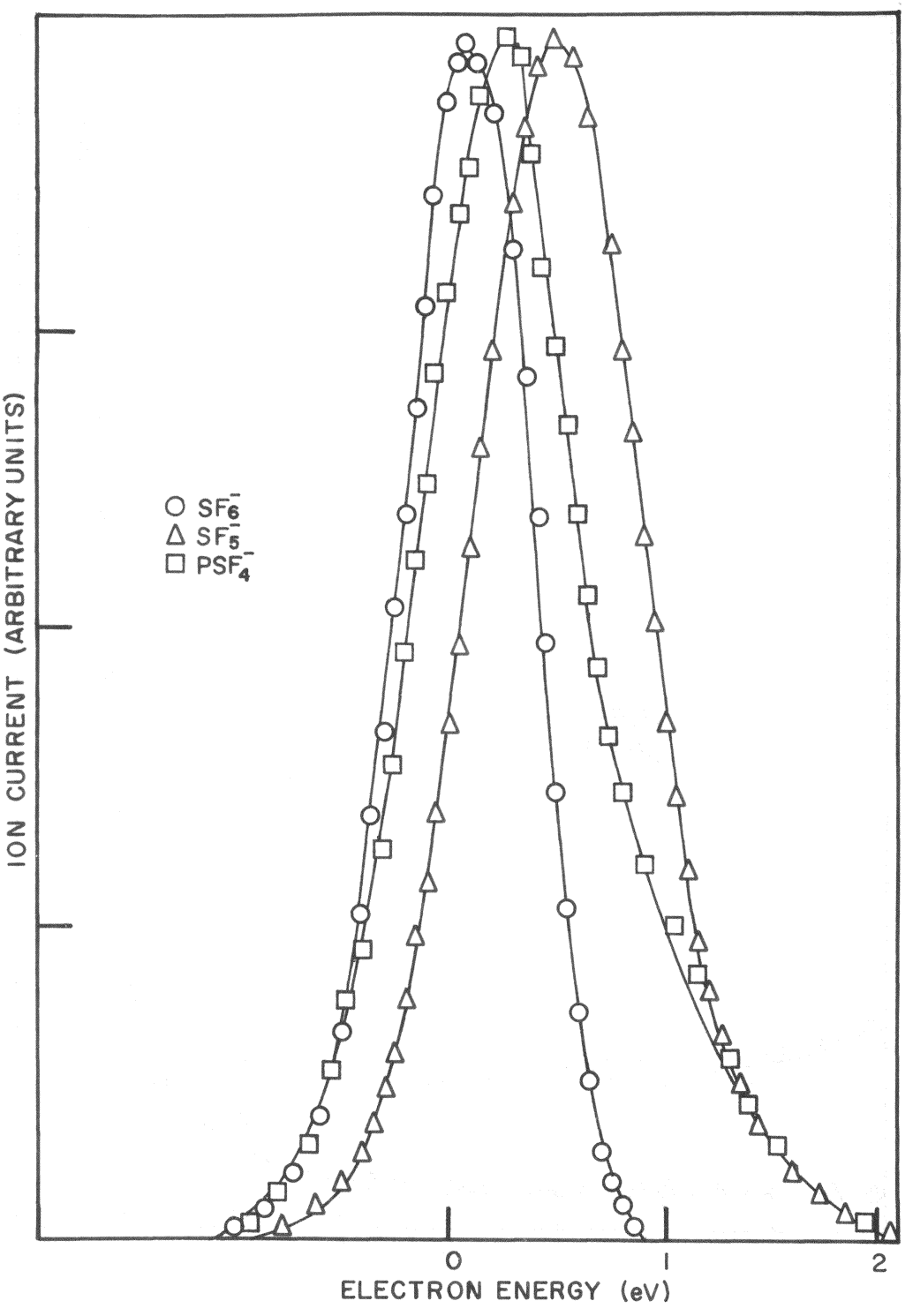

FIGURE 28. IONIZATION EFFICIENCY CURVES FOR SF_6^-, SF_5^- AND PSF_4^- AT 6.0V REPELLER

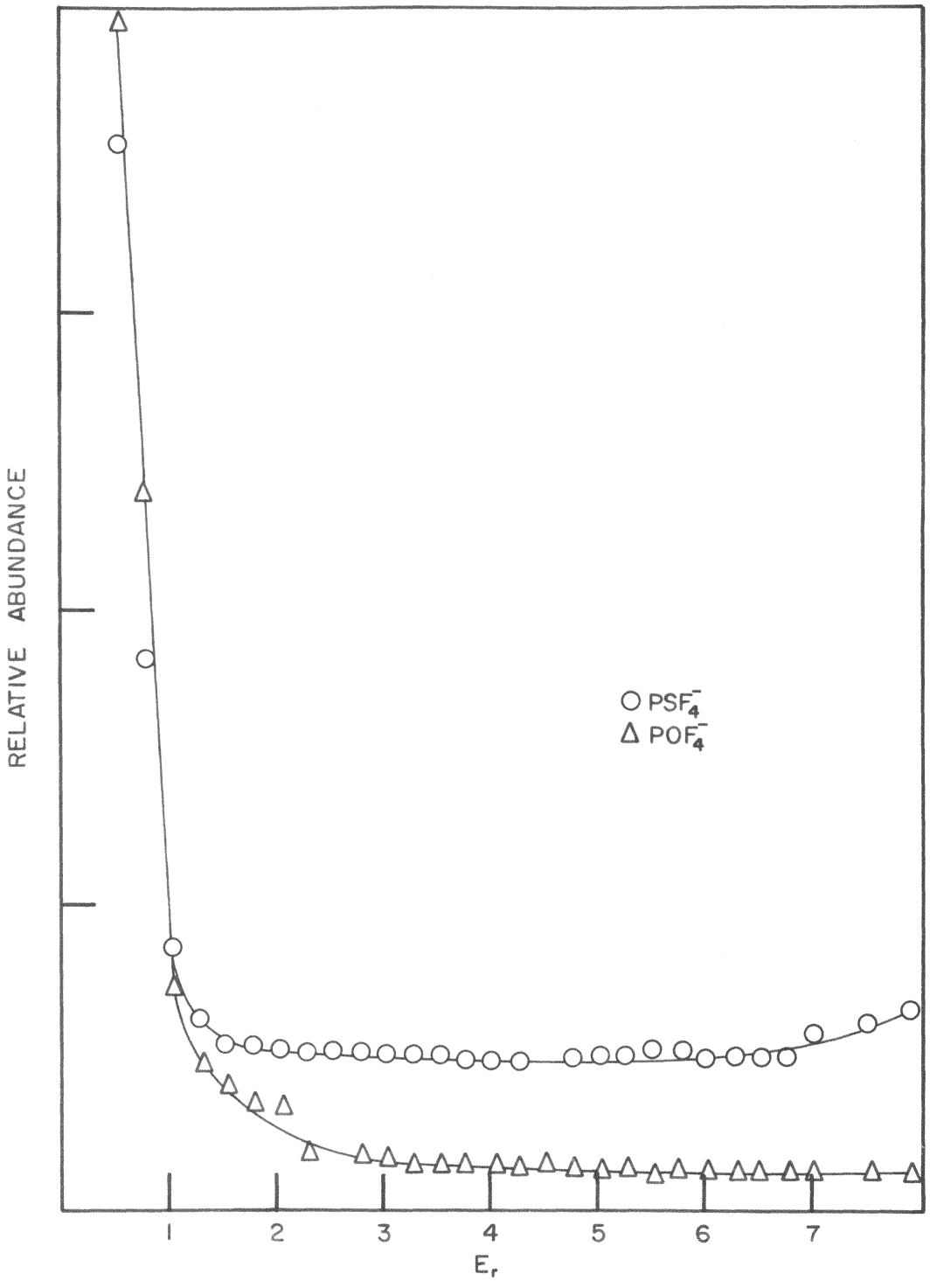

FIGURE 29. FRACTIONAL ABUNDANCE OF POF_4^- AND PSF_4^- AS A FUNCTION OF REPELLER VOLTAGE

endothermicity of 24 kcal/mole, so that $\Delta H_f(PSF_4^-) = -349$ kcal/mole.

A shoulder on the ionization efficiency curve of POF_4^- was also observed at high repeller voltages, but the variation in ion abundance for POF_4^- as a function of repeller voltage, shown in Figure 29, indicates that the identification of an endothermic reaction involving SF_5^- cannot be accomplished from the data available. The absence of an increase in POF_4^- ion current at high repeller voltages can only be rationalized by the assumption that the cross section for the reaction

$$SF_5^- + POF_3 \rightarrow POF_4^- + SF_4 \qquad (100)$$

is much smaller than that for PSF_4^- formation.

Pentafluorosilicate (IV): SiF_5^-

The heat of formation of the SiF_5^- anion is determined to be $\Delta H_f(SiF_5^-) = -441$ kcal/mole from combination of the heats of formation of ions and neutrals in the reaction

$$SF_6^- + SiF_4 \rightarrow SiF_5^- + SF_5 \qquad (101)$$

MacNeil and Thynne (110) have determined a value for $\Delta H_f(SiF_5^-)$ which is -583 kcal/mole, from the ion-molecule reaction

$$SiF_3^- + SiF_4 \rightarrow SiF_5^- + SiF_2 \qquad (102)$$

This value may be compared with the $\Delta H_f(SiF_5^-)$ determined here, and the difference probably is the result of internal and/or kinetic energy in the reactants and products. These quantities were not measured in either of the determinations of $\Delta H_f(SiF_5^-)$.

Examination of the ionization efficiency curve for SiF_5^- at high repeller voltages reveals that a shift in the curve is observed,

suggesting the occurrence of an endothermic process as described for PF_6^-. The fractional abundance of SiF_5^-, when plotted as a function of repeller voltage, showed an increase at high repeller voltage similar to that observed for PF_6^- in Figure 27. The extrapolated onset for formation of SiF_5^- by the endothermic process was found to occur at a repeller voltage of 4.5 volts, so that the endothermicity of the reaction for formation of SiF_5^- was 39 kcal/mole. Therefore the heat of formation of SiF_5^- was calculated to be $\Delta H_f(SiF_5^-) = -466$ kcal/mole for the endothermic process.

Comparison of the two values obtained for $\Delta H_f(SiF_5^-)$ from this study shows that the heat of formation obtained from the endothermic process is more negative than that from reaction 101 by about 25 kcal/mole, suggesting that the $\Delta H_f(SiF_5^-)$ obtained from the endothermic reaction has fewer contributions from internal and/or kinetic energy.

Tstrafluoroborate (III) and Tstrafluorophosphate (III): BF_4^- and PF_4^-

Upper limits for the heats of formation of the secondary ions BF_4^- and PF_4^- are calculated by combining the heats of formation of reactants and products in reaction 96 to obtain $\Delta H_f(BF_4^-) = -327$ kcal/mole and $\Delta H_f(PF_4^-) = -275$ kcal/mole.

Other investigators have evaluated ionic heats of formation of BF_4^- from lattice energy calculations (108,109) to be -407 kcal/mole. This estimate compares at least qualitatively with the present value and the discrepancy likely arises from the fact that the value obtained in the ion-molecule reaction study does not take into account the internal energy or kinetic energy of the reactants and products. Such contributions may be

significant in negative ion formation and reaction processes.

Shoulders were also observed on the ionization efficiency curves of the ions BF_4^- and PF_4^- at high repeller voltages, and the variation of relative ion abundance for BF_4^- and PF_4^- formation as a function repeller voltage is similar to that shown for POF_4^- in Figure 29 in that no increase was observed at high repeller voltage. Therefore no estimates of ionic heats of formation of these ions may be determined.

Tetrafluoroarsenate (III) and Hexafluoroarsenate (V): AsF_4^- and AsF_6^-

The primary ion AsF_4^- is formed near 0 eV by the process

$$AsF_5 + e^- \rightarrow AsF_4^- + F \qquad (103)$$

as observed in this study, and taking the appearance potential of AsF_4^- to be 0, the heat of formation of AsF_4^- is -308 kcal/mole.

Based on the reactions of SF_6^- with AsF_3 and AsF_5 to form the secondary ions AsF_4^- and AsF_6^-, respectively, upper limits for the heats of formation of these ions are $\Delta H_f(AsF_4^-) = -273$ kcal/mole and $\Delta H_f(AsF_6^-) = -351$ kcal/mole. The formation of secondary ions in pure AsF_5 was also observed, and AsF_6^- is formed by the process

$$AsF_4^- + AsF_5 \rightarrow AsF_6^- + AsF_3 \qquad (104)$$

The heat of formation of AsF_6^- may be calculated from this process since the heats of formation of AsF_5 and AsF_3 are known and $\Delta H_f(AsF_4^-)$ has been determined from measurements of the appearance potential of AsF_4^- formed by reaction 103. The heat of formation of AsF_6^- formed in reaction 104 is thus $\Delta H_f(AsF_6^-) = -384$ kcal/mole. If the value of $\Delta H_f(AsF_4^-)$ determined from the reaction of SF_6^- with AsF_3 is used in calculating $\Delta H_f(AsF_6^-)$,

then the heat of formation determined is -349 kcal/mole. This value is much closer to the $\Delta H_f(AsF_6^-)$ determined from the SF_6^- reaction with AsF_5, and is less negative than the previous value by 33 kcal/mole. It is interesting to note that this difference is at the upper limit of estimates for the electron affinity of SF_6 and is therefore approximately the limit of excitation energy to be contained in SF_6^- formed at 0.08 eV electron energy. It is not probable, however, that all of this energy is transferred to the secondary ion in the ion-molecule reaction since the energy transferred to products must be distributed according to the ratio of reduced masses of the products. SF_5 would therefore be expected to retain a share of the internal energy of SF_6^-, and it appears that the difference of 33 kcal/mole cannot be attributed entirely to excitation in SF_6^-. The $\Delta H_f(AsF_6^-)$ = -384 kcal/mole is assumed to be the more meaningful value for the heat of formation of AsF_6^- since, being more negative, it likely contains fewer contributions from excitation energy than does the value obtained from the ion-molecule reaction of SF_6^- and AsF_5.

Examination of the ionization efficiency curves for the secondary ions AsF_4^- and AsF_6^- formed at high repeller voltages reveals that shoulders are observed similar to that for PF_6^-, suggesting that an endothermic process similar to reaction 98 is occurring. However, since reliable ion current measurements for these ions were not obtained at repeller voltages greater than 5 V, no onset for such a process was observed and no calculations of $\Delta H_f(AsF_4^-)$ or $\Delta H_f(AsF_6^-)$ from endothermic reactions were carried out.

Pentafluoroarsenate (IV): AsF_5^-

The heat of formation of AsF_5^- may be evaluated from the reaction

$$AsF_4^- + AsF_5 \rightarrow AsF_5 + AsF_4 \quad (105)$$

if $\Delta H_f(AsF_4)$ is known. This quantity may be calculated from the relationship

$$AsF_5 \rightarrow AsF_4 + F \quad (106)$$

where the heat of formation of AsF_4 is given by

$$\Delta H_f(AsF_4) = D(AsF_4\text{-}F) + \Delta H_f(AsF_5) - \Delta H_f(F) \quad (107)$$

In order to evaluate the bond dissociation energy of AsF_5 the reaction

$$AsF_5 \rightarrow AsF_3 + 2F \quad (108)$$

is considered since the heats of formation of all the quantities are known. From the relationship

$$D(AsF_4\text{-}F) + D(AsF_3\text{-}F) = \Delta H_f(AsF_3) + 2\Delta H_f(F) - \Delta H_f(AsF_5) \quad (109)$$

the bond dissociation energy for the two As-F bonds is determined to be 114 kcal/mole and $D(AsF_4\text{-}F)$ is taken as one-half this energy, or 57 kcal/mole.

Equation 107 may now be utilized to obtain $\Delta H_f(AsF_4) = -258$ kcal/mole, and the heat of formation of AsF_5^- formed by reaction 103 is calculated to be $\Delta H_f(AsF_5^-) = -346$ kcal/mole. If one assumes that AsF_5^- may be formed by the process

$$AsF_5 + e^- \rightarrow AsF_5^- \quad (110)$$

then the near-zero appearance potential observed for AsF_5^- may be utilized to calculate $\Delta H_f(AsF_5^-) = -296$ kcal/mole.

It is worthwhile to emphasize again that the heats of formation of ions calculated here are upper limits and do not correspond to equilibrium values since no provision for kinetic energy in the ionic and neutral species was made. Therefore the calculated values may differ from equilibrium values by as much as several eV.

Charge-Transfer Reactions and Relative Molecular Electron Affinities

As the result of experiments in this study it has been proposed that AsF_5^- is formed via charge transfer with AsF_4^- according to the reaction

$$AsF_4^- + AsF_5 \rightarrow AsF_5^- + AsF_4 \qquad (105)$$

No other nonmetal fluoride studied here (except SF_6) formed a parent negative ion or participated in a reaction similar to reaction 105. SF_6, when introduced into the mass spectrometer, forms the parent negative ion SF_6^-. This ion does not undergo charge transfer with AsF_5 since addition of AsF_5 to SF_6 in the mass spectrometer caused no change in the SF_6^- ion current after the initial process of passivating the ion source was completed. The SF_6^- ion current showed no dependence on AsF_5 pressure, and thus it is proposed that the reactions

$$SF_6 + AsF_4^- \rightarrow SF_6^- + AsF_4 \qquad (111)$$

$$SF_6 + AsF_5^- \rightarrow SF_6^- + AsF_5 \qquad (112)$$

do not occur. Since both the $\Delta H_f(AsF_4)$ and $\Delta H_f(AsF_4^-)$ have been determined in this study the electron affinity of AsF_4 may be estimated to be .65 eV< E.A.(AsF_4)<2.2 eV depending upon which value for $\Delta H_f(AsF_4^-)$ is selected from the table. Since the value of $\Delta H_f(AsF_4^-)$ = -308 kcal/mole has been designated as the "best" value, the E.A.(AsF_4) is probably about 2.2 eV.

This is greater than estimates for the electron affinity of SF_6 (93,104), and thus charge transfer from AsF_4^- to SF_6 is not expected. Since this behavior is indeed observed, it may be concluded that E.A.(SF_6)<E.A.(AsF_4).

No charge transfer was observed from SF_6^- to any of the nonmetal fluorides by reactions such as

$$SF_6^- + BF_3 \rightarrow BF_3^- + SF_6 \qquad (113)$$

so that for each of the nonmetal fluorides the molecular electron affinity is less than that of SF_6.

III. REACTION CROSS SECTION AS A MEASURE OF ACCEPTOR PROPERTIES

The nonmetal fluorides investigated in this study are well-known for their behavior as Lewis acids in solution. PF_5 forms the PF_6^- anion in solution (17,18,19) and many salts containing this anion have been isolated (18,19). PF_3 is known to form a 1:1 adduct with trimethylamine (112). BF_3 forms many complexes with Lewis bases, and the acidity of BF_3 has been studied by many workers (18,19,113,114). Wilkins and Grant (115) and Muetterties (116) have investigated adduct formation with SiF_4, and the SiF_5^- anion has been isolated by Clark and Dixon (100). The acceptor properties of AsF_3 are well known and the AsF_4^- anion has been identified by Woolf and Greenwood (117) and by Muetterties and Phillips (118). AsF_5 is a strong acid and forms the AsF_6^- ion in solution (18,19). The acceptor properties of POF_3 and PSF_3 are less well-characterized than are the other nonmetal fluorides studied here. Muetterties, Bither, Farlow, and Coffman (17) have noted that POF_3 has little tendency to form adducts with typical organic bases. The chemical behavior of PSF_3 has not been

widely investigated since it is spontaneously flammable in air (74).

The nonmetal fluorides described here are thus divided into two groups, those having strong acceptor properties (BF_3, AsF_5, AsF_3, PF_5, and SiF_4) and those having relatively weak or unknown acceptor properties (PF_3, POF_3, and PSF_3).

Addition of a fluoride ion to the nonmetal fluoride molecule is analogous to the addition of a pair of electrons to the molecule, and the ability of the nonmetal fluoride to accept the fluoride ion is certainly related to the ease with which the electron pair from F^- may be incorporated into the bonding sphere of the molecule. Steric factors probably do not play a large role in the addition of F^- to the molecule since the fluoride ion is extremely small.

Since the fluoride ion transfer reactions studied here involve addition of F^- to the bonding sphere of the neutral nonmetal fluoride by the gas-phase process

$$SF_6^- + AF_n \rightarrow \left[AF_{n+1}\right]^- + SF_5 \qquad (114)$$

a determination of the relative ease of incorporation of this fluoride ion should provide information regarding the Lewis acidity of the free molecule.

Since the Lewis base SF_6^- in reaction 114 is common to reactions involving the nonmetal fluorides, no differences in reactivity of the base should be involved in comparisons of relative reactivities toward this base. SF_6^- is generated by resonance electron capture of thermal energy electrons, and since the width of the ionization efficiency curve reflects the energy distribution of the electrons used in forming SF_6^- (16),

it is possible to select ions of uniform energy distributions by observing the width of the electron capture curve. This procedure was followed in these experiments, so that in all cases the reactant ion SF_6^- was in very nearly the same energy state. In addition, the studies were all carried out at a constant temperature of approximately 100° C, and therefore differences in reactivity of the base due to differences in population of excited vibrational or electronic states in reaction 114 should be minimized.

The reaction cross section for the process illustrated by reaction 114 is an indication of the reactivity of the free nonmetal fluoride molecule, unaffected by solvent interactions, toward the radical anion SF_6^-, and since the process for formation of secondary ions has been identified as common to each of the species forming secondary ions in mixtures with SF_6, comparison of the reaction cross section for these processes should be a valid measure of the relative acceptor strength exhibited by the nonmetal fluoride molecules.

The reaction cross sections for the formation of secondary ions by reaction 114 are summarized in Table XV. Since the reaction forming AsF_4^- from AsF_3 exhibits the largest cross section at all repeller voltages for those reactions studied, a scale of Lewis acidities may be constructed relative to the reactivity of AsF_3. By taking the reactivity of AsF_3 to be unity at each repeller voltage, the reactivity of each of the nonmetal fluorides may be determined relative to this cross section and the order determined should be independent of repeller voltage. The relative Lewis acid strengths of the nonmetal fluorides determined in this way are presented in Table XVI. It is apparent that the relative acidity is indeed

TABLE XV

SUMMARY OF REACTION CROSS SECTIONS FOR THE FORMATION OF SECONDARY IONS AS A FUNCTION OF REPELLER VOLTAGE

Repeller Voltage	Cross Section (A^2/molecule) Secondary Ion							
(V)	AsF_4^-	BF_4^-	SiF_5^-	AsF_6^-	PF_6^-	POF_4^-	PF_4^-	PSF_4^-
1.5	100.7	73.6	68.8	72.4	34.4	4.64	3.88	0.429
2.0	84.7	73.9	56.5	55.8	31.9	5.50	2.88	0.412
2.5	78.7	57.3	52.1	39.6	28.5	4.28	2.60	0.413
3.0	73.7	56.7	50.1	34.7	25.7	3.71	1.09	0.404
3.5	69.7	46.9	47.2	32.7	24.9	3.45	1.68	0.404
4.0	69.5	51.2	48.8	30.4	23.3	3.02	1.59	0.381

independent of the repeller voltage at which the cross section was determined, indicating that the Lewis acid strength listed here reflects the acidity of the molecule rather than experimental conditions in the ion source. Examination of these data suggest an order of acid strength of $AsF_3 > BF_3 > SiF_4 > AsF_5 > PF_5 >> POF_3 > PF_3 > PSF_3$.

This order of Lewis acid strength is in general agreement with solution studies, since AsF_3, AsF_5, BF_3, PF_5, and SiF_4 are denoted as strong Lewis acids and PF_3 is considered to be a weak Lewis acid (74). Clifford, Beachell, and Jack (18) have determined relative acidities of fluorides in HF solution, and BF_3 and AsF_5 were found to exhibit a strong acid nature whereas PF_5 was designated a weak acid and SiF_4 was described as extremely weak. This is in contrast to the order determined from ion-molecule reaction studies, since the cross section for SiF_5^- formation is larger than that for PF_6^- by a factor of 2 and is nearly as large as the cross section for BF_4^- formation.

The prediction that SiF_4 is a strong Lewis acid based on the gas-phase ion-molecule reactions described here and the reverse prediction from studies in HF solution (18) reflect the basic difference in the experiments conducted. The solution study involved equilibria in which the dissociation of hydrogen fluoride provides an excess of fluoride ions which may be added to SiF_4 to give the SiF_6^- anion, whereas the gas-phase experiments are non-equilibrium processes with respect to the "saturation" of silicon with fluorines, since only one reactive collision is allowed per SiF_4 molecule at pressures used in this study. The anion formed is immediately extracted from the reaction zone (the ion source) and therefore the observed cross section reflects the addition of only

TABLE XVI

RELATIVE LEWIS ACID STRENGTH FOR NONMETAL FLUORIDES

Repeller Voltage	Relative Lewis Acidity Nonmetal Fluoride							
(V)	AsF_3	DF_3	SiF_4	AsF_5	PF_5	POF_3	PF_3	PSF_3
1.5	1.00	0.73	0.68	0.72	0.34	0.046	0.038	0.004
2.0	1.00	0.87	0.67	0.66	0.38	0.065	0.034	0.005
2.5	1.00	0.74	0.66	0.50	0.36	0.055	0.033	0.005
3.0	1.00	0.77	0.68	0.47	0.35	0.050	0.026	0.005
3.5	1.00	0.67	0.66	0.47	0.31	0.050	0.024	0.006
4.0	1.00	0.78	0.75	0.46	0.36	0.046	0.024	0.006
Average	1.00	0.76	0.68	0.55	0.35	0.052	0.030	0.005

one fluoride ion to form the SiF_5^- ion.

The prediction of relative stability of the hexafluoro anions is in accord with that observed in solution (17,18,19), and the weak acceptor properties of PF_3 compare with that proposed from solution studies by Muetterties, Bither, Farlow and Coffman (17).

Arsenic pentafluoride is often classified a stronger Lewis acid than BF_3 (18,19), and the order predicted here is the opposite, although both are certainly classified as having strong acceptor properties. The AsF_5 system studied here was found to be much more complicated than the other nonmetal fluorides, with ion-molecule reactions being observed in the pure gas as well as in mixtures of AsF_5 and SF_6. Reactions of SF_6^- with AsF_5 should occur independent of those occurring with AsF_4^-, and the method of calculation of the cross section for the SF_6^- reaction should remove only those contributions from the AsF_4^- reaction. Therefore no reason is immediately obvious why the Lewis acidity given in Table XVI cannot be taken as the true reactivity of AsF_5 toward the Lewis base.

The general agreement of the order of Lewis acidities determined from gas-phase studies of negative ion-molecule reactions suggests that such studies may be a means of establishing a quantitative scale of Lewis acidities of inorganic molecules.

IV. THE EFFECT OF STRUCTURAL PARAMETERS ON REACTIVITY

Understanding the relationship between structure and reactivity may be considered the ultimate goal of the chemical kineticist, and a determination of this relationship must come from experimental observations of rates and mechanisms of reactions. The determination of the relationship

of structure to reactivity involves a study of chemical reactions for a series of molecules with various structural parameters. To eliminate effects of solvents, and condensed phase interactions, it is important to carry out these investigations in the gas phase where molecular reactivity may be evaluated. Unfortunately many reactions cannot be studied in this way, since reactions which occur in solution are not energetically possible in the gas phase where a solvent cannot provide activation energy and/or a stabilizing influence on the products formed.

However, it has been demonstrated that gas-phase reactions of negative ions with nonmetal fluoride molecules provide a system of gaseous ionic reactions which is useful for relating intrinsic reactivity of the molecule to structural parameters.

Effect of Electron Density Distribution on Reactivity

Schaefer and Henis (60) have proposed an electron density rearrangement model for ion-molecule reactions which assumes that the dominant effect in low energy exothermic reactions may simply be the extent of electron density rearrangement required in proceeding from reactants to products. The general negative ion molecule reaction

$$A^- + BC \rightarrow AB^- + C \qquad (111)$$

is considered in terms of the relative electronegativities at the reaction centers A and B. If the electronegativity of A is larger than B, then little rearrangement of electron density will be necessary upon proceeding to the AB^- ion since the more electronegative A moisty will command a larger share of the electron density in the product ion. Similarly, if

the electronegativity of B is much larger than that of A, then formation of the product ion will require a net shift of electron density to B at or near the time of reaction. The authors (60) thus predict that for the situation requiring little effective rearrangement of electron density the reaction will be enhanced and a large reaction cross section ($Q > 1 A^2$/molecule) will probably be observed. Likewise, if the relative values of the electronegativities of A and B are such that extensive rearrangement occurs, then a small cross section is expected for the reaction.

Applying the criteria of Schaefer and Henis (60) to the fluoride ion transfer reactions results in the prediction of large reaction cross sections for each of the reactions reported. The electronegativities (119) for atoms of interest in these reactions are: F = 4.0, P = 2.2, As = 2.2, B = 2.0, Si = 1.9, O = 3.4, and S = 2.6. Since the electronegativity of fluorine is much larger than either of the atoms occupying the reaction center of the neutral molecule, then little electron density rearrangement should be required upon transfer of a fluoride ion to the neutral molecule to form the secondary ion. Calculations of electronic distributions in the molecules SF_6 and PF_5 tend to support this prediction for the binary nonmetal fluorides.

Santry and Segal (120) have pointed out that the electronic distribution in SF_6 involves a net shift of electron density to the fluorine atoms. These authors also suggest that the electronic distribution in PF_5 is quite similar to that in SF_6, with electron density on the fluorine atoms being significant due to inefficient back-donation of electrons to the phosphorus. Similar electronic distributions may be expected with the arsenic, boron, and silicon fluorides. Mitchell (121) has suggested that

the unpaired electron in SF_6^- may lie in a molecular orbital having a large contribution from the sulfur atomic orbitals, thus maintaining significant electron density on the fluorine atoms. Since both the reactant ion and the neutral are likely characterized by a high electron density on the fluorine atoms, little rearrangement of electron density is necessitated by transfer of fluoride ion to the neutral molecule and the prediction of a high reaction cross section for this process is deemed reasonable. The interpretation of the electron density rearrangement model is somewhat more involved, however, for phosphoryl and thiophosphoryl fluoride.

Oxygen and sulfur both have electronegativities greater than that of phosphorus, and the electron density in POF_3 and PSF_3 is likely distributed toward both the fluorines and the oxygen or sulfur atom, giving the phosphorus atom a distinctly positive character. Transfer of a fluoride ion to these molecules would require little rearrangement of electron density since in both the reactant and product electron density on the fluorine atoms is significant. Therefore the Schaefer-Henis theory predicts a large cross section for this process. The formation of POF_4^- is found to have a cross section larger than that for PF_4^- formation, but the reaction involving PSF_3 does not agree with the predictions of the Schaefer-Henis model.

In addition, the large range of values of reaction cross section observed for these reactions is not explained in a satisfactory manner by the electron density rearrangement model. It is suggested that factors in addition to the rearrangement of electron density must be considered in order to obtain more meaningful predictions.

Effect of Dipole Moment on Reactivity

Of the nonmetal fluorides discussed here, BF_3, SiF_4, PF_5, and AsF_5 have zero dipole moments, whereas each of the other nonmetal fluoride reactants has a nonzero moment. Since neutral molecules having a permanent dipole should exhibit different behavior in colliding with an ion than should molecules with a symmetrical charge distribution, it is instructive to consider the effect of dipole moment on reaction cross sections determined for ion-molecule reactions in the gas phase.

Moran and Hamill (57) have proposed that in collisions involving ions and neutral species with permanent dipole moments, the reaction cross section is quite large if the possibility of orientation of the ion-dipole forces is allowed. However, at high ion velocities the alignment becomes less likely, and the cross section is observed to decrease. Thus the effect of dipole attractions is to enhance the reaction cross sections if the alignment of ion and dipole may be readily accomplished.

The nonmetal fluorides having zero dipole moments will not be affected by the negative charge upon approaching SF_6^- in a reactive collision. Therefore the reaction cross sections for these ions will not be dependent on any particular orientation with respect to the ion. However, the molecules PF_3, AsF_3, POF_3, and PSF_3 each have a permanent dipole, and orientation effects probably are important in these molecules.

The dipole moments determined for PF_3, AsF_3, POF_3 and PSF_3 are 1.07 (122), 2.81 (123), 1.77 (122), and 0.63 (124) Debye units, respectively. Following the argument of Moran and Hamill (57) these molecules are predicted to have a high reaction cross section if interaction with the impacting ion may be accomplished with the proper orientation of the dipole

with respect to the charge of the ion. If such alignment is achieved, then the molecule will be locked in with the ion and the reaction process will be enhanced. However, if the required orientation cannot be assumed by the molecule, reaction will be less likely to occur and the reactivity of the molecule will probably be quite low. Within the group of molecules with a dipole moment, the order of increasing observed cross section should parallel the order of increasing dipole moment, and this is indeed the case observed.

The effect of the dipole is not always strong enough to enhance the reaction, however, since only AsF_3 exhibits a larger cross section than the molecules having a symmetrical charge distribution. Electronegative substituents at the positive end of the dipole may shield the phosphorus atom from the negative charge on SF_6^- and thus nullify the enhanced reactivity expected from contributions of the dipole moment.

POF_3 and PSF_3 are symmetric top molecules with the oxygen and sulfur atom oriented away from the fluorines. The presence of the oxygen and sulfur atoms at the positive end of the molecule apparently nullifies the lock-in effect of the dipole with the charge of the ion, and the fluoride ion transfer to the phosphorus in thus retarded. PF_3 has no electronegative atom at the positive end of its dipole, but charge delocalization in the molecule results in considerable π-bond character being attributed to the P-F bonds (125). Thus the electron pair in phosphorus is not so tightly bound as that in AsF_3, and the donation of these electrons is possible as in the formation of PF_3 complexes similar to those of carbon monoxide. Phosphorus trifluoride is expected to have a low reactivity toward the negative SF_6^-, and this is the observed behavior. In PF_3, the

electron pair apparently functions in the same manner as the oxygen and sulfur atom in POF_3 and PSF_3, and the effect of the dipole in overcoming this obstruction is reflected in the observed order of reaction cross sections for these molecules.

The previous discussions have illustrated the importance of molecular parameters such as electron density distribution and dipole moment in determining the reactivity of the nonmetal fluorides toward SF_6^-. In addition, the structure of the molecule determines to a large extent the ability of the molecule to assume a proper orientation which will enhance the fluoride ion transfer, and the ability of the central atom to expand its bonding sphere to include the incoming fluoride ion is instrumental in the transfer process.

The role of oxidation state and coordination number is evident in the relative reactivities of the phosphorus and arsenic fluorides. Phosphorus (V) readily expands its coordination number in forming the PF_6^- anion, whereas trivalent phosphorus cannot accommodate another atom in its coordination sphere so easily, apparently due to the presence of the electron pair. Molecules containing four-coordinate phosphorus also are not able to expand their coordination number with the facility evident in the formation of PF_6^-, and the symmetrical octahedral structure of the six-coordinate phosphorus may be a factor which contributes to the stability observed.

The six-coordinate structure attained in AsF_6^- also illustrates the ease of expanding the coordination sphere from five coordination to six-coordination, and the large reaction cross section observed for this process is in agreement with the expected behavior. Arsenic trifluoride

has long arsenic-fluorine bonds (1.72 Å compared to 1.53 Å in PF_3), indicating that the effective charge on the As atom is probably quite positive with respect to the fluorines. This positive effective charge apparently enhances the addition of a fourth fluorine, and the large cross section observed for this reaction indicates that effective charge at the reaction center is important in determining the reactivity of the molecule. The highly polar bonds in SiF_4 and BF_3 likewise contribute to the effective positive character of the nonmetal, and the high cross section for addition of F^- to these molecules reflects the importance of this parameter in determining reactivity.

The investigation of gaseous negative ion-molecule reactions thus enables the correlation of varied structural parameters with reactivity in the absence of any solvent effects. In these experiments the chemical behavior observed is that of free ions and molecules, and the conclusions drawn from these studies should therefore aid in attaining the goal of relating structural parameters to the inherent chemical reactivity of molecules.

VI. LITERATURE CITED

1. J. J. Thomson, "Rays of Positive Electricity and Their Application to Chemical Analyses," Longmans, Green, and Co., London, 1913.

2. R. W. Kiser, "Introduction to Mass Spectrometry," Prentice Hall, Inc., Englewood Cliffs, N. J., 1965.

3. H. F. Chalcote and D. E. Jensen, Advan. Chem. Ser., 58, 291 (1966).

4. B. Steiner, J. Chem. Phys., 49, 5097 (1968).

5. C. E. Melton, J. Phys. Chem., 74, 582 (1970).

6. F. C. Fehsenfeld, A. L. Schmeltekopf, H. I. Schiff, and E. E. Ferguson, Planet. Space Sci., 15, 373 (1966).

7. A. A. Frost and R. G. Pearson, "Kinetics and Mechanism," 2nd. ed., John Wiley and Sons, Inc., New York, N. Y., 1964, pp. 147-157.

8. T. O. Tiernan and B. M. Hughes, presented at the Seventeenth Annual Conference on Mass Spectrometry and Allied Topics, Dallas, Texas, May, 1969.

9. W. K. Stuckey and R. W. Kiser, Nature, 211, 963 (1966).

10. R. D. Dougherty, J. Chem. Phys., 50, 1896 (1969).

11. E. W. McDaniel, "Collision Phenomena in Ionized Gases," John Wiley and Sons, Inc., New York, N. Y., 1964, pp. 368-422.

12. J. R. Case and F. Nyman, Nature, 193, 473 (1962).

13. G. C. Demitras and A. G. MacDiarmid, Inorg. Chem., 3, 1198 (1964).

14. L. Brewer, C. Cheng, and B. King, Inorg. Chem., 9, 814 (1970).

15. K. D. Asmus and J. H. Fendler, J. Phys. Chem., 72, 4285 (1968).

16. W. M. Hickam and R. E. Fox, J. Chem. Phys., 25, 642 (1956).

17. E. L. Muetterties, T. A. Bither, M. W. Farlow, and D. D. Coffman, J. Inorg. Nucl. Chem., 16, 52 (1960).

18. A. F. Clifford, H. C. Beachell, and W. M. Jack, J. Inorg. Nucl. Chem., 5, 57 (1957).

19. K. O. Christe and A. E. Pavlath, Z. Anorg. Allgem. Chem., 335, 210 (1965).

20. A. J. Dempster, Phil. Mag., 31, 438 (1916).

21. T. R. Hogness and E. G. Lunn, Phys. Rev., 26, 44 (1925).

22. H. Eyring, J. O. Hirschfelder, and H. S. Taylor, J. Chem. Phys., 4, 479 (1936).

23. M. P. Langevin, Ann. Chem. Phys., 5, 245 (1905).

24. T. R. Hogness and R. W. Harkness, Phys. Rev., 32, 784 (1928).

25. G. C. Eltenton, "Monthly Reports of Shell Development Co.," Emeryville, Calif., April, 1940; cited by D. P. Stevenson in "Mass Spectrometry," C. A. McDowell, Ed., McGraw-Hill Book Co., Inc., New York, N. Y., 1963, p. 591.

26. V. L. Tal'rose and A. K. Lyubimova, Dokl. Akad. Nauk SSSR, 86, 929 (1952).

27. G. Gioumousis and D. P. Stevenson, J. Chem. Phys., 29, 294 (1958).

28. J. L. Franklin, F. H. Field, and F. W. Lampe, Adv. Mass Spectrometry, 1, 308 (1959).

29. F. W. Lampe, J. L. Franklin, F. H. Field, Progr. Reaction Kinetics, 1, 69 (1961).

30. M. S. B. Munson and F. H. Field, J. Amer. Chem. Soc., 88, 2621 (1966); F. H. Field, Accounts Chem. Res., 1, 42 (1968).

31. E. E. Muschlitz, J. Appl. Phys., 28, 1414 (1957).

32. C. E. Melton and G. A. Ropp, J. Amer. Chem. Soc., 80, 5573 (1958).

33. A. Henglein and G. A. Muccini, J. Chem. Phys., 31, 1426 (1959).

34. E. E. Ferguson, F. C. Fehsenfeld, and A. L. Schmeltekopf, Adv. Atomic Molecular Phys., 5, 1 (1969).

35. J. F. Paulson, Advan. Chem. Ser., 58, 28 (1966).

36. J. F. Paulson, J. Chem. Phys., 52, 959 (1970).

37. F. C. Fehsenfeld, A. L. Schmeltekopf, D. B. Dunkin, and E. E. Ferguson, ESSA Technical Report ERL 135-AL 3, U. S. Government Printing Office, Washington, D. C., September, 1969.

38. J. A. Rutherford and B. R. Turner, J. Geophys. Res., 72, 3795 (1967).

39. J. L. Moruzzi and A. V. Phelps, J. Chem. Phys., 45, 4617 (1966).

40. P. Kebarle, S. K. Searles, A. Zolla, J. Scarborough, and M. Arshadi, Adv. Mass Spectrometry, 4, 621 (1968).

41. J. G. Dillard and J. L. Franklin, J. Chem. Phys., 48, 2349 (1968).

42. J. G. Dillard and J. L. Franklin, J. Chem. Phys., 48, 2353 (1968).

43. J. G. Dillard, J. L. Franklin, and W. A. Seitz, J. Chem. Phys., 48, 3828 (1968).

44. V. K. Kraus, W. Muller-Duysing, and H. Neuert, Z. Naturforsch., 16A, 1385 (1961).

45. K.A.G. MacNeil and J.C.J. Thynne, J. Phys. Chem., 74, 2257 (1970).

46. K.A.G. MacNeil and J.C.J. Thynne, Int. J. Mass Spectrom. Ion Phys., 3, 455 (1970).

47. S. Cradock, P. W. Harland, and J.C.J. Thynne, Inorg. Nucl. Chem. Lett., 6, 425 (1970).

48. J. G. Dillard and T. C. Rhyne, J. Amer. Chem. Soc., 91, 6521 (1969).

49. T. C. Rhyne and J. G. Dillard, Inorg. Chem., in press.

50. C. E. Melton in "Mass Spectrometry of Organic Ions," F. W. McLafferty, Ed., Academic Press, New York, N. Y., 1963, Chapters 2, 4.

51. E. E. Ferguson, Adv. Electronics Electron Phys., 24, 1 (1968).

52. I. Dzidic, A. Good, and P. Kebarle, Can. J. Chem., 48, 664 (1970).

53. N. Boelrijk and W. H. Hamill, J. Amer. Chem. Soc., 84, 730 (1962).

54. R. F. Pottie, A. J. Lorquet, and W. H. Hamill, J. Amer. Chem. Soc., 84, 529 (1962).

55. L. P. Theard and W. H. Hamill, J. Amer. Chem. Soc., 84, 1134 (1962).

56. D. A. Kubose and W. H. Hamill, J. Amer. Chem. Soc., 85, 125 (1963).

57. T. F. Moran and W. H. Hamill, J. Chem. Phys., 39, 1413 (1963).

58. J. C. Light, Discussions Faraday Soc., 44, 14 (1967).

59. F. A. Wolf, J. Chem. Phys., 44, 1619 (1966).

60. J. Schaefer and J. M. S. Henis, J. Chem. Phys., 49, 5377 (1968).

61. E. C. Beaty and P. L. Patterson, Phys. Rev., 137, A 346 (1965).

62. Z. Herman, J. Kerstetter, T. Ross, and R. Wolfgang, J. Chem. Phys., 46, 2844 (1967).

63. Roy H. Neynaber, Adv. Atomic Molecular Phys., 5, 57 (1969).

64. S. E. Butrill, Jr., J. Chem. Phys., 50, 4125 (1969).

65. R. P. Clow and J. H. Futrell, Int. J. Mass Spectrom. Ion Phys., 4, 165 (1970).

66. J. H. Futrell and C. D. Miller, Rev. Sci. Instrum., 37, 1521 (1966).

67. G. E. Wells and C. E. Melton, Rev. Sci. Instru., 28, 1065 (1957).

68. F. H. Field and J. L. Franklin, "Electron Impact Phenomena and the Properties of Gaseous Ions," Academic Press, New York, N. Y., 1957.

69. F. C. Fehsenfeld, J. Chem. Phys., 53, 2000 (1970).

70. G. M. Begun and R. N. Compton, J. Chem. Phys., 51, 2367 (1969).

71. F. W. Lampe, J. L. Franklin, and F. H. Field, J. Amer. Chem. Soc., 79, 6129 (1957).

72. G. W. Dulaney, "MADCAP IV," DECUS Program Library No. 8-237, Digital Equipment Corporation, Maynard, Mass., 1969.

73. "Biomedical Computer Programs," W. J. Dixon, Ed., University of California Press, Berkeley and Los Angeles, 1968, pp. 289-296.

74. R. D. W. Kemmitt and D. W. A. Sharp, Adv. Fluorine Chem., 4, 142 (1965).

75. F. A. Cotton and G. Wilkinson, "Advanced Inorganic Chemistry," 2nd ed., Interscience Publishers, New York, N. Y., 1962.

76. R. E. Rondeau, J. Chem. Eng. Data, 11, 124 (1966).

77. L. H. Long and D. Dollimore, J. Chem. Soc., 1954, 4457.

78. T. D. Coyle and F. G. A. Stone, J. Chem. Phys., 32, 1892 (1960).

79. G. Mitra, J. Amer. Chem. Soc., 80, 5639 (1958).

80. C. W. Tullock and D. D. Coffman, J. Org. Chem., 25, 2016 (1960).

81. G. G. Meisels, W. H. Hamill, and R. R. Williams, J. Chem. Phys., 25, 790 (1956).

82. C. D. Wagner, P. A. Wedsworth, and D. P. Stevenson, J. Chem. Phys., 28, 517 (1958).

83. F. H. Field and F. W. Lampe, J. Amer. Chem. Soc., 80, 5583 (1958).

84. T. W. Shannon and A. G. Harrison, J. Chem. Phys., 43, 4201 (1965).

85. A. G. Harrison, A. Ivko, and T. W. Shannon, Can. J. Chem., 44, 1351 (1966).

86. S. K. Gupta, E. G. Jones, A. G. Harrison and J. J. Myher, Can. J. Chem., 45, 3107 (1967).

87. D. P. Stevenson and D. O. Schissler, J. Chem. Phys., 23, 1353 (1955).

88. H. Gutbier, Z. Naturforsch., A, 12, 499 (1957).

89. D. P. Stevenson and D. O. Schissler, J. Chem. Phys., 29, 282 (1958).

90. V. Aquilanti, A. Galli, A. Giardini-Guidoni, and G. G. Volpi, J. Chem. Phys., 43, 1969 (1965).

91. F. Fehsenfeld, E. E. Ferguson, and A. L. Schmeltekopf, J. Chem. Phys., 45, 404 (1966).

92. F. C. Fehsenfeld, A. L. Schmeltekopf, and E. E. Ferguson, J. Chem. Phys., 46, 2802 (1967).

93. R. N. Compton, L. G. Christophorou, G. S. Hurst, and P. W. Reinhardt, J. Chem. Phys., 45, 4634 (1966).

94. D. Edelson, J. E. Griffiths, and K. B. McAfee, J. Chem. Phys., 37, 917 (1962).

95. J. M. S. Henis and C. A. Mabie, J. Chem. Phys., 53, 2999 (1970).

96. J. B. Hasted and S. Beg, Brit. J. Appl. Phys., 16, 1779 (1965).

97. C. E. Klots, J. Chem. Phys., 46, 1197 (1967).

98. R. K. Curran, J. Chem. Phys., 34, 1069 (1961).

99. D. W. A. Sharpe, Adv. Fluorine Chem., 1, 68 (1960).

100. H. C. Clark and K. R. Dixon, Chem. Commun., 717 (1967).

101. F. H. Field, J. L. Franklin, and F. W. Lampe, J. Amer. Chem. Soc., 79, 2419 (1957).

102. K. R. Ryan and J. H. Futrell, J. Chem. Phys., 42, 824 (1965).

103. A. G. Harrison, J. J. Myher, and J. C. J. Thynne, Advan. Chem. Ser., 58, 150 (1966).

104. C. Lifshitz and T. O. Tiernan, presented at the Eighteenth Annual Conference on Mass Spectrometry and Allied Topics, San Francisco, California, June, 1970.

105. D. D. Wagman, W. H. Evans, V. B. Parker, I Harlow, S. M. Bailey, and R. H. Schumm, "Selected Values of Chemical Thermodynamic Properties. Tables for the First Thirty-Four Elements in the Standard Order of Arrangement," National Bureau of Standards, Technical Note 270-3, U. S. Government Printing Office, Washington, D. C. 1968.

106. D. R. Stull, JANAF Thermochemical Tables, PB-168, 370, Department of Commerce Clearinghouse, Springfield, Virginia.

107. P.A.G. O'Hare and W. N. Hubbard, J. Phys. Chem., 69, 4358 (1965).

108. A. P. Altschuler, J. Chem. Soc., 17, 6187 (1955).

109. R. C. Waddington, "Lattice Energies," Advances in Inorganic Chemistry and Radiochemistry, H. J. Emeleus and A. G. Sharpe, Ed., Vol. 1, Academic Press, Inc., New York, N. Y., 1959, p. 157.

110. K.A.G. MacNeil and J.C.J. Thynne, Inorg. Chem., 9, 1946 (1970).

111. R. S. Berry, Chem. Rev., 69, 533 (1969).

112. J. Chatt and A. A. Williams, J. Chem. Soc., 1951, 3061.

113. N. N. Greenwood and R. L. Martin, Quart. Rev., 8, 1 (1954).

114. H. S. Booth and D. R. Martin in "Fluorine Chemistry," Ed. by J. H. Simons, Vol. 1, Academic Press, New York, N. Y., 1950, p. 201.

115. C. J. Wilkins and D. K. Grant, J. Chem. Soc., 927 (1953).

116. E. L. Muetterties, J. Amer. Chem. Soc., 82, 1082 (1960).

117. A. A. Woolf and N. N. Greenwood, J. Chem. Soc., 2200 (1950).

118. E. L. Muetterties and W. D. Phillips, J. Amer. Chem. Soc., 79, 3686 (1957).

119. A. L. Allred, J. Inorg. Nucl. Chem., 17, 215 (1961).

120. D. P. Santry and G. A. Segal, J. Chem. Phys., 47, 158 (1967).

121. K.A.R. Mitchell, Chem. Commun., 368 (1969).

122. S. N. Ghosh, R. Trambarulo, and W. Gordy, J. Chem. Phys., 21, 308 (1953).

123. R. G. Schulman, B. P. Dailey, and C. H. Townes, Phys. Rev., 78, 145 (1950).

124. N. J. Hawkins, V. W. Cohen, and W. S. Koski, J. Chem. Phys., 20, 528 (1952).

125. M. C. Day, Jr., and J. Selbin, "Theoretical Inorganic Chemistry," 2nd Ed., Rheinhold Book Corporation, New York, N. Y., 1969, p. 329.

VII. APPENDICES

Appendix A. The FOCAL language program used to calculate rate data for the fluoride ion transfer reaction forming AsF_4^- from AsF_3 is presented here. This program requires few changes to be applicable to any of the other reactions studied except the AsF_5 system. Only the headings listing the secondary ion and statement 2.30 must be changed to complete the transition to any of the systems desired. Statement 2.30 converts the measured ion current to a value representing the total ion current for all the isotopic peaks observed for an ion. Since SF_5^- contains one sulfur atom, the measured SF_5^- ion current for the sulfur-32 isotope is divided by the fractional abundance of ^{32}S, giving the total SF_5^- ion current. Since arsenic is monoisotopic (as is fluorine) no correction for the AsF_4^- ion current is necessary. The program calculates the reaction rate constant and reaction cross section from values of temperature, pressure of the neutral species, the repeller voltage, and the ion currents measured for all the ions observed. In addition, the per cent of total ion current for each ion observed is calculated by the subroutine in group 7.00.

Appendix B. The program listed here was used to calculate the rate data for processes occurring in pure AsF_5. Both an ion transfer and a charge transfer reaction were observed in pure AsF_5, and this program calculates the individual rate constants and

cross sections for these processes.

Appendix C. The FOCAL program listed here was used to calculate rate data for processes occurring in SF_6-AsF_5 mixtures. Three processes were observed in such mixtures, with two reactions yielding a common product. The subroutine in group 10.00 was utilized to subtract the contribution from the reaction occurring in pure AsF_5, allowing determination of rate data for the SF_6^- reaction forming AsF_6.

APPENDIX A

```
C-8K MODV 11-219

Ø1.Ø1 C-CHANGE 1217 FROM 4551 TO 76ØØ TO SUPPRESS:
Ø1.Ø2 C-CHANGE 6ØØ2 FROM 4551 TO 76ØØ TO SUPPRESS =
Ø1.1Ø T !!!!!!!!!!!!!!!!
Ø1.2Ø S N=1; T "IMR RATE CONSTANT AND CROSS
Ø1.3Ø T " SECTION CALCULATION" !
Ø1.4Ø A !, "DATE  " Z9,Z8,Z7; T "                "
Ø1.5Ø T "SEC. ION : ASF4-"
Ø1.6Ø A !, #, "TEMPERATURE,C " T
Ø1.7Ø S M=146; T %4, "   PRIMARY ION MASS = " M
Ø1.8Ø A !, "IS PRESSURE CONSTANT ? " YY
Ø1.81 I (YY-25) 1.9,1.85,1.9
Ø1.85 A "   PRESSURE " P
Ø1.9Ø T !!; A "REPELLER VOLTAGE " V

Ø2.1Ø A !, "I(ASF4-) " IS; A "   I(SF6-) " IP
Ø2.2Ø A  "   I(SF5-) " IZ
Ø2.3Ø S IP=2.465*IP/.95Ø18; S IZ=IZ/.95Ø18
Ø2.5Ø I (YY-25) 2.6,2.7
Ø2.6Ø A !, "PRESSURE " P; G 2.9
Ø2.7Ø T !, %3.Ø2, "PRESSURE =" P
Ø2.9Ø T "  MICRON"; I (P-1) 3.1,3.1,2.91
Ø2.91 T "S"

Ø3.1Ø S A=1; S B=IS; S A=IP; S R=B/(A+B)
Ø3.15 D 7
Ø3.4Ø S K(I)=FSQT[(8.6Ø67*R↑2*(T+273.16)↑2*V)/(P↑2*M)]
Ø3.5Ø S Q(I)=FSQT[(K(I)↑2*M*5.53Ø7)/(V)]
Ø3.6Ø S QR(I)=[6.9ØØ*R*(T+273.16)]/P

Ø4.1Ø T !!, %1Ø.Ø6, "K  =" K(I)
Ø4.15 T "  *1Ø↑-1Ø CC/MOLECULE-SEC"
Ø4.2Ø T !, "Q  =" Q(I)
Ø4.3Ø T "  A↑2"
Ø4.4Ø T !, "QR =" QR(I); D 4.3

Ø5.1Ø A  "                SAME V? " ZZ
Ø5.15 I (ZZ-25) 5.3,5.4,5.3
Ø5.3Ø T !!, ".........."; S N=N+1
Ø5.35 I (N-4) 1.9,5.8,5.8
Ø5.4Ø T !!, ".........."; S N=N+1
Ø5.45 I (N-4) 5.95,5.9,5.9
Ø5.8Ø T !!!!!!!!!!!!!!!!!!!!; S N=Ø; G 1.9
Ø5.9Ø T !!!!!!!!!!!!!!!!!!!!; S N=Ø
Ø5.95 T !!, %4.Ø2, "REPELLER VOLTAGE =" V; G 2.1
```

```
Ø7.1Ø T !!, "                        ASF4-         SF6-"
Ø7.15 T "          SF5-"
Ø7.2Ø S DN=IS+IP+IZ
Ø7.3Ø T !, #, %8.Ø6, "% ION CURRENT    " 1ØØ*IS/DN
Ø7.35 T "    " 1ØØ*IP/DN
Ø7.4Ø T "    " 1ØØ*IZ/DN
Ø7.7Ø R

*
```

APPENDIX B

```
C-8K MODV 11-219

01.01 C-CHANGE 1217 FROM 4551 TO 7600 TO SUPPRESS:
01.02 C-CHANGE 6002 FROM 4551 TO 7600 TO SUPPRESS =
01.10 T !!!!!!!!!!!!!!!!
01.20 S N=1; T "IMR RATE CONSTANT AND CROSS
01.30 T " SECTION CALCULATION" !
01.40 A !, "DATE   " Z9,Z8,Z7; T "                    "
01.50 T "SEC. ION : ASF6-,ASF5-"
01.60 A !, #, "TEMPERATURE,C " T
01.70 S M=151; T %4, "   PRIMARY ION MASS " M
01.80 A !, "IS PRESSURE CONSTANT ? " YY
01.81 I (YY-25) 1.9,1.85,1.9
01.85 A "   PRESSURE " P
01.90 T !!; A "REPELLER VOLTAGE " V

02.30 S Z=1;  A !!, "I(ASF6) " IS
02.40 A "  Q(ASF4) " IP; A "  I(ASF5) " IZ
02.50 I (YY-25) 2.6,2.7
02.60 A !, "PRESSURE " P; D 2.9; G 3.1
02.70 T !, %3.02, "PRESSURE =" P
02.90 T "  MICRONS"

03.10 S B=IS; S A=IP; S C=IZ; S R1=B/(A+B)
03.11 S R2=C/(A+C)
03.15 T !!; D 7
03.30 S R=R1; S Z6=1; S I=1
03.40 S K(I)=FSQT[(8.6067*R↑2*(T+273.16)↑2*V)/(P↑2*M)]
03.50 S Q(I)=FSQT[(K(I)↑2*M*5.5307)/(V)]
03.60 S QR(I)=[6.900*R*(T+273.16)]/P

04.10 I (Z6-1) 5.1,4.2
04.20 S Z6=0; S R=R2; S I=2
04.30 D 3.4; D 3.5; D 3.6
04.40 D 6

05.10 A !!, "SAME V? " ZZ; I (ZZ-25) 5.3,5.4,5.3
05.30 T !!, ".........."; S N=N+1
05.35 I (N-4) 1.9,5.8,5.8
05.40 T !!, ".........."; S N=N+1
05.45 I (N-4) 5.95,5.9,5.9
05.80 T !!!!!!!!!!!!!!!!!!!!; S N=1; G 1.9
05.90 T !!!!!!!!!!!!!!!!!!!!; S N=1
05.95 T !, %4.02, "REPELLER VOLTAGE =" V; G 2.3
```

```
06.04 T !!!, %8.05, "           K*10↑10          Q"
06.05 T "            QR              R"
06.06 T !, "          CC/M-SEC          A↑2"
06.07 T "           A↑2"
06.10 T !, %8.05, "IMR    " K(1), "    " Q(1)
06.11 T "    " QR(1)
06.15 T %10.09, "     " R
06.20 T !, #, %8.05, "CTR    " K(2), "    " Q(2)
06.21 T "    " QR(2)
06.25 T %10.09, "     " R
06.30 R

07.10 T !, "                      ASF4-          ASF5-"
07.11 T "         ASF6-"
07.20 S DN=IS+IP+IZ
07.30 T !, %8.06, "% ION CURRENT    " 100*IP/DN
07.35 T "    " 100*IZ/DN
07.40 T "    " 100*IS/DN
07.60 R

*
```

APPENDIX C

```
C-8K MODV 11-219

01.01 C-CHANGE 1217 FROM 4551 TO 7600 TO SUPPRESS:
01.02 C-CHANGE 6002 FROM 4551 TO 7600 TO SUPPRESS =
01.10 T !!!!!!!!!!!!!!!!
01.20 S N=1; T "IMR RATE CONSTANT AND CROSS
01.30 T " SECTION CALCULATION" !
01.40 A !, "DATE  " Z9,Z8,Z7; T "                "
01.50 T "SEC. ION : ASF6-,ASF5-"
01.60 A !, #, "TEMPERATURE,C " T
01.70 S M=151; T %4, "   PRIMARY ION MASS " M
01.80 A !, "IS PRESSURE CONSTANT ? " YY
01.81 I (YY-25) 1.9,1.85,1.9
01.85 A "   PRESSURE " P
01.90 T !!; A "REPELLER VOLTAGE " V

02.30 S Z=1;  A !!, "I(ASF6-) =" IS
02.40 A "  I(ASF4-) ="  IP; A "  I(ASF5-) =" IZ
02.45 A !, "I(SF6-) =" I1; A "   I(SF5-) =" I2
02.46 S I1=I1*2.465/.95018; S I2=I2/.95018
02.50 I (YY-25) 2.6,2.7
02.60 A !, "PRESSURE " P; D 2.9; G 3.1
02.70 T !, %3.02, "PRESSURE =" P
02.90 T "  MICRONS"

03.10 D 10; D 8
03.15 T !!; D 7
03.30 S R=R1; S Z6=1; S I=1
03.40 S K(I)=FSQT[(8.6067*R↑2*(T+273.16)↑2*V)/(P↑2*M)]
03.50 S Q(I)=FSQT[(K(I)↑2*M*5.5307)/(V)]
03.60 S QR(I)=[6.900*R*(T+273.16)]/P

04.10 I (Z6-1) 5.1,4.2
04.20 S Z6=0; S R=R2; S I=2
04.30 D 3.4; D 3.5; D 3.6
04.40 S R=R3; S I=3; S M=146
04.50 D 3.4; D 3.5; D 3.6
04.55 S M=151
04.60 D 6

05.10 A !!, "SAME V? " ZZ; I (ZZ-25) 5.3,5.4,5.3
05.30 T !!, "........."; S N=N+1; I (N-4)1.9,5.8,5.8
05.40 T !!, "........."; S N=N+1; I (N-4) 5.95,5.9,5.9
05.80 T !!!!!!!!!!!!!!!!!!!!; S N=1; G 1.9
05.90 T !!!!!!!!!!!!!!!!!!!!; S N=1
05.95 T !, %4.02, "REPELLER VOLTAGE =" V; G 2.3
```

```
Ø6.Ø4 T !!!, %8.Ø5, "          K*1Ø↑1Ø          Q"
Ø6.Ø5 T "          QR            R"
Ø6.Ø6 T !, "          CC/M-SEC          A↑2          A↑2"
Ø6.1Ø T !, %8.Ø5, "IMR    " K(1), "    " Q(1)
Ø6.15 T "    " QR(1); T %1Ø.Ø9, "    " R1
Ø6.2Ø T !, #, %8.Ø5, "CTR    " K(2), "    " Q(2)
Ø6.25 T "    " QR(2); T %1Ø.Ø9, "    " R2
Ø6.3Ø T !, #, %8.Ø5, "SF6 RXN" K(3), "    " Q(3)
Ø6.35 T "    " QR(3); T %1Ø.Ø9, "    " R3
Ø6.4Ø R

Ø7.1Ø T !, "              ASF4-       ASF5-       ASF6-"
Ø7.11 T "       SF6-        SF5-"
Ø7.2Ø S DN=IS+IP+IZ+I1+I2
Ø7.3Ø T !, %6.Ø4, "% I. C.    " 1ØØ*IP/DN
Ø7.35 T "    " 1ØØ*IZ/DN
Ø7.4Ø T "    " 1ØØ*IS/DN
Ø7.6Ø T "    " 1ØØ*I1/DN
Ø7.7Ø T "    " 1ØØ*I2/DN
Ø7.8Ø R

Ø8.1Ø S XR=FSQT[(KR↑2*P↑2*M)/(8.6Ø67*(T+273.16)↑2*V)]
Ø8.2Ø S IR=XR*IP/(1-XR); S I3=IS-IR; S R3=I3/(I3+I1)
Ø8.4Ø S R1=IR/(IR+IP); S R2=IZ/(IZ+IP)
Ø8.6Ø R

1Ø.1Ø I (1.25-V) 1Ø.15
1Ø.12 S KR=5.6; R
1Ø.15 I (1.75-V) 1Ø.2Ø,1Ø.17,1Ø.18
1Ø.17 S KR=4.1; R
1Ø.18 S KR=4.65; R
1Ø.2Ø I (2.25-V) 1Ø.25,1Ø.22,1Ø.23
1Ø.22 S KR=3.95; R
1Ø.23 S KR=3.82; R
1Ø.25 I (3.5-V)1Ø.3,1Ø.27,1Ø.28
1Ø.27 S KR=3.58; R
1Ø.28 S KR=3.6Ø; R
1Ø.3Ø I (4.Ø-V)1Ø.35,1Ø.32,1Ø.33
1Ø.32 S KR=3.53; R
1Ø.33 S KR=3.45; R
1Ø.35 I (4.5-V)1Ø.4Ø,1Ø.37,1Ø.38
1Ø.37 S KR=3.7; R
1Ø.38 S KR=3.75; R
1Ø.4Ø I (5-V) 1Ø.45,1Ø.42,1Ø.43
1Ø.42 S KR=3.3; R
1Ø.43 S KR=3.65; R
1Ø.45 I (5.5-V) 1Ø.5Ø,1Ø.47,1Ø.48
1Ø.47 S KR=3.Ø; R
1Ø.48 S KR=3.2; R
1Ø.5Ø S KR=3.35; R

*
```

The vita has been removed from the scanned document

NEGATIVE ION-MOLECULE REACTIONS: AN INVESTIGATION OF FLUORIDE ION TRANSFER REACTIONS IN SELECTED NONMETAL FLUORIDES

Thomas C. Rhyne

ABSTRACT

In this study of negative ion-molecule reactions a high pressure mass spectrometer was utilized to investigate the formation of fluoroanions. The reactions of SF_6^- and SF_5^- with the nonmetal fluorides PF_3, PF_5, POF_3, PSF_3, BF_3, SiF_4, AsF_3, and AsF_5 were investigated.

Reactant negative ions were produced by electron bombardment at low electron energies in the mass spectrometer by resonance electron capture processes. From an examination of the electron capture ionization efficiency curves for primary ions (SF_6^- and SF_5^-) and secondary ions at low electron energies, SF_6^- was identified as the reactant ion. A study of the pressure dependence of the primary and secondary ion currents confirmed that the reactions are simple bimolecular processes.

Reaction rate constants and reaction cross sections were determined for the fluoride ion transfer processes, and the variation of the reaction cross section with energy of the reactant ion was investigated. Shifts in the electron capture ionization efficiency curves for secondary ions formed at high repeller voltages (and therefore at high reactant ion energies) suggested that the primary ion SF_5^- might also react to form $\left[AF_{n+1}\right]^-$ ions if supplied with sufficient energy.

Heats of formation of the secondary ions were evaluated from a knowledge of the heats of formation of primary ions and neutral species and application of Hess's Law. Since no kinetic energy measurements were carried out, the enthalpy data reported here represent upper limits for the actual heats of formation of the secondary ions.

The reaction cross sections determined for the fluoride ion transfer reactions were considered as a measure of the relative acceptor strength of the nonmetal fluorides. A scale of Lewis acidities was established from the cross section data obtained, and the order of Lewis acid strength was determined to be $AsF_3 > BF_3 > SiF_4 > AsF_5 > PF_5 >> POF_3 > PF_3 > PSF_3$.

The effect of structural parameters on reactivity was evaluated from a consideration of the measured reaction cross sections and the varied structural parameters exhibited by the nonmetal fluorides. The electron density rearrangement description of ion-molecule reactions was applied to the reactions investigated, and this model was found to be of limited use in predicting the magnitude of the reaction cross section. Factors in addition to the rearrangement of electron density were observed to correlate well with the observed cross section measurements.

The influence of a permanent dipole moment on the reactive ion-molecule collision was found to be quite marked, and the stereochemistry of the reactant molecules is suggested as important in determining the ease of ion transfer to the neutral species. Molecular symmetry and coordination number of the neutral also determine to a large extent the ability of the neutral species to incorporate an additional species into the bonding sphere. Therefore, the correlation of these parameters with the reaction cross sections measured for the fluoride ion transfer

reactions suggests that studies of gas-phase ion-molecule reactions may be quite useful in understanding the effect of structure on chemical reactivity.